Structural design of self-unloading mining ship and unsteady flow computations over its vertical riser

Guemini Ramzi

Master Thesis

presented in partial fulfillment
of the requirements for the double degree:
“Advanced Master in Naval Architecture” conferred by University of Liege
"Master of Sciences in Applied Mechanics, specialization in Hydrodynamics, Energetics and Propulsion” conferred by Ecole Centrale de Nantes

developed at West Pomeranian University of Technology, Szczecin
in the framework of the

“EMSHIP”
Erasmus Mundus Master Course
in “Integrated Advanced Ship Design”

Ref. 159652-1-2009-1-BE-ERA MUNDUS-EMMC

Supervisors:	Prof. Zbigniew Sekulski West Pomeranian University of Technology, Szczecin Prof. Tomasz Abramowski Inter Ocean Metal organization, Szczecin
Reviewer:	Prof. Mathias Paschen University of Rostock, Germany

Szczecin, February 2014

Structural design of self-unloading mining ship and unsteady flow computations over its vertical riser

Guemini Ramzi

Master Thesis

presented in partial fulfillment
of the requirements for the double degree:
“Advanced Master in Naval Architecture” conferred by University of Liege
"Master of Sciences in Applied Mechanics, specialization in Hydrodynamics, Energetics and Propulsion” conferred by Ecole Centrale de Nantes

developed at West Pomeranian University of Technology, Szczecin
in the framework of the

“EMSHIP”
Erasmus Mundus Master Course
in “Integrated Advanced Ship Design”

Ref. 159652-1-2009-1-BE-ERA MUNDUS-EMMC

ABSTRACT

The Inter Ocean Metal organization (IOM) has proposed some initial considerations which can be used in developing the design of a polymetallic nodules mining ship.
The requirements for cargo volume and deadweight are studied on the basis of assumed production output. A novel concept for cargo discharging to a shuttle transport ship by self-unloading is proposed by IOM company, the analysis of cargo characteristics showed that there are several issues which affect the subdivision of the ship and the approach to the problem of arranging its structure.
Accidental stress or damage caused during the loading or discharging of self-unloading mining ship could ultimately lead to catastrophic structural failure.

The primary aim of this thesis is to perform a structural design of the concerned mining ship by means calculating the shear forces and bending moments in any load or ballast condition and to asses these against the assigned maximum permissible values.
When we consider the primary hull structure, the two most important load effects are the still water and the wave-induced shear force and bending moments. The reference is made to the cross section by creating a scantling of proposal structural arrangement according to the DNV Rules given by Nauticus Hull software used for this study.
The values of load effects in the various components of the ship structure show a good correspondence to the requirements of DNV (Det Norske Veritas) classification society.
One component related to mining applications that can be subjected to large deformations is the riser which is controlled by a lifting system installed in the mining support vessel.

The secondary aim is to find a means of alleviating vortex-shedding-induced vibration of a deep-ocean mining riser with 0.7 m outer diameter and 5,000 m in length, and to deduce on the power requirements for towing the whole riser through the water depth in vertical position.
An unsteady analysis of flow was performed around three riser configurations at different Reynolds number, for their effectiveness in reducing vortex- shedding intensity.
The computational implementation was accomplished by the commercial software Fluent Ansys and the flow was analyzed by means of studying pressures, velocities, vorticities distributions, also lift and drag forces variations and torsional moment applied on the risers.
The numerical results of drag coefficient and Strouhal number which signifies the vortex shedding in function of Reynolds number are coincident with the previous experiments.

CONTENTS

Index of figures

Index of tables

Symbols and Abbreviations

Symbol	Entity	Definition
A_{WP}	m^2	Water plane area of vessel at draught T
B	m	Rule breadth of the ship
b_b	m	Distance between tank sides
b_t	m	Breadth of top of tank
b	m	The largest athwart ship distance from the load point
C_B	-	Rule block coefficient of the ship
C_D	-	Drag coefficient
C_L	-	Lift coefficient
C_W	-	Wave coefficient
D	m	Rule depth of the ship
F	N	Hydrodynamic force per unit length along pipes
F_D	N	Hydrodynamic drag
F_i	N	Hydrodynamic inertia force per unit length
f	m	Vertical distance from the waterline to the top ship's side
f_1	-	Material factor
H	m	Height of the tank (or stowage height)
h	m	Filling height
h_0	m	Vertical distance from the waterline at draught to the load point
h_s	m	Vertical distance from the load point to the top of tank
hp	m	Vertical distance from the load point to the top of air pipe
h_b	m	Vertical distance from the load point to the deepest waterline
I_N	cm^4	Moment of inertia about the transverse neutral axis
I_C	cm^4	Moment of inertia about the vertical neutral axis
k_a	-	Correction factor for aspect ratio of plate field
k_f	m	The smallest of T and f
L	m	Rule length of the ship
L_1	m	Ship’s length but need not be taken greater than 300
l	m	Stiffener span, measured along the top flange of the member
l_t	m	Length of top of tank
*l*s	m	Effective sloshing length

M_W	kNm	Wave bending moment
M_{WH}	kNm	Wave bending moment about the vertical axis
M_{WT}	kNm	Wave torsional moment
M_S	kNm	Design still water bending moment
p	kN/mm^2	Design pressure
p_0	kN/mm^2	Tank pressure
p_{bhd}	kN/mm^2	Sloshing pressure on wash or end bulkheads
Q_S	kN	Design still water shear force
Q_W	kN	Wave shear force
S	m	Girder span
s	m	Stiffener spacing measured along the plating
T	m	Rule draught of the ship
T_M	m	Minimum design draught
t	mm	Rule thickness of plating
V	Knots	Maximum service speed
x	m	Distance in m from A.P. to section considered.
y	m	Horizontal distance from the center line to the load point
Z	cm^3	Rule section modulus in of stiffeners and simple girders
z	m	Vertical distance from the baseline to the load point
z_a	m	Vertical distance from the baseline to the point in question
z_n	m	Vertical distance from the baseline to the neutral axis of girder
z_e	m	Distance from the shear center of the midship section to 0.7 T
ρ	t/m^3	Density of liquid
Δp_{dyn}	kN/mm^2	Calculated pressure drop
σ_F	N/mm^2	Minimum upper yield stress of material
τ_L	N/mm^2	Shear stress
σ_L	N/mm^2	Normal stress
σ_v	N/mm^2	Von Mises stress
σ_y	N/mm^2	Normal stress component in the transversal direction
σ_x	N/mm^2	Normal stress component in the longitudinal direction

ABS	American Bureau of Shipping
DNV	Det Norske Veritas
GL	Germanischer Lloyd
LR	Lloyd Register
IACS	International Association of Classification Societies
IMO	International Maritime Organization
SOLAS	IMO convention for Safety Of Life At Sea
2D	Two-dimensional
3D	Three-dimensional
CFD	Computational Fluid Dynamics
RMS	Root Mean Square
VIV	Vortex-Induced Vibrations

Declaration of Authorship

I declare that this thesis and the work presented in it are my own and have been generated by me as the result of my own original research.

Where I have consulted the published work of others, this is always clearly attributed.

Where I have quoted from the work of others, the source is always given. With the exception of such quotations, this thesis is entirely my own work.

I have acknowledged all main sources of help.

Where the thesis is based on work done by myself jointly with others, I have made clear exactly what was done by others and what I have contributed myself.

This thesis contains no material that has been submitted previously, in whole or in part, for the award of any other academic degree or diploma.

I cede copyright of the thesis in favour of West Pomeranian University of Technology, Szczecin.

Szczecin, January 11th 2014 *Guemini ramzi*

INTRODUCTION

Tough market conditions bring intense operational demands on the 4500 bulk carriers that transport 30% of world ocean cargo. Heavy and high density cargo , mineral ores and coal for exemple,also make high physical demands on ship's structure , especially on their cargo hold areas.

The International Association of Classification Societies (IACS) casualty database shows that from 1983 to June 1997, 73 bulk carriers were lost (or written off) due to known or possible structural failure. At least 40 more ships suffered serious damage.

Typically, the bulk carriers have a high number of lives lost in accidents, which shows that the consequences of bulk carrier casualties are more severe than other ship types.

The research into bulk carrier's casualties shows that over 70% of total losses had three factors in common. The ships were all at least 18 years old, carrying heavy cargoes, and experienced water ingress to hold in bad weather. (IACS, 2001)

The self-unloading mining ship proposed by Abramovski and Cepowski, (2013) is designed with limitation imposed upon their operability; a structural design of a bulk carrier is required to ensure that the structural integrity is maintained.

The improper handling of cargo during loading and discharge may cause excessive stress of the ship structure and physical damage to holds and bulkheads. Over time, this may reduce or threaten structural safety margins when the ship is at hard sea conditions.

The ship's approved loading manual provides a description of the operational loading conditions upon which the design of the hull structure has been based.

The loading instrument provides a mean to readily calculate the still water shear force and bending moments in any load or ballast condition, and access these values against the design limits.

Current technology in deep sea mining applications dictates that the slurry produced by the seabed mining tool is transported to the mining support vessel using a flexible riser to the vertical riser inlet similar to oil & gas risers.

Because of the extreme depths involved (generally from several hundred up to thousands of meters), the risers are subjected to numerous forces that induce high stress levels in the pipe material. Therefore, an appropriate pipe design is essential to render them more resistant and to avoid possible breaks and subsequent dispersal of oil and gas which could be transported towards sensitive areas near coastal environments. (A. Pollio, M. Mossa, 2006)

Alleviation of these problems has been possible using vortex-shedding reduction or suppression devices, including streamlined (mechanical) fairings, perforated-shroud, and he1ical-strake

arrangements around the circular cylinder, from the criteria for selecting the optimal configuration.

A series of flow-visua1ization simulations was carried out in order to obtain, in addition to the force measurements and moments, physical information regarding the effectiveness of the model devices in reducing the intensity and regularity of vortex shedding relative to the bare cylinder to which these devices were attached.

External flows past objects have been studied extensively because of their many practical applications.

In particular, the present thesis focuses on three main aspects:

- Firstly, the structural design of the self-unloading mining ship more than 100 m length,

is carried out for a typical cargo ship by performing a scantling calculation of a chosen cross section to study the safety margin and to judge damage tolerance and survivability which can be assessed by a comparison of their ultimate strength with expected extreme hull girder loads using Nauticus Hull DNV software, by means calculating the vertical and horizontal bending moments, shear forces and stresses acting on the ship hull in both still water and wave conditions, then combined in accordance with the proposed ultimate load criterion and compared with the DNV standards under which the ship will be designed.

- Secondly, to simulate a 2D flow laminar and turbulent past a circular cylinder using Fluent Ansys package and to study the influence of Reynolds number on quantities such as Strouhal number and compare the results with the previous experiments.

The Navier-Stokes equations with appropriate boundary conditions are approached numerically. The incompressible flow equations are solved using the CFD software package, Fluent, which is a finite-volume solver. CFD calculates numerical solutions to the equations governing fluid flow.

- Lastly, to perform a 3D turbulent flow simulation over three basic riser configurations including cylindrical, streamlined fairing and straight cables model used in mining application and to investigate the effect of vortex shedding and pressure distribution, flow velocity and vorticity around the riser, also to deduce on the drag, lift force and torsional moments.

The numerical result of drag force in function of Reynolds number for the cylindrical riser is validated with the previous study and finally, the power requirement for towing the whole vertical risers with 5000 m length from seafloor is carried out.

1. MINING SHIP AND UNLOADING DEVICES

1.1. Self-unloading ships

Self-unloaders are specialized ships equipped with onboard cargo-handling systems, enabling them to discharge without shore-based unloading equipment. Their rapid discharging rate, and reduced infrastructure and labor requirements, make this bulk cargo handling option an effective and competitive solution that helps keep costs down and minimize environmental impacts**.** Self-unloaders provide ideal solutions for shipping and handling commodities such as salts, fertilizers, aggregates, coal, grains, ores and minerals. An example of self-unloader is presented in fig.1-1.

It was mentioned in the bulk carrier guide that self-unloader bulk carriers are similar in hull structure to other bulk carriers, these vessels are fitted with one of two systems for discharging cargo:

- *A gravity fed self-unloader:* the cargo is dropped onto a conveyor belt running in a duct keel under the cargo holds that carries the cargo towards the bow or stern of the vessel where another conveyor lifts it for discharge ashore. The discharging arm is connected to a boom that can be slewed into position for discharge
- *A hybrid self-unloader:* commonly used, this method does not require any special structural design of the vessel. The cargo is discharged by grabs into hoppers where it feeds onto a conveyor belt. The hoppers can be permanently fitted on the ship or may be placed on the deck of the vessel when discharging.

Figure.1-1 self-unloading bulk carrier

http://www.nordnes.nl/history.php

1.2. Cargo unloading system and its influence on ship subdivision

The devices for cargo trans-shipment are a crucial part of the mining ship design. They should be able to transfer the accumulated nodules at a sufficient loading rate, shortening the time of this operation to a minimum. Several options are available in this regard; starting from standard grab cranes installed above the cargo holds, as well as systems installed onboard the so-called self-unloading bulk cargo vessels. The latter are a particularly tempting option - due to a consistent structure of such a design, there is a single system of conveyor belt(s) placed along the whole length of the ship, gathering nodules from all cargo holds.

Such a system can easily be designed to include a dewatering or drying mechanism. Dewatering conveyor belt devices are commonly used in mines and on ships as well.

Self-unloaders have a capital cost which is 20-35 per cent higher than conventional bulkers and also provide less space for cargo than conventional ships of the same size do. However, these disadvantages are balanced by a facilitation of cargo discharging, which is a crucial function of a nodule mining ship. The use of such a system for a mining ship brings about another advantage as there is no need to unload the vessel in ports, in consequence it is unnecessary to provide full-size hatch covers which simplifies the design and improves longitudinal strength of the hull. The drawback of such a system is that there is no watertight subdivision along the length of the cargo part. This complicates the design process and a solution can either be to use additional watertight compartments or to arrange various function areas of the ship in such a way as to allow shorter floodable compartments.

For the sake of prototype design suitable for further investigations, it was assumed that the discharging boom will be located in the aft part of the ship. According to Abramowski and Cepowski, (2013).

The most advanced diamond mining vessel in the world is a South African ship called

‘*Peace in Africa’*

The ship was built at a cost of $15 million at the A&P Tyne shipyard in Newcastle. It stays out at sea for two and a half years with a crew of 60 people working 12 hour shifts (the crew changes monthly, ever 28 days). See fig.1-2.

Figure.1-2 The De Beers diamond mining vessel '*Peace in Africa'*
http://teeveetee.blogspot.com/2010/05/programming-note-watch-south-africas.html

1.3. Self-unloading mining ship description

The assumptions given by Abramowski and Cepowski,(2013) was that eight holds are planned; four on each board with a "V" shaped cross section, with trimming tops fulfilling also the wing tanks function. The gates for the discharge of nodules are situated at the base point of each hold. Upper and lower wing tanks for ballast and fuel occupy the spaces created by the shape of the holds, and double bottom ballast tanks are also included. During the discharging operation, the nodules are driven by gravity from the holds through hydraulically operated hopper gates to two dewatering conveyor belts which run aft beneath the holds. They are then raised from hold level to boom height by a vertical conveyor, from where it joins the boom conveyor belt to be discharged. The boom unloads nodules at any point up to 35 m from the ship's sides, which makes possible to transfer the cargo to the most typical large bulk cargo ships. Floatation of the ship during unloading is corrected by ballasting. The operation takes place concurrently with unloading.

The reason for fitting eight holds, four on each ship's board is to shorten the breadth of a single hold and decrease the risk of stability loss due to cargo free surface effects. This solution

improves damage stability characteristics in longitudinal direction, due to the presence of watertight longitudinal bulkhead.

Free surface effect affects the stability of a ship due to a shift of its center of gravity. The shift of the center of gravity occurs due to a change in mass distribution caused by ship motions, especially rolling.

Such motions may be due to sharp turns (operational), or due to natural reasons such as wind or wave forces acting on a ship. The changes of ship mass distribution may be due to liquid or otherwise easily occurring cargo shifts in a cargo hold.

1.4. Initial proposal for self-unloading mining ship design

The presented initial design was prepared assuming constant yearly production of nodules. Whether the self-unloading system proposed here is feasible for operation at the assumed unloading rate in the environment of Clarion Clipper ton Zone.

The general arrangement of the designed ship is presented in fig.1-3.

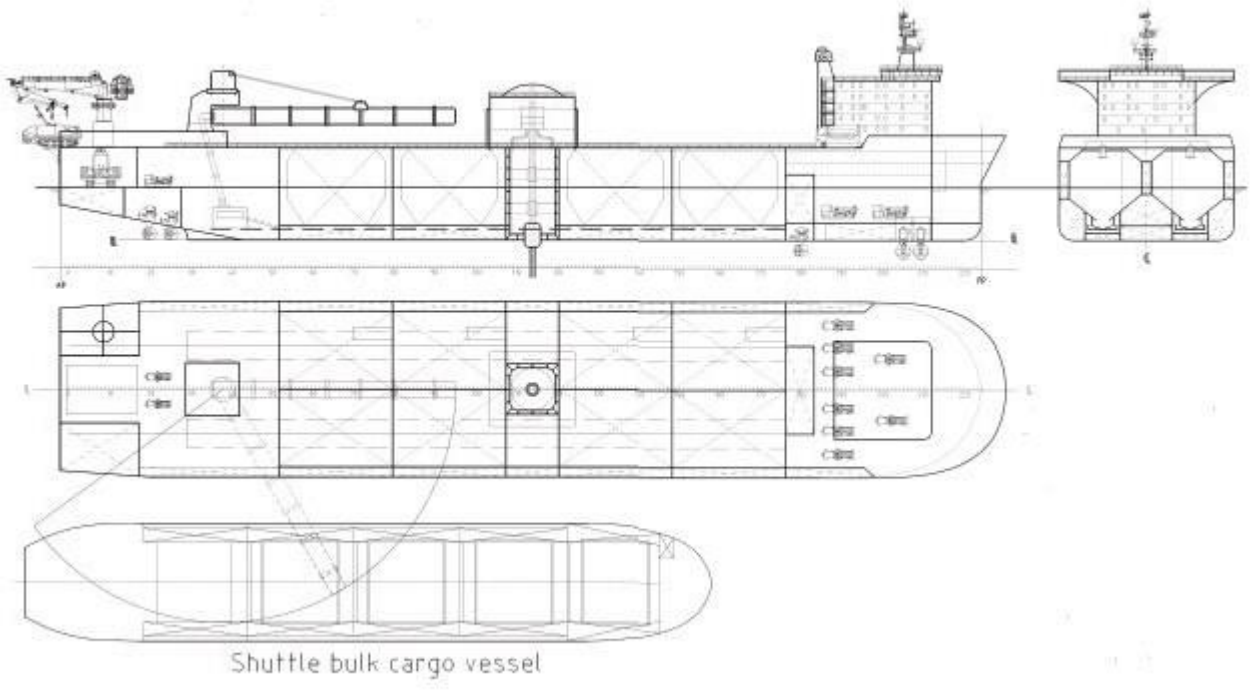

Figure.1-3 Initial proposal for general arrangement of the polymetalic nodules mining ship (Abramowski and Cepowski, 2013)

The design proposal has been prepared for the purposes of presentation of the above considerations, while the presented results by (IOM Company) can serve as a starting point for further, more detailed analysis. The assumptions for the design are given in Table.1-1.

Table.1-1 The assumptions for the design of self-unloading mining ship (Abramowski and Cepowski)

Assumptions for the design of mining ship	Magnitude	Unites
Yearly production of wet nodules , YPO	3,000,000	t/y
Working days WD	320	days
Daily production DP	9375	t/d
Nodules stowage factor NSF	0.4	m3/t
Cargo hold volume coefficient CVC	0.7	-
Self-discharging rate SR	6000	t/h
Unloading cycle, UC	7–8	days
Duration of unloading cycle DUC	déc-15	h
Deadweight of the designed ship DWT	72	t
Overall cargo volume OCV	41	m3

Definition of hull shape (see appendix A1) allowed for calculating the principal hydrostatic characteristics which are given in Table.1-2.

Table.1-2 Hydrostatic characteristics of the self-unloading mining ship (Abramowski and Cepowski)

Data of self-unloading mining ship	**Magnitude**	**Unites**
Displacement, D	110840	[tones]
Draft, T	12.9	[m]
Length of waterline, LWL	227	[m]
Breadth, B	43.2	[m]
Midship area, AM	554	[m2]
Waterplane area, AW	9352	[m2]
Block coeff. CB	0.845	-
Midship coeff. CM	0.996	-
Waterplane area coeff. CWP	0.950	-
Long. center of buoyancy, LCB from AP	115.8	[m]
Center of floatation, LCF from AP	109.6	[m]
Height of buoyancy center, KB	6.8	[m]
Trans. metacentric radius, rT	12.7	[m]
Long. metacentric radius, rL	344.2	[m]
Trans. metacenter, KMT	19.5	[m]
Long. metacenter, KML	351	[m]
Immersion (tons per cm draft)	95.9	[tone/cm]
Wetted surface area	14349	[m^2]

1.5. Structural design principles

The proposed concept of combining a mining ship with a self-discharging bulk carrier requires a structural study of this new ship based on the assumptions and the actual data presented in the previous section. The interest will be on bulk carrier by performing a global structural design using Nauticus Hull package.

'Careful cargo handling helps maintain bulk carrier safety –bad practice lowers safety margins and increases risk '

This IACS booklet is part of continuing series of publications dedicated to safer bulk carrier operations. Summarizing the main problems in loading and discharging heavy and high density cargo, it then considers technical factors from the viewpoints of design limitations and the ship safety responsibilities of the ship's officers. See fig.1-4 for stress cycle in bulker.

The main cargo handling risks are:

- Poor ship-to-shore communications
- Ignoring loading plans
- Inadequate pre-planning of cargo operations
- Improper load distribution between holds
- Overloading by high capacity systems
- Physical damage during discharging

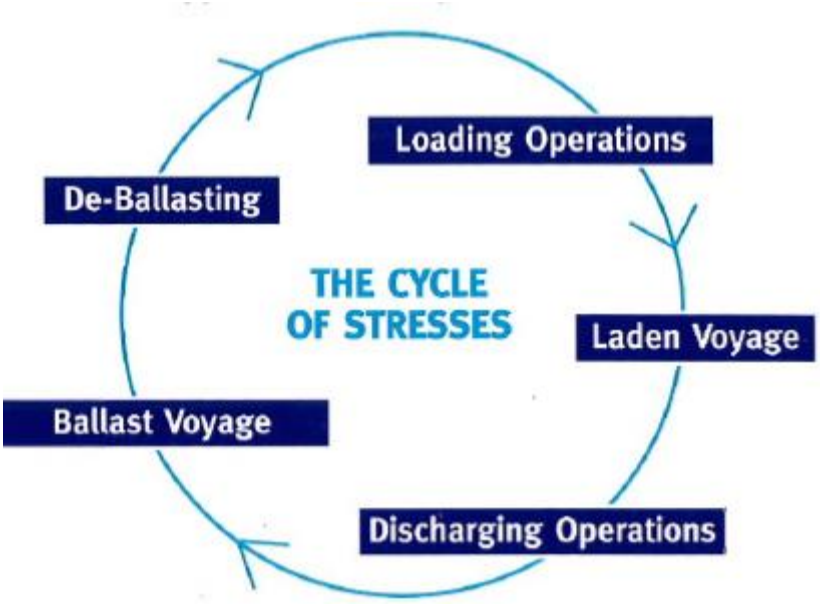

Figure.1-4 Typical bulker operation (IACS, 2001)

1.6. Potential problems

Terminal operating staff needs to share with ship's officer's awareness that heavy/high density cargo operations with bulk carriers involve the following nine main risks of hull or local structure over-stressing and consequent weakness. A typical transverse section in way of cargo hold is detailed in fig.1-5.

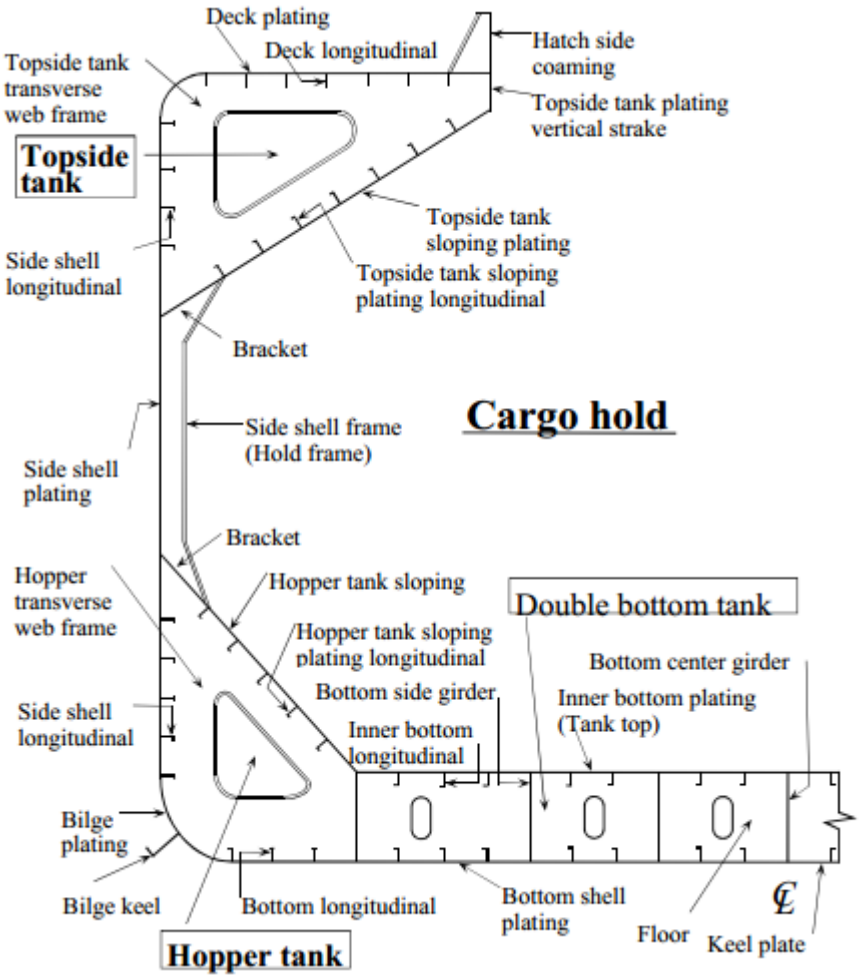

Figure.1-5 Nomenclature for typical transverse section in way of cargo hold

http://www.iacs.org.uk/document/public/Publications/Guidelines_and_recommendations/PDF/REC_76_pdf216.pdf

The potential problems of bulk carrier's hull structure are:

- **Deviations from the loading manual**

Exceeding permissible limits in the ship's approved loading manual will to over-stressing of the ship's structure and may result in catastrophic failure of the hull structure.

It is important to be aware that over-stressing of the local structural members can occur even when the hull girder still water shear force (SWSF) /Still water bending moment (SWBM) have remained within their permissible limits.

- **Shallow draught loading**

To minimize the risks of over–stressing the local structure, the largest possible number of non-successive cargo pours should be used for each hold.

- **Sensitivity of the hull girder to overloading**

High loading rates may cause significant overloading within a very short space of time.

Local structure overloading and synchronization of ballasting where ballast pumping capacity is low versus cargo loading rate, are the three main problems associated with high loading rates

- **Asymmetric cargo and ballast distribution**

Cargo and water ballast distribution have an important influence on the resultant hull structural stresses.

High density cargo should be stowed uniformly over the cargo space and trimming applied to level the cargo as far as practicable. This will minimize the risks of cargo shift in heavy weather and of damage to the hull structure.

When heavy cargo is poured into a cargo space at one end of the cargo hold, and piles up the lateral cargo pressure acting on the transverse bulkhead will increase loads carried by the bulkhead structure and the magnitude of transverse compressive stresses in the cross deck structure.

The double bottom structure may also be severely overloaded.

If the same loading pattern is applied to an adjacent hold, lateral pressure on the transverse bulkhead will be laterally cancelled out, but vertical forces will be transferred to the bulkhead.

Cargo should always be stowed symmetrically in the longitudinal direction, and trimmed as far as practical.

Stowing cargo asymmetrically about the ship's centerline in a cargo space induces torsional loads, causing twisting of the hull girder and warping of the hull structure.

➢ **Stresses resulting from asymmetrical cargo distribution**

1. On transverse bulkheads and cross deck structure.

2. On transverse bulkheads if cargo is asymmetrically distributed in adjacent holds.

3. Asymmetric stowage about the ship's centerline can induce torsional loads and twisting of the hull girder. See to fig.1-6.

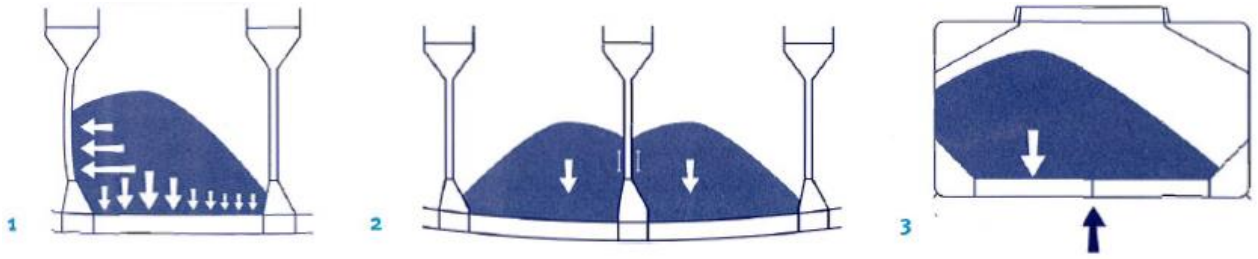

Figure.1-6 Stresses resulting from asymmetrical cargo distribution (IACS, 2001)

- Asymmetrical distribution of water ballast induces torsional loads and torsional loading of the hull girder is considered to be an important contributory factor in recurring cracking at the hatch corners, and to problems with hatch cover alignment and fittings.

Extreme cases may even lead to buckling of the cross deck structure between hatch openings.

➢ **Partially filled ballast tanks or holds**

In partially filled ballast holds or tanks, there is the probability of sloshing, due to the ship's motion in a seaway, sloshing will magnify dynamic internal pressures acting on the hold/tank boundary surfaces and may ultimate damage their internal surface.

➢ **Inadequate cargo weight measurement during loading**

Overloading the cargo hold through inaccurate weighing will increase the stress levels in the ship's structure.

- During cargo operations, it is important to determine the cargo weight loaded into each individual hold and the associated loading rate.
- Inaccurate terminal weighing equipment limited checking time at high loading rate terminals, and hold overloading to compensate for partial bunkers may all contribute to structural overloading. (IACS,2001)

1.7 Hull structure failure

Accidental stress or damage caused during the loading or discharging of bulk carriers could ultimately lead to catastrophic structural failure either alongside or at sea. In terms of lives ships and cargoes lost, the casually record of bulk carriers in recent years has been unacceptable. An exemple of hull structure failure is presented in fig.1-7 showing the wreck of the *Selendang Ayu* cargo ship.

The Selendang Ayu was a 738 ft., 73,000 DWT dry bulk freighter carrying a cargo of soybeans from Seattle to China along the Great Circle Route that intersects the Aleutian Islands at Unimak Pass and a pass near Shemya Island. The freighter grounded on the Western shore of Unalaska Island on December 8, 2004 after drifting for more than two days subsequent to a failed attempt to repair its main propulsion engine. Four vessels ranging from 1,550 hp to 6,800 hp attempted to take the freighter under tow prior to grounding but severe sea conditions either broke the towline or otherwise rendered rescue too hazardous. The grounding occurred in a severe storm that broke the vessel in half, causing a spill that ultimately released more than 335,000 gallons of fuels and lubricants that primarily consisted of the persistent heavy fuel oil IFO 380. A U.S. Coast Guard helicopter attempting to rescue the freighter crew crashed while lifting personnel off of the freighter deck, causing the loss of six Selendang Ayu crewmembers.

Figure.1-7 The wreck of the *Selendang Ayu* bulk carrier

http://www.aleutiansriskassessment.com/documents/SelendangAyu.pdf

The Principal factors contributing to loss were corrosion and cracking of the structure within the cargo space. Factors that could have contributed to hull structural failure were over stressing due to incorrect loading and physical damage to side structures during cargo discharging. Mechanical and coatings damage during cargo discharge will contribute to local weaknesses. See figure1.8 for more details.

Hold bottom (A);

Hopper tank plating (B);

Bulkheads (C);

Side shell frames (D);

Brackets (E).

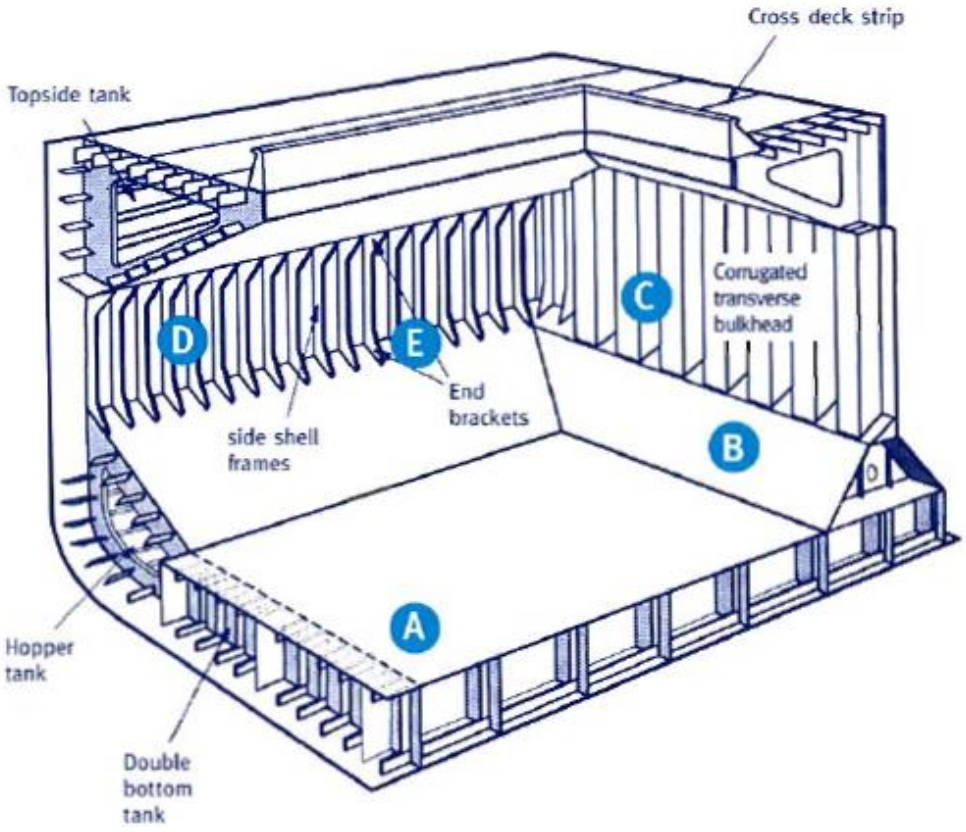

Figure.1-8 Typical Cargo hold structural configuration for a single side skin bulk carrier (IACS,2001)

1.8. Bending and shearing of the hull girder

1.Shearing of the hull girder results from local differences in the opposite-acting vertical forces of hull/cargo weight versus buoyancy. See Fig.1-9

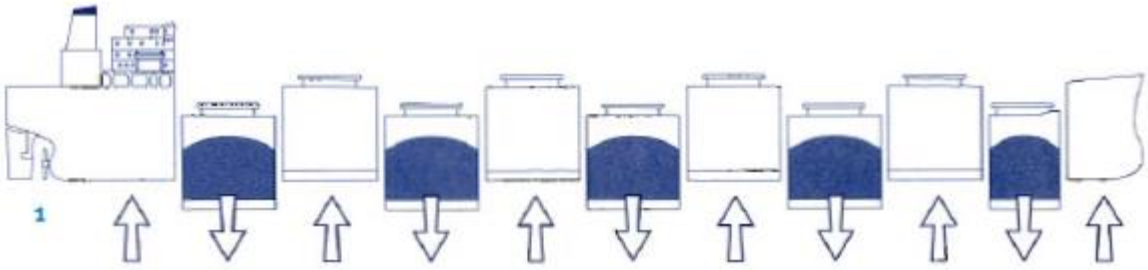

Figure.1-9 Shearing action of the hull girder in still water

2. Bending of the hull girder will produce sagging if weight is incorrectly coocentrated in the middle of the ship. See Fig.1-10

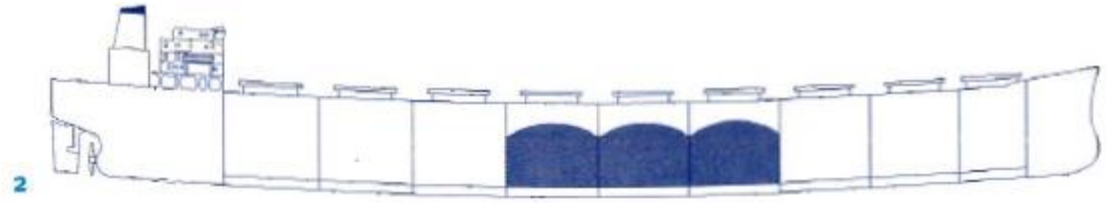

Figure.1-10 Bending action of the hull girder "sagging" in still water

3. Bendingwill produce hogging effect if weight wrongly concentrated at opposite ends of the ship. See Fig.1-11

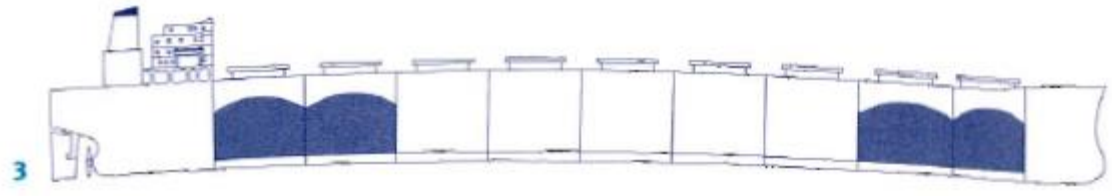

Figure.1-11 Bending action of the hull girder "hogging" in still water

2. DNV RULES REQUIREMENTS FOR THE STRUCTURAL DESIGN

2.1. Design procedure

It was noted (DNV, 2012), that hull scantlings are in general based on the two design aspects, load (demand) and strength (capability).

The probability distribution for the load and the strength of a given structure may be as illustrated in the fig.2-1.

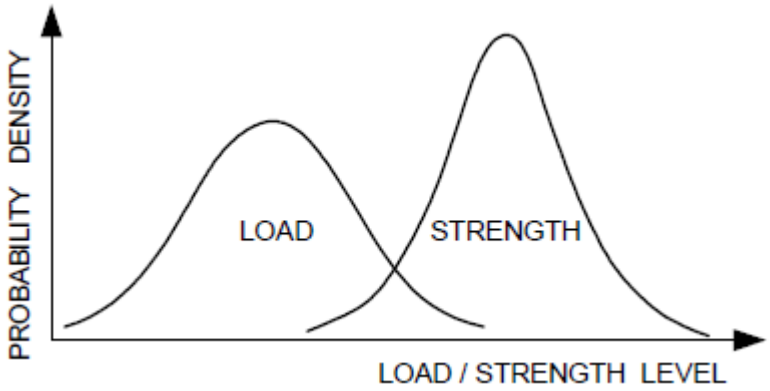

Fig.2-1. Probability distribution for the load and the strength

The rules have established design loads corresponding to the loads imposed by the sea and the containment of cargo, ballast and bunkers.

2.2. Loading conditions

- Static loads are derived from loading conditions submitted by the builder or standard conditions prescribed in the rules. The standard conditions are expected to give suitable flexibility with respect to the loading of ordinary ship types.
- Unless specifically stated, dry cargoes are assumed to be general cargo or bulk cargo (coal, grain) stowing at 0.7t/m^3. Liquid cargoes are assumed to have density equal to or less than that of seawater.
- Unless especially stated to be otherwise, or by virtue of the ship's class notation (e.g. Container Carrier) or the arrangement of cargo compartments, the ship's cargo and ballast conditions are assumed to be symmetric about the centerline. For ships for which unsymmetrical cargo or ballast condition(s) are intended, the effect of this shall be considered in the design.
- The determination of dynamic loads is based on long term distribution of motions that the ship will experience during her operating life.

- Any pertinent effects of surge, sway, heave; roll, pitch and yaw in irregular seas are considered. A uniform probability is normally assumed for the occurrence of different ship-to-wave heading angles. The effects of speed reduction in heavy weather are allowed for. Wave-induced loads determined according to accepted theories, model tests or full scale measurements may be accepted as equivalent basis for classification.

2.3. Hull girder and buckling strength

A minimum strength standard determined by the section modulus at bottom and deck is required for the hull girder cross-section amidships.

Requirements for structural stability are given by the classification societies to prevent buckling or tripping of structural elements when subjected to compressive stresses and shear stresses.

2.4. Fatigue

In general the susceptibility of hull structures to fatigue cracking has been taken care of by special requirements to detail design. However in some cases e.g. where high tensile steel is applied in stiffening members subjected to high frequency fluctuating loads, a special calculation evaluating dynamic stresses, stress concentration factors and environment may have to be performed.

2.5. Local vibrations

Vibrations in the hull structural elements are not considered in relation to the requirements for scantlings given in the rules. It is, however, assumed that special investigations are made to avoid harmful vibrations, causing structural failures, especially in after body and machinery space tank structures, malfunction of machinery like riser system, crane and conveyor used for the mining application and instruments or annoyance to crew and passengers.

2.6. Wave coefficient according to ship length

The wave coefficient varies according to the ship length as shown in table.2-1.

Table.2-1 Wave coefficient according to the ship length.

L	**C_W**
$L \leq 100$	0.0792 L
$100 < L < 300$	$10.75-[(300-L)/100]^{3/2}$
$300 \leq L \leq 350$	10.75
$L > 350$	$10.75-[(L-350)/150]^{3/2}$

2.7. Pressures and Forces

A bulk carrier typical load is presented in fig.2-2 showing the external and internal pressures considered to influence the scantling of panels:

- Static and dynamic sea pressures
- Static and dynamic pressures from liquids in a tank
- Static and dynamic pressures from dry cargoes, stores and equipment.

The design sea pressures are assumed to be acting on the ship's outer panels at full draught.

The internal pressures are given for the panel in question irrespectively of possible simultaneous pressure from the opposite side. For outer panels sea pressure at ballast draught may be deducted. The gravity and acceleration forces from heavy units of cargo and equipment may influence the scantlings of primary strength members.

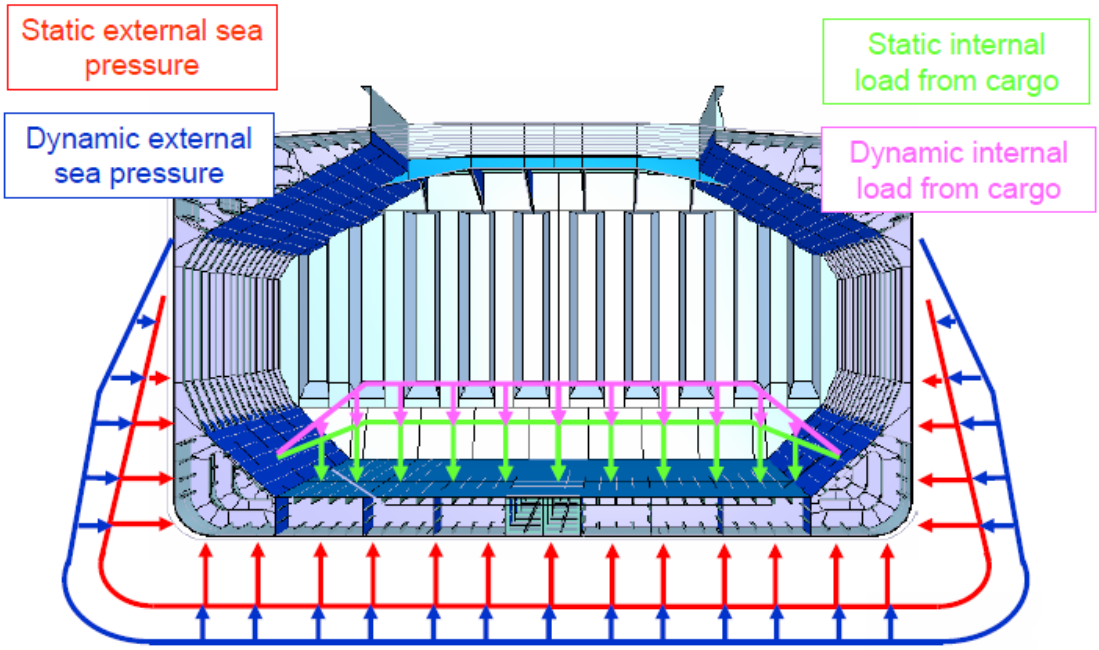

Figure.2-2 Bulk Carrier typical load (DNV, 2011)

2.7.1. Sea pressures

- The pressure acting on the ship's side, bottom and weather deck shall be taken as the sum of the static and the dynamic pressure as:

➢ for load point below summer load waterline:

$$p_1 = 10\ h_0 + p_{dp} \quad [kN/m^2] \qquad (1)$$

➢ for load point above summer load waterline:

$$p_2 = a\ (p_{dp} - (4 + 0.2\ k_s)\ h_0) \quad [kN/m^2] \qquad (2)$$

p_2= minimum $6.25 + 0.025\ L_1$ for sides

p_2= minimum 5 for weather decks.

The pressure p_{dp} is taken as:

$$p_{dp} = p_l + 135\,(y/B + 75) - 1.2\,(T - z) \qquad [KN/m^2] \tag{3}$$

$$p_l = k_s\, C_W + k_f \tag{4}$$

$$= (k_s\, C_W + k_f)\,(0.8 + 0.15\, V/\sqrt{L}) \quad \text{if } V/\sqrt{L} > 1.5$$

$$k_S = 3C_B + 2.5/\sqrt{C_B} \quad \text{at AP and aft} \tag{5}$$

$$k_S = 2 \text{ between } 0.2\ L \text{ and } 0.7\ L \text{ from AP}$$

$$= 3C_B + 4/C_B \text{ at FP and forward.}$$

The sea pressure at minimum design draught which may be deducted from internal design pressures shall be taken as:

$$p = 10\,(T_M - z) \quad [kN/m^2] = \text{minimum } 0 \tag{6}$$

The design pressure on watertight bulkheads (compartment flooded) shall be taken as:

$$p = 10\, h_b \qquad [kN/m^2] \tag{7}$$

- The design pressure on inner bottom (double bottom flooded) shall not be less than:

$$p = 10\ T\ [kN/m^2] \tag{8}$$

2.7.2. Liquids in tanks

- Tanks for crude oil or bunkers are normally to be designed for liquids of density equal to that of sea water, taken as $\rho = 1.025\ t/m^3$
- Tanks for heavier liquids may be approved after special consideration. Vessels designed for 100% filling of specified tanks with a heavier liquid will be given the notation HL **(ρ)**, indicating the highest cargo density applied as basis for approval. See figures(fig.2-3,Fig.2-4)

The pressure in full tanks shall be taken as the greater of:

$$p = \rho\,(g_0 + 0.5\, a_v)\, h_s \quad [kN/m^2] \qquad [1] \tag{9}$$

$$p = \rho\, g_0\, [0.67(h_s + \varphi\, b) - 0.12\, \sqrt{(Hb_t\varphi)}] \quad [kN/m^2 \qquad [2] \tag{10}$$

$$p = \rho\, g_0\, [0.67(h_s + \theta\, l) - 0.12\, \sqrt{Hl_t\theta}\,] \, [kN/m^2] \qquad [3] \tag{11}$$

$$p = 0.67\,(\rho\, g_0\, hp + \Delta\, p_{dyn}) \, [kN/m^2] \qquad [4] \tag{12}$$

$$p = \rho\, g_0\, h_s + p_0 \, [kN/m^2\,] \qquad [5] \tag{13}$$

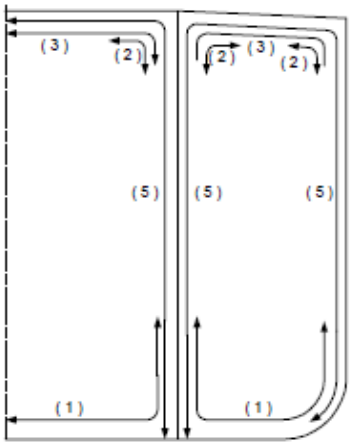

Figure.2-3 Section in cargo tanks

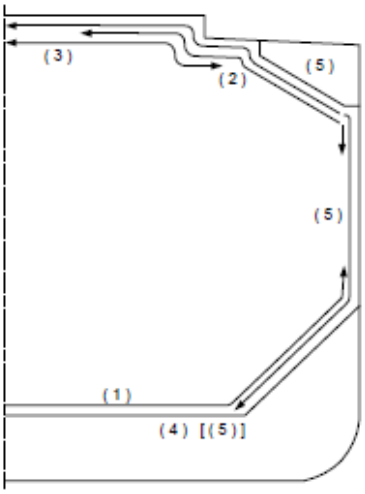

Figure.2-4 Section in bulk cargo hold

• Tanks with l_b < 0.13 L and b_b < 0.56 B shall have scantlings for unrestricted filling height.

For strength members located less than 0.25 l_b away from wash and end bulkhead. Refer to fig.2-5, the pressure shall not be taken less than:

$$p = \rho\,[4\text{-}L/200]\; l_b \;\; [KN/m^2] \qquad (14)$$

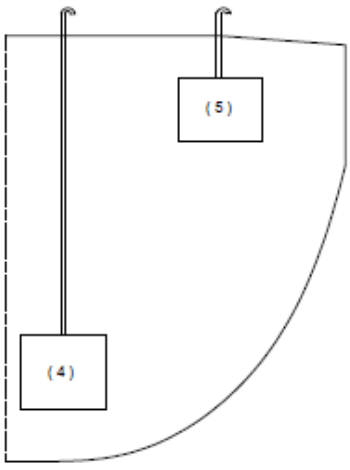

Figure.2-5 Section in engine room

- For strength members located less than 0.25 b_b away from longitudinal wash bulkheads and tank sides the pressure shall not be taken less than:

$$p = \rho [3-B/100] b_b \ [KN/m^2] \quad (15)$$

The minimum sloshing pressure on web frames and girder panels in cargo and ballast tanks, except ballast tanks in double side and double bottom, shall be taken as 20 kN/m^2 .
In double side and double bottom ballast tanks the minimum sloshing pressure shall be taken as 12 kN/m^2.
In long or wide tanks with many web frames or girders the sloshing pressure on the frames or girders near to the wash or end bulkheads shall be taken as:
For web frames:

$$P = p_{bhd} (1-s/l_s)^2 \qquad [KN/m^2] \quad (16)$$

For longitudinal girders:

$$P = p_{bhd} (1-s/b_s)^2 \qquad [KN/m^2] \quad (17)$$

2.7.3. Sloshing pressure

For strength members located less than 0.25 ls away from transverse wash and end bulkheads the pressure shall not be taken less than :

$$p = 7\rho \ g_0 \ k_f (bs/B - 0.3) \ GM^{0.75} \quad [KN/m^2] \quad (18)$$

$$k_f = 1.2 (0.7 - h/H)^2 \ , \ (h/H)_{max} = 1 \quad (19)$$

2.7.4 Dry cargoes, stores, equipment and accommodation

The pressure on inner bottom, decks or hatch covers shall be taken as:

$$p = \rho (g_0 + 0.5 a_v) H \ [kN/m^2] \quad (20)$$

This pressure in calculated manually to deduce on the loads applied in the deck.

2.8. Longitudinal strength

In this section the requirements regarding the longitudinal hull girder scantlings with respect to bending and shear are given.
These values are applied when determining the section modulus and the shear area of the hull girder and in connection with control of buckling and ultimate strength. Reduced values will have to be used when considering combined local and longitudinal stresses in local elements,

2.8.1. Still water bending moment and shear force

The design still water bending moments, M_S, and still water shear forces, Q_S, shall be calculated along the ship length for design cargo and ballast loading conditions.

For these calculations, downward loads are assumed to be taken as positive values, and shall be integrated in the forward direction from the aft end of L.

- **Bending moments**

The design still water bending moments amidships (sagging and hogging) are:

Sagging

$$M_{SO} = -0.065\, C_{WU}\, L^2\, B\, (C_B + 0.7)\ (kNm) \qquad (21)$$

Hogging

$$M_{SO} = C_{WU}\, L^2\, B\, (0.1225 - 0.015\, C_B)\ (kNm) \qquad (22)$$

$C_{WU} = C_W$ for unrestricted service.

When required in connection with stress analysis or buckling control, the stillwater bending moments at arbitrary positions along the length of the ship are normally not to be taken less than:

$$M_S = k_{sm}\, M_{SO}\ (kNm) \qquad (23)$$

k_{sm} = 1.0 within 0.4 L amidships

= 0.15 at 0.1 L from A.P. or F.P.

= 0.0 at A.P. and F.P.

Between specified positions k_{sm} shall be varied linearly. Values of k_{sm} may also be obtained from fig.2-6.

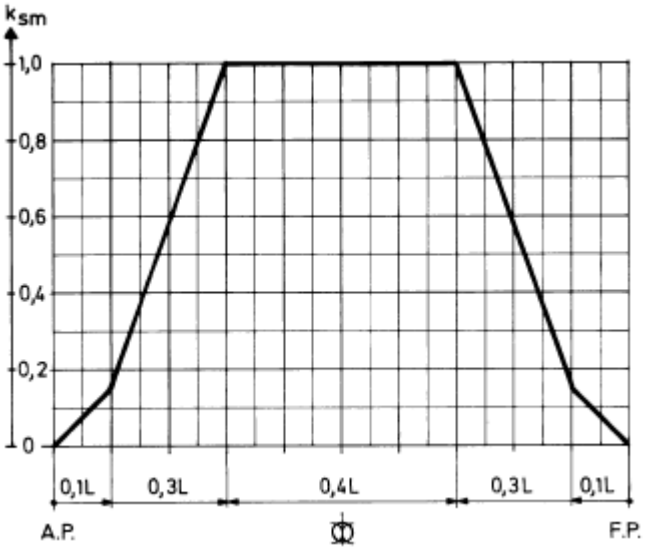

Figure.2-6 Stillwater bending moment

- **Shear forces**

The design values of still water shear forces along the length of the ship are normally not to be taken less than:

$$Q_S = k_{sq}\, Q_{SO} \quad [kN] \tag{24}$$

$$Q_{SO} = 5\, M_{SO}/L \; [KN] \tag{25}$$

k_{sq} = 0 at A.P. and F.P.

= 1.0 between 0.15 L and 0.3 L from A.P.

= 0.8 between 0.4 L and 0.6 L from A.P.

= 1.0 between 0.7 L and 0.85 L from A.P.

2.8.2. Wave bending moment and shear force

- **Bending moment**

The rule vertical wave bending moment amidships is presented in figure2.7 and given by:

$$M_W = M_{WO} \text{ (kNm)} \tag{26}$$

Sagging

$$M_{WO} = -0.11\, \alpha\, C_W\, L^2\, B\, (C_B + 0.7) \text{ (kNm)} \tag{27}$$

Hogging

$$M_{WO} = 0.19\, \alpha\, C_W\, L^2\, B\, C_B \text{ (kNm)} \tag{28}$$

α= 1.0 for seagoing conditions

= 0.5 for harbour and sheltered water conditions (enclosed fjords, lakes, rivers).

When required in connection with stress analysis or buckling control, the wave bending moments at arbitrary positions along the length of the ship are normally not to be taken less than:

$$M_W = k_{wm}\, M_{WO} \text{ (kNm)} \tag{29}$$

k_{wm} = 1.0 between 0.40 L and 0.65 L from A.P

= 0.0 at A.P. and F.P.

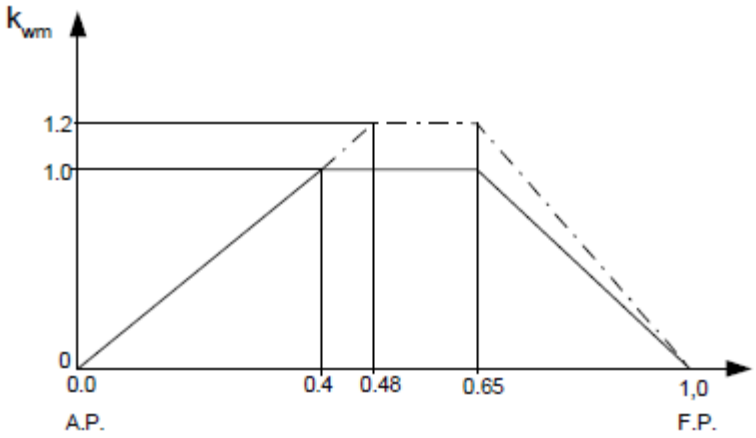

Figure.2-7 Wave bending moment distribution

- **Shear forces**

The rule value of vertical wave shear forces along the length of the ship is presented in fig.2-8 and given by:

Positive shear force, to be used when positive still water shear force:

$$Q_{WP} = 0.3\ \beta\ k_{wqp}\ C_W\ L\ B\ (C_B + 0.7) \qquad [kN] \qquad (30)$$

Negative shear force, to be used when negative still water shear force:

$$Q_{WN} = -\ 0.3\ \beta\ k_{wqn}\ C_W\ L\ B\ (C_B + 0.7) \qquad [kN] \qquad (31)$$

Positive shear force when there is a surplus of buoyancy forward of section considered.

Negative shear force when there is a surplus of weight forward of section considered.

β = 1.0 for seagoing conditions

= 0.5 for harbour and sheltered water conditions (enclosed fjords, lakes, rivers)

k_{wqp} = 0 at A.P. and F.P.

= 1.59 CB/(CB + 0.7) between 0.2 L and 0.3 L from A.P.

= 0.7 between 0.4 L and 0.6 L from A.P.

= 1.0 between 0.7 L and 0.85 L from A.P.

k_{wqn} = 0 at A.P. and F.P.

= 0.92 between 0.2 L and 0.3 L from A.P.

= 0.7 between 0.4 L and 0.6 L from A.P.

= 1.73 CB/(CB + 0.7) between 0.7 L and 0.85 L from A.P.

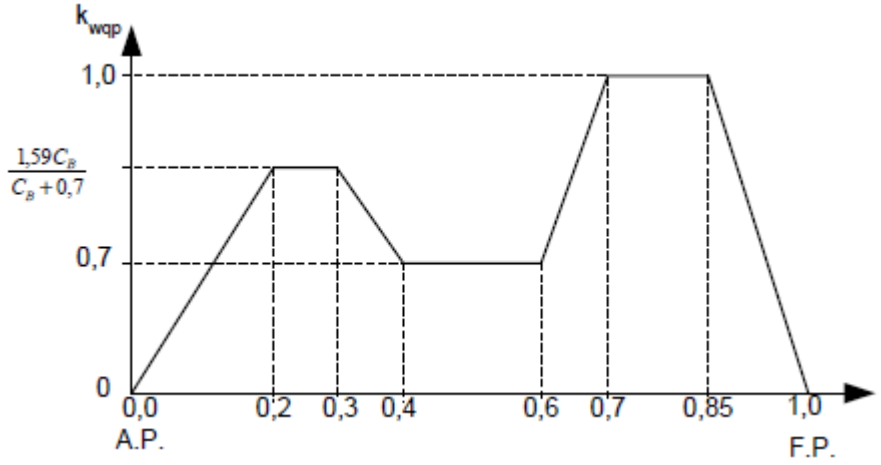

Figure.2-8 Wave shear force distribution

2.8.3. Horizontal wave bending moment

The rule horizontal wave bending moments along the length of the ship are given by:

$$M_{WH} = 0.22\ L^{9/4}\ (T + 0.3\ B)\ C_B\ (1 - \cos(360\ x/L)) \quad (32)$$

x = distance in m from A.P to cross section.

2.8.4. Wave torsional moments

The rule wave torsional moments along the length of the ship due to the horizontal wave- and inertia forces and the rotational wave- and inertia moment loads are given by:

$$M_{WT} = K_{T1}\ L^{5/4}\ (T + 0.3\ B)\ C_B\ z_e \pm K_{T2}\ L^{4/3}\ B^2\ C_{SWP} \quad (33)$$

$K_{T1} = 1.40 \sin(360\ x/L)$

$K_{T2} = 0.13\ (1 - \cos(360\ x/L))$

$C_{SWP} = A_{WP}/(LB)$

3. STRUCTURAL DESIGN OF SELF-UNLOADING MINING SHIP

3.1. Nauticus Hull DNV software

3.1.1. General

Is an autonomous and independent foundation with the objectives of safeguarding life, property and the environment, at sea and onshore. DNV undertakes classification, certification, and other verification and consultancy services relating to quality of ships, offshore units and installations, and onshore industries worldwide, and carries out research in relation to these functions.

DNV Software is commercial software owned by DNV classification society, and is a leading provider of software for managing risk in oil & gas, offshore, petrochemical, refineries and maritime industries. DNV software products are recognized market leaders in design, engineering, strength assessment, risk and reliability, safety and integrity management.

Nauticus Hull is DNV's software solution for strength analysis of ships and FPSOs. It offers all the programs required for hull design and verification according to DNV rules for ships and FPSOs and IACS common structural rules. Based on DNV's strong industry knowledge and expertise, the system provides a highly efficient environment for design and verification.

Already in use by more than 200 shipyards and ship design offices around the world.

3.1.2. Section scantling

Section scantling is well established as the market leader for hull scantling design. It is used for designing ship cross-sections. A rule check can be performed to verify the hull girder longitudinal strength, local strength and buckling of plates and stiffeners. Shear flow calculations are also included in the program. The model data defined by section scantlings may later be expanded into 3D finite element models.

3.1.3. Fatigue strength

Fatigue calculations of longitudinal are done directly from the section scantlings program. Structural data such as stiffener dimensions, end connection and bracket geometry are all input in the section scantlings program and used to calculate the fatigue strength. As a result of this, user interaction is reduced to a minimum and results are presented directly in the section scantlings report.

3.1.4. Rule Check XL

Together with section scantlings, rule check XL provide all features needed to carry out rule check and hull structural analysis according to the DNV Rules for Ships and the IACS common

structural rules. The rule check XL programs are all fully integrated into the Nauticus Hull system and share common ship data with the other Nauticus Hull modules.

3.1.5. 3D Beam software

The 3D Beam module is a highly efficient three-dimensional general beam element analysis program offered in the rule check extended package. 3D Beam program is an important supplement to the rule check programs and a valuable tool for strength evaluation of both ship and frame structures. (DNV, 2013)

3.2. Material designation and properties

The hull material used is NV-NS denotes normal strength structural steel with yield point not less than 235 N/mm^2.The material factor f_1 included in the various formulae for scantlings and in expressions giving allowable stresses, is dependent on strength group.

In ships intended to operate for longer periods in areas with low air temperatures (i.e. regular service during winter to Arctic or Antarctic waters), the materials in exposed structures will be specially considered.

In important structural cross-joints where high tensile stresses are acting perpendicular to the plane of the plate, special consideration will be given to the ability of the plate material to resist lamellar tearing. Aluminum alloy for marine use may be applied in superstructures, deckhouses, hatch covers, hatch beams and sundry items, provided the strength of the aluminum structure is equivalent to that required for a steel structure. (DNV, 2012)

The majority of ships operating today are built of mild steel. High tensile steel has been used in shipbuilding, but its recent popularity is due to the fact that plates can be thinner without losing any strength. Whereas a normal side plate will be 25-30mm thick, this can be reduced to 18mm by using HT steel. The weight saving which might amount to several thousand tons cuts building costs and also enables the ship to carry more cargo.

The high tensile steel HTS ships need at least as much care and maintenance as those build of mild steel, especially as they too are frequently subject to greater stresses in cargo loading and unloading than was originally envisaged.

Regarding the current new project of self-discharging mining ship, the entire structural ship is made of NV-NS denotes normal strength structural steel, except for some equipements in the deck panel which are made of aluminum alloy; the steel has the following characteristics:

Yield stress σ_y = 235 N/mm^2

Young modulus E=206000 N/mm^2

Strain hardening parameter; C = 825 MPa

Poisson's ratio ν = 0.3.

3.3. Structural design concept

The self-unloading mining ship is designed with a configuration of bulk carrier: double hull, flat bow, round bilge and 8 cargo holds four on each board with a “V” shaped cross section.

Two conveyors belts are installed in the tunnel below the holds for both ship’s boards.

The double bottom consisting of ballast tanks, upper and lower wing tanks for ballast with wing ballast tanks located outboard, the fuel occupy the spaces created by the shape of the holds in the ship centerline and a fresh water tank in top center.

The structure includes main and tween deck, longitudinal bulkheads, transvers frames and in addition to side stringers and cofferdams. Some transversal stiffeners are fixed in the bottom to support the cargo holds load in addition to side and center girder to ensure more reinforcement of the hull structure.

The large length of bulk carrier 227 m requires longitudinal stiffening system; the longitudinal framing system resistes to longitudinal bending, load produced by distributed hull weight, cargo weight, self-unloading and mining system, buoyancy force and wave force.

This system has more resistance to the buckling stress than the transversal system and it’s complicated to produce, from economical point of view , the drawback of longitudinal system is that it requires high costs. The proposed cross section design is introduced in fig.3-1.

A scantling requirements details with all input and output data are presented in the report given by Nauticus Hull software Annex. A1. For global scantling results refer to Appendix A1.

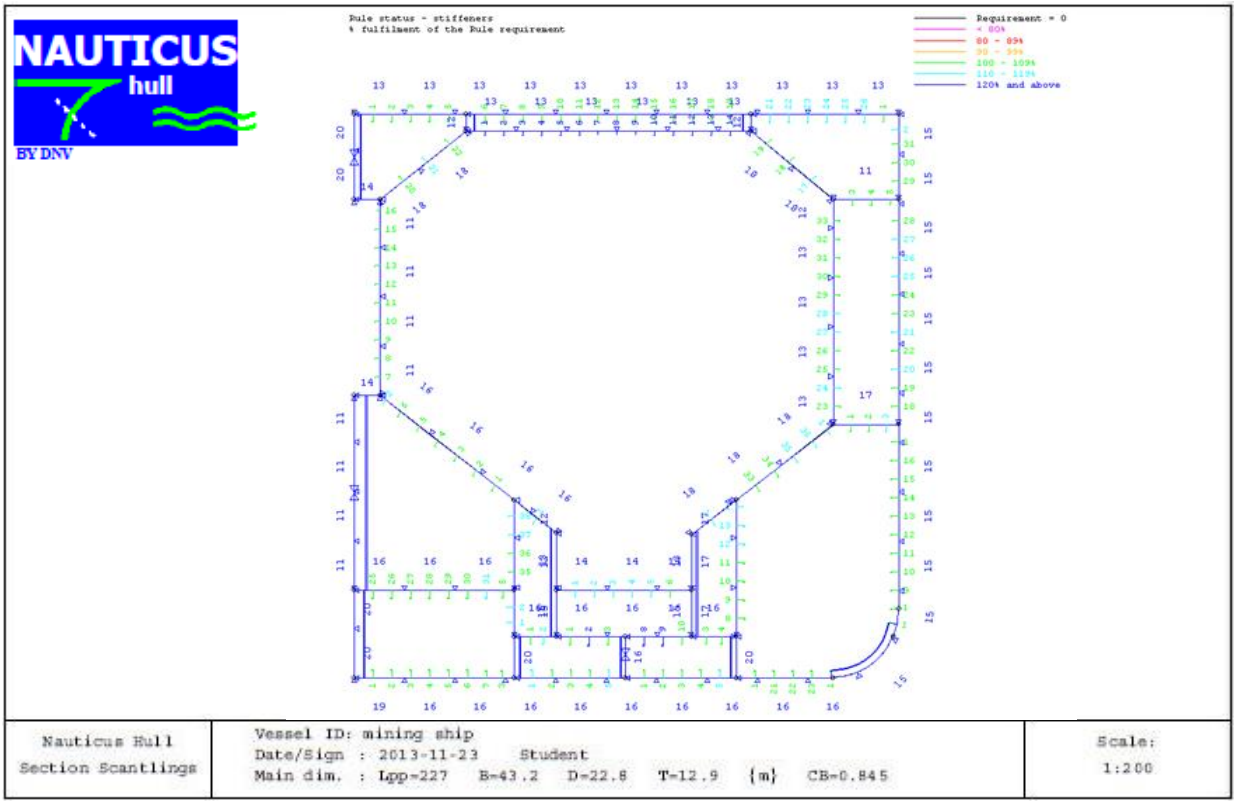

Figure.3-1 Structural design of cross section (105 m from AP) using Nauticus Hull

3.3.1. Ship structure details

- **Deck**

The deck structure is longitudinally stiffened and transversally framed with 13 mm thickness, it contains in fore part a deckhouse with helicopter landing platform, In addition to a crane and a boom for conveying the cargo to the shuttle vessel or to harbor both fixed in the aft ship.

A mining lifting system is installed in the amid ship which requires more reinforcement in this area. The main deck is large containing eight hatch covers; the size of the hatch covers is limited by the amount of steel necessary in the deck to resist wracking.

- **Double bottom**

The ship bottom is also longitudinally stiffened with 16 mm thickness and 19 mm in the centerline below the center girder to ensure more reinforcement to the load resulting from the mining lifting system (mining riser) installed in the midship section.

- **The cargo hold**

The cargo hold structure with topside tanks at both shoulders and double bottom arrangements with bilge hoppers at both wings has been designed as the best structure for mining bulk cargo transportation. Each hold is accessed through a large hatch that is closed watertight with a hatch cover. Coal and light bulk cargoes are stowed in every cargo hold. Iron ore, however, is usually shipped in alternate cargo holds because of its high specific gravity.

This is done for the purpose of avoiding excessively stiff ship motion and also for the convenience of loading facilities.

- **Topside and hopper tanks**

The topside and bilge hopper tanks compose a double hull surrounding the cargo space, which together with the double bottom provides hull strength and rigidity. Double hulled side shells provided with individual transverse frames are located between the topside and bilge hopper tanks. The shape of topside tanks provides sufficient stability to prevent dangerous cargo shift and bilge hoppers contribute to convenience in collecting the cargoes on discharge.

A cut out is designed with transvers stiffeners for both bottom ballast tank , the heavy fuel tank and the fresh water tank in the top centerline to ensure the stability of the bulk carrier ship, and reduce the free surface effect.

- **Longitudinal bulkheads**

Longitudinal bulkheads are typically corrugated with upper and lower stools that follow the hoppers. While the longitudinal structure provides to the vessel a global resistance to bending moment loads, it is the longitudinal bulkheads that will experience the localized loading of the static weight of cargo or any sloshing loads associated with ballast or accidental flooding.

- **Longitudinal stiffeners**

The longitudinal stiffeners are of HP bulb profile with various dimensions respecting DNV standards used in Nauticus Hull package.

The long bulk carrier requires the use of longitudinal stiffeners, fixed on the deck, the side shell and bottom, along the tanks and the hold cargo, also in both sides of the two longitudinal bulkheads supporting the hold.

- **Transvers stiffeners**

The transvers stiffeners used are flat bar profile fixed in the bulkheads below the holds in both sides of the machinery space for more reinforcement of the hull structure. Other traversal stiffener designed in the round bilge area for more transversal reinforcement of the hull because of the large bulk carrier.

Two transvers stiffeners are designed between the cargo hatches and the deck to ensure more support to the loads.

- **Longitudinal girders**

Girder provided in double-bottom tanks usually indicates a strong frame, usually with the full depth, provided in ship's longitudinal direction. For the center line, a longitudinal center girder is fixed along the bottom of the ship to resist to the bending moment for both sagging and hogging conditions. To avoid the free surface effect, ballast tank and center girder divide the ballast tank into two tanks. Two longitudinal side girders are fixed in the bottom ballast tank to support the heavy hold loads.

- **The conveyor belt system**

The void space formed between the underside of these hoppers and the double bottom tank top along the length of the ship is called the 'tunnel'. Two conveyors belt run in the tunnel along the ships length, and fed by cargo through the 'gates'. Gravity is utilised and the flow of cargo is controlled; governed by the load on the belt. The cargo is then lifted up vertically (loop or elevator lifts) or by gradual inclines and is transferred to the ships boom.

The boom is an extended structure with freedom of direction situated on the main deck , and encases the boom belt,it unloads nodules at any point up to 35 m from the ship's sides(to the shuttle vessel or shore terminal).

The selection of two convoyors belts is to ensure the efficiency and gain time during the unloading operations of self-unloading system in this new mining ship project.

3.3.2. Main data of the mining ship

The main data of self-unloading mining ship described in section1.3.are presented in table.3-1.

Table.3-1 Main data of the designed mining ship

Item	Magnitude	Unit
Length between perpendiculars L_{bp}	227	[m]
Rule length ,L	220.19	[m]
Breadth moulded ,B	43.2	[m]
Depth moulded, D	22.8	[m]
Draught moulded ,T	12.9	[m]
Block coefficient, C_b	0.845	[m]
Min.design draught at AP	8	[m]
Min.design draught at FP	8	[m]
Waterplane area coefficient ,C_{wp}	0.950	-
Area of the waterplane	9352	[m^2]
Maximum service speed, V	15	[knots]

3.3.3. Cross section identification

The presence of the lifting system (riser) in the amidship section, makes the design more complex (unknown dimensions), The cross section that is taken as a reference for the assessment of hull structure strength is frame 140 within the frame 120 and frame 160, 105 m starting from Aft part of the ship (stern).The location cross section is well shown in figure.3-2.

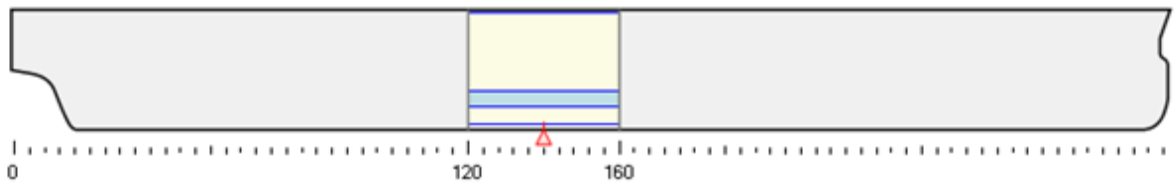

Figure.3-2 Actual position of cross section, 105 m from AP

3.3.4. Compartment loads

The ship's structure is designed to withstand the static and dynamic loads likely to be experienced by the ship throughout its service life.

On designing a mining self-unloading bulk carrier, loading patterns and sequences reflecting the specific gravities of intended cargoes and ballasting patterns in various operation modes are taken into consideration.

Regarding local loads, external (hydrostatic and hydrodynamic) pressures and internal (static and inertial) pressures are considered as lateral loads in still water and in waves.

The internal static pressures are induced by the weights carried, while the internal inertial pressures are induced by the accelerations on the masses.

The loads acting on the hull structure when the ship is floating in (calm) water are:

Static loads from the weight of the vessel and the corresponding buoyancy is well understood. These loads are imposed by the:

- Actual weight of the ship's structure, outfitting, equipment and machinery(Engines, lifting system and self-unloading system;
- Cargo load (weight);
- Ballast load assigned for the carriage of salt water ballast;
- Hydrostatic pressure (sea water pressure acting on the hull).

The different compartments in the designed cross section are shown in figures (fig.3-3, fig.3-4).

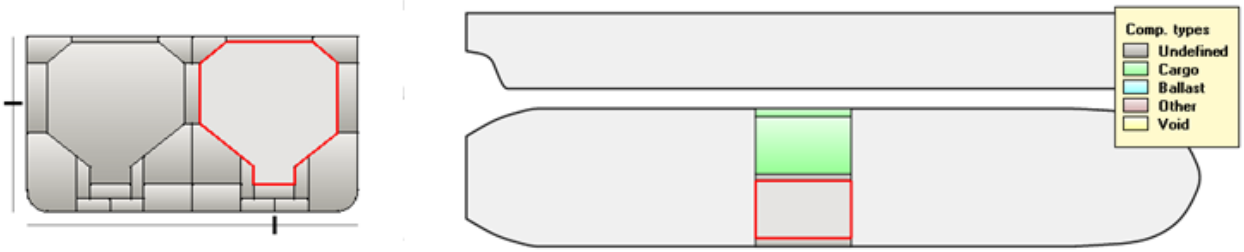

Figure.3-3 Compartments and loads for self-unloading mining ship

Dynamic loads are those additional loads exerted on the ship's hull structure through the action of the waves and the effects of the resultant ship motions (acceleration forces, slamming and sloshing loads).

Sloshing loads may be induced on the ship's internal structure through the movement of the fluids in tanks /holds with slamming of the bottom shell structure forward may occur due to emergence of the fore end of the ship from the sea in heavy weather.

Cargo over-loading in individual hold spaces will increase the static stress levels in the ship's structure and reduce the strength capability of the structure to sustain the dynamic loads exerted in adverse sea conditions.

Table.3-2 shows more details about load distribution of water ballast, Heavy fuel oil tank, Fuel oil tank and Fresh water tank with various pressures and density, in addition to the gravity center of each compartment.

Basically, the density of nodules is changing from abt. 2 t/m^3 to 3.5 t/m^3 in slurry. This results in stowage factor of 0.28 - 0.5 m3/t and this is a typical range for iron ore.

Table.3-2 Bulk cargo and liquid loads for self-unloading mining ship

Ref	compartment category	Load type	Density t/m^3	Volume (m^3)	Pressure valve setting (KN/m^2)	Centre of gravity(m)		
						From A.P x	From CL y	Above baseline z
1	WB	Water ballast	1.025	469.5	15	105	19.207	21.306
2	WB	Water ballast	1.025	1354.7	15	105	0	1.775
3	Void space	Heavy fuel oil tank	0.9	2331.4	25	105	0	6757
4	Void space	Fresh water tank	1.025	634.3	25	105	0	21.431
5	Void space	Fuel oil tank	0.95	494.2	25	105	0	15.39
6	WB	Water ballast	1.025	440.9	15	105	10.76	0.835
7	WB	Water ballast	1.025	1761.7	15	105	18.469	4.83
8	WB	Water ballast	1.025	706.3	15	105	20.305	14.805
9	Void space	Machinery space	-	301.2	-	105	10.7	2.61
10	Void space	Bulk cargo hold	1	7911.4	-	105	10.22	14.082
11	Void space	-	-	260.1	-	105	14.309	4.109
12	Void space	-	-	243.6	15	105	7.157	4.116
13	Void space	-	-	227.5	-	105	10.09	22.465

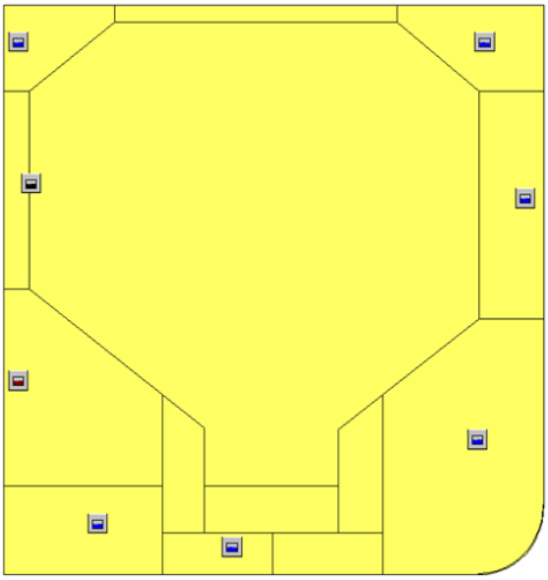

Figure.3-4 Cross section compartments and loads

3.3.5. Deck loads

Careful planning is required in the loading of self-unloading mining ship. Not only it is critical that the final departure condition be sound, but how the ship is loaded and offloaded is very important for a successful operation.

At ocean, the self-unloading mining ship is subject to both static and dynamic loading.

Classification societies (BV, DNV, GL, and LR) often define structural requirements as a function of static loading with a margin for dynamics in the form of allowable still water shear force and bending moment.

The main loads acting on the self-unloading mining ship is the load of lifting system when launching or towing the whole riser from the seafloor and the loads of the helicopter, the crane and the boom of self-unloading system when transferring the nodules and minerals received from the conveyors installed in the ship.The tank loads are defined by the density of the fluid.

The load acting on the deck is taken in the range of the maximum load calculated manually according to DNV rules,(2012) by applying the next formula :

$P_1=a(p_{dp}-(4+0.2k_s))h_0$

The different loads applied are presented in table.3-3.

Table.3-3 Loads applied on the deck of the self-unloading mining ship

Load No	Stowage rate ,ro (t/m^3)	Stowage height , H (mm)	Extent (distance from CL)		Panel
			Y_1 (mm)	Y_2 (mm)	
1	12	1000	0	4430	Deck
2	12	1000	4430	15750	Deck
3	12	1000	15750	21600	Deck

3.3.6. Calculation of input parameters used for the scantling

The designed cross section is located within 0.4 L from ship stern, the applied formulas are the same as for amid ship section.

The total results of the manual calculations applying DNV rules are presented in table.3-4.

- **Still water bending moment**

The extreme still water bending moment (M_{SW}) may be taken as the maximum value of the still water bending moments resulting from the worst load condition for the ship, considering both hogging and sagging.

The design still water bending moment, M_S, and still water shear forces, Q_S, shall be calculated along the ship length for design cargo and ballast loading conditions.

- **Wave coefficient C_W**

For $100 < L < 300$ $C_W = 10.75 - [(300 - L)/100]3/2$

C_W= 10.12

Sagging $M_{SOS} = -0.065\, C_{WU}\, L^2\, B\, (C_B + 0.7)$

M_{SOS}= -2262339.7 KNm

Hogging $M_{SOH} = C_{WU}\, L^2\, B\, (0.1225 - 0.015\, C_B)$

M_{SOH}= 2474099.6 KNm

- **Still water shear force**

The design value of Stillwater shear force along the length of the ship is:

$$Q_S = k_{sq}\, Q_{SO}$$

$$Q_{SO} = \frac{M_{SO}}{L}$$

K_{sq}= 0.8 between 0.4 L and 0.6 L from A.P.

Q_S= 39865 KN

- **Wave bending moment**

The prediction of the behavior of the ship in waves represents a key point in the quantification of both global and local loads acting on the ship.

The design minimum wave-induced bending moment M_{wv} is normally taken as the mean value of the extreme wave-induced bending moment that the ship is likely to encounter during its lifetime, the rule vertical wave bending moment amidship is:

Sagging $M_{WO} = -0.11\, \alpha\, C_W\, L^2\, B\, (C_B + 0.7)$

α = 1 for seagoing conditions

M_{WOS} = -3828574.8 KNm

Hogging $M_{WO} = 0.19\, \alpha\, C_W\, L^2\, B\, C_B$

M_{WOH} = 3616814.9 KNm

- **Wave shear force**

The rule values of vertical wave shear force along the length of the ship

$$Q_W = 0.3\, \beta\, k_{wqp}\, C_W\, L\, B\, (C_B + 0.7)$$

β = 1 for seagoing conditions

k_{wqp} = 0.7 between 0.4 L and 0.6 L from A.P.

Q_W = 32198.6 KN

- **The horizontal wave bending moment**

The rule M_{WH} along the length of the ship is:

$$M_{WH} = 0.22\, L^{9/4}\, (T + 0.3\, B)\, C_B\, (1 - \cos(360\, x/L))$$

x = distance in m from A.P. to the section (frame 140).

M_{WH} = 1518129.37 KNm

Table.3-4 Total results of the hand calculations

	Still water		**waves**	
	Sagging	Hogging	Sagging	Hogging
Bending moment (KNm)	-2262339.7	2474099.6	-3828574.8	3616814.9
Shear force (KN)	39865		32198.6	
Horizontal wave bending moment (KNm)	1518129.37			

3.4. Scantling description

The self-unloading mining bulk cargo is double hull ship, the reference cross section is located in frame 140 (105 m AP) within frame 120 and frame 160.

The scantling is done with respect to DNV standards for the minimum ship members dimensions (plates , longitudinal stiffeners, transvers stiffeners , bulkheads, stringers, girders) The structural design should be optimized several times with new dimensions (thiknesses , webs , flanges, depth , width..), the results are given by Nauticus Hull software after runing the calculation to arrive to the optimum scantling with less ship weight.

The structure is longitudinally stiffened with 750 mm spacing and transversely framed, the span between regular frames is 750 mm and 3000 mm for main frames, with round bilge hull form and 8 holds**.**

For more scantling details see figure.3-5 which presents a global cross section of the designed bulk cargo ship. Or refer to Nauticus Hull report in Annex.A1 in the electronic version of this master thesis.

A detailed description of the scantling is presented in table.3-5.

Table.3-5 Main particulars and structural data of the ship hull describing the scantling.

Material	NV-NS denotes normal strength structural steel			
Yield stress [Mpa]	235			
Items [mm]	**Magnitudes for different panels**			
	Deck	**Shell**	**Bottom**	**Bulkheads**
Plate thickness	13	15	16	11/20
Web frames				
Span (main frames)	3000	3000	3000	
Thickness (t)	13	15	16	
spacing(regulars frames)	750	750	750	
Longitudinal Stiffeners HPbulb profil				
Web thickness (t)	13	11/12	12/13	10/12
Web depth (h)	300	280/320	320/340	200 /340
Spacing (S)	750	750	750	750
Transversal Stiffeners Flat bar profil				
Web thickness (t)	14	13	12/20	11/14
Web depth (h)	340	320	232/500	240/340
Span	3450	2995	1669	670/2318
Cut out breadth (b)	200/600			

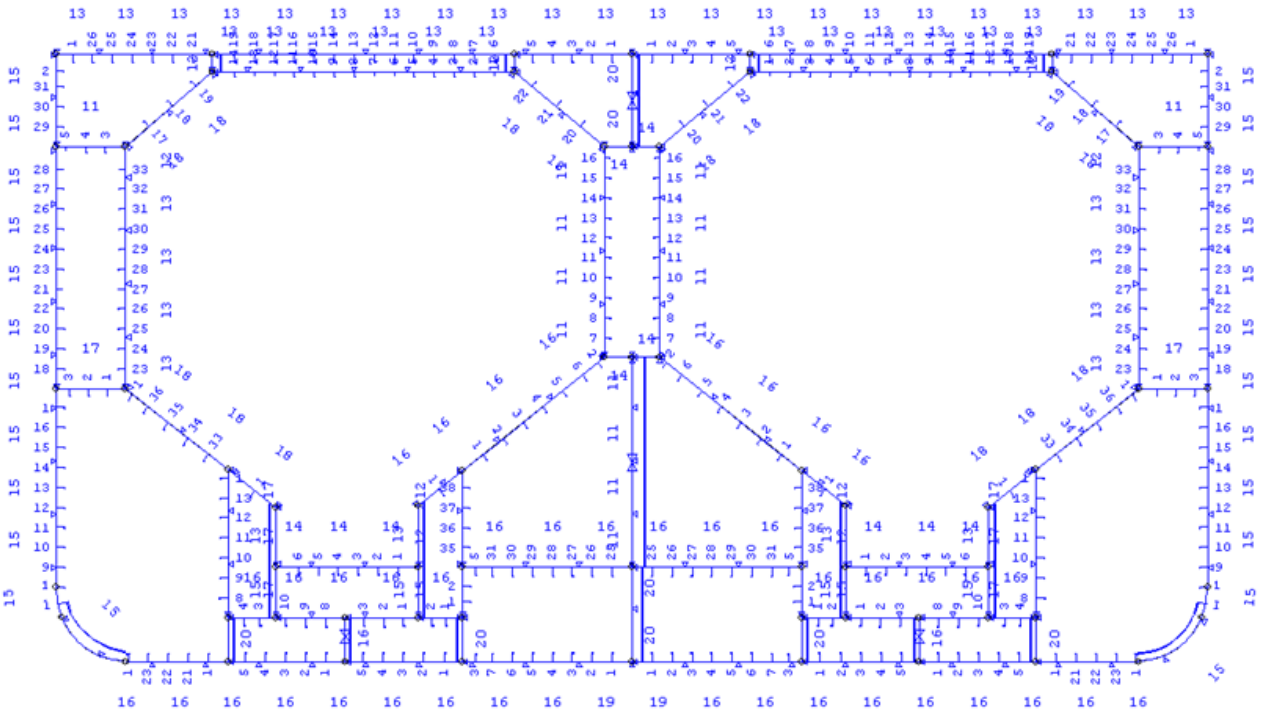

Figure.3-5 Detailed scantling of cross section using Nauticus Hull software

3.5. Results from Nauticus Hull software

The distributions of vertical and horizontal bending moments and shear forces given by Nauticus Hull package for still water and wave sea state, are presented in figures (Fig.3-6, Fig.3-7, Fig.3-8, Fig.3-9, Fig.3-10, Fig.3-11, Fig.3-12,Fig.3-13).

From the results , it is necessary to note that:

- A thickness reduction in the bottom plating largely affects the hogging strength, while a thickness reduction in the deck plating largely reduces the sagging strength.
- The ultimate sagging capacity in intact and damaged bulk carrier vessels is considerably less than the ultimate hogging capacity.
- Damages in upper side shell and deck structures subject to in-plane compressive loading reduce the residual strength substantially in sagging condition.
- For bulk carriers in the hogging condition, the stresses of deck elements reach the material yield stress point first and then the bottom structure approaches the critical stress point in the yield zone of that material, with the increasing of ship hull girder curvature.
- Stiffeners do not have much torsional rigidity and tripping stress is lower than beam column stress of the stiffener with associated plate. This fact leads to more reduction of the ultimate bending moment in sagging compared with the moment in hogging, where the bottom is in tension.

- For the collision damage scenarios, the safety index is greater in the hogging condition than in the sagging condition. It means that collision damage to the topside has more effect on the decrease of ultimate strength in the sagging state than in hogging state.
- Because of the large bulk carrier studied, it is subjected to horizontal bending moment which has significant influence on the lateral ship structure.
- For still water sea state, the vertical bending moment is minimum for sagging and hogging condition in the amid ship area and zero for aft and fore ship. See figures (Fig.3-6, Fig3-7)
- For wave sea state, the vertical bending moment is maximum for hogging condition in the amid ship and zero in both aft and fore ship. See figures (Fig.3-8, Fig.3-9).
- Wave horizontal bending moment reaches its maximum value in the amid ship while its zero for ship's extremities. See fig.3-10.

The design values of bending moments are shown in tables (tab.3-6,tab3-7) for amidship and cross section (105 m AP).

Table.3-6 Design bending moments at amid ship.

Amidship	**Sagging (kNm)**	**Hogging (kNm)**
Still water bending moment standard according to rules, M_{SO}	2111178	2308789
Design still water bending moments, M_S	2262340	2474100
Design wave bending moments, M_W (input)	3828575	3616815
Horizontal wave bending moment according to rules, M_{WH}	1795695	

Table.3-7 Design bending moments at actual position (105 m from AP)

Frame 140 (105 m from AP)	**Sagging (kNm)**	**Hogging (kNm)**
Still water bending moments standard according to rules, M_S	2111178	2308789
Design still water bending moments, M_S (input)	2262340	2474100
Design wave bending moments, M_W (input)	3828575	3616815
Design wave bending moments, M_W for buckling check input	3983033	3616815
Horizontal wave bending moment according to rules, M_{WH}	1744383	

3.5.1. Bending moment distribution

The Figures present the vertical and horizontal bending moment and shear force for both sagging and hogging condition given by Nauticus Hull software with respect to DNV rules.

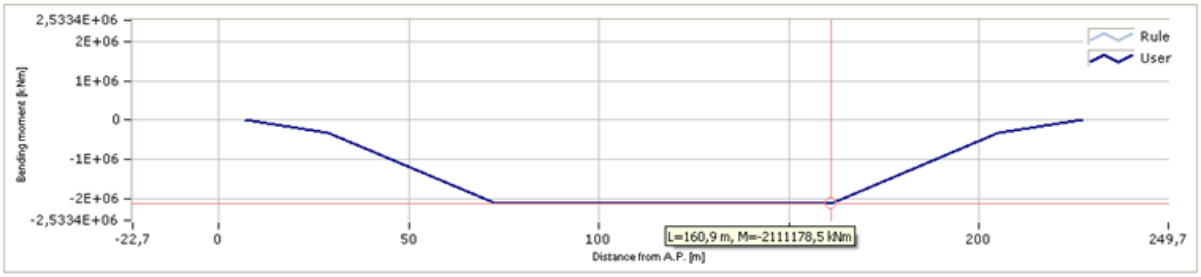

Figure.3-6 Still water bending moment (Sagging)

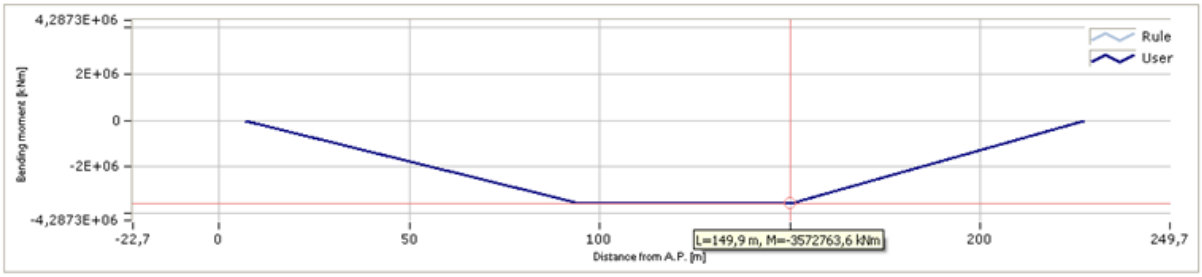

Figure.3-7 Still water bending moment (Hogging)

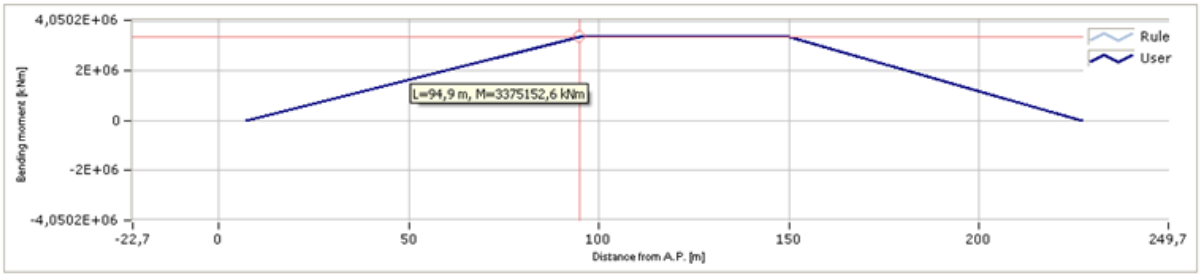

Figure.3-8 Wave bending moment (Sagging)

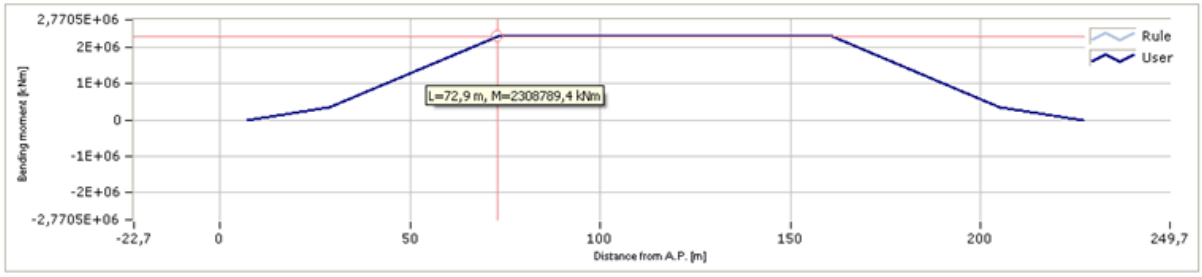

Figure.3-9 Wave bending moment (Hogging)

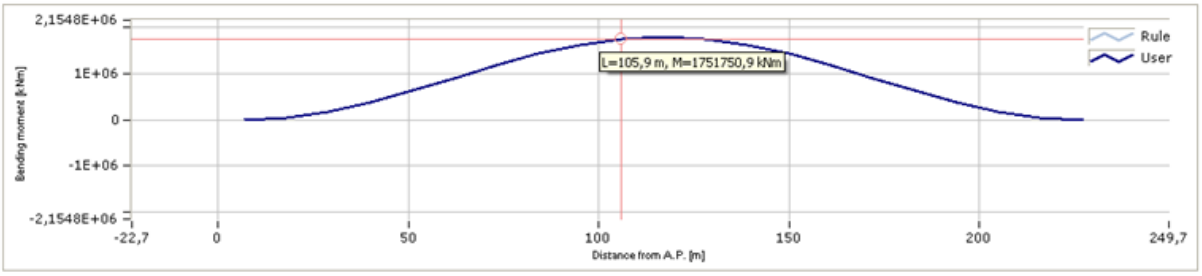

Figure.3-10 Wave horizontal bending moment

3.5.2. Shear force distribution

For sagging and hogging sea conditions, wave shear force is in accordance with DNV rules .see figures (Fig.3-12, Fig.3-13)

Shear force distribution varies according to the cargo load pattern in the self-unloading mining ship , Nauticus Hull software gave zero for still water sea state , may be because of the small value of shearing when the mining ship is in the harbor. The manually calculations and graphs show a negative shear force for hogging condition and positive in sagging condition.

- The still water shear force distribution is given by Nauticus Hull DNV software as zero in the graph because of its minimum value. see fig.3-11.

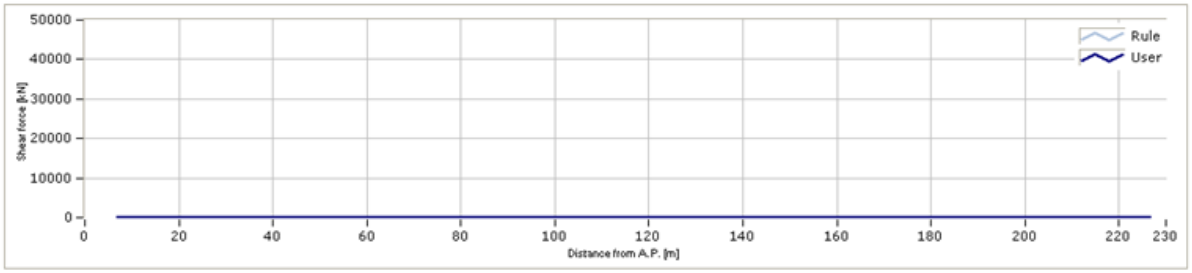

Figure.3-11. Still water shear force

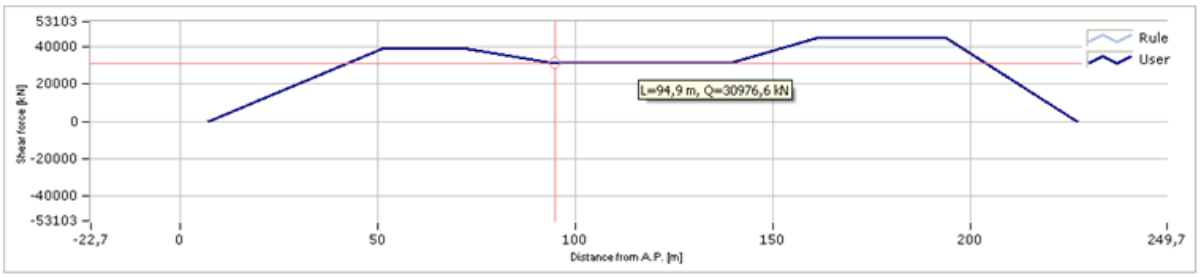

Figure.3-12 Wave shear force (Sagging)

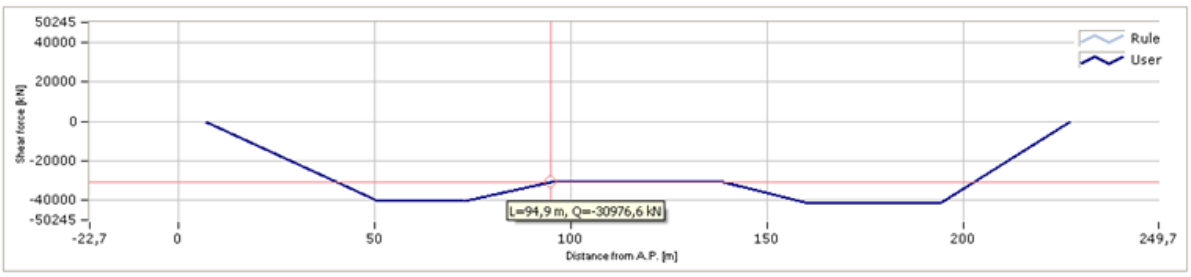

Figure.3-13 Wave shear force (Hogging)

3.5.3. Global design stresses

The yield strength of the material σ_{yield} is defined as the measured stress at which appreciable nonlinear behavior accompanied by permanent plastic deformation of the material occurs.

The ultimate strength is the highest level of stress achieved before the test specimen fractures. For most shipbuilding steels, the yield and tensile strengths in tension and compression are assumed equal.

The margin against yield failure of the structure is obtained by a comparison of the structure's Von Mises equivalent stress, σ_e, against the permissible stress (or allowable stress), σ_0, giving the result:

$$\sigma_e \leq \sigma_0 = f_1 \times \sigma_y$$

σ_e : Von Mises equivalent stress $\sigma_e = (\sigma_x^2 + \sigma_y^2 - \sigma_x \sigma_y + 3\tau^2)^{1/2}$

f_1 : partial safety factor defined by DNV classification societies, which depends on the loading conditions and method of analysis.

$f_1 = 1$ for NV-NS denotes normal strength steel used in the structural design of the self-unloading mining ship.

$\sigma_{yield} = 235$ N/mm^2 : minimum yield point of the mild steel.

According to DNV rules:

- Equivalent stress for NV-NS should be less than $\sigma_{e\ max} = 205$ N/mm^2
- Nominal stress for NV-NS $\sigma_{max} = 190$ N/mm^2
- Shear stress for NV-NS $\tau_{max} = 110$ N/mm^2

➢ The longitudinally continuous upper deck of a bulk carrier suffers hull girder stress. The longitudinal bending causes an axial force on the upper deck that may cause cracking of the deck plate at the locations where the stress is concentrated.

The designed vessel is subjected to high double bottom stresses therefore plating is built with increased thickness.

➢ From scantling, combined stress at bilge 130.2 [N/mm^2] and 158.3[N/mm^2] at deck corners

➢ Bulk carriers have cargo hatchways for the convenience of cargo-handling facilities. These hatchways reduce the ship's torsional strength and invite concentrated stress at the hatchway corners which may be evident by cracking of the deck plates in these areas.

The table.3-8 shows the good correspondence between the equivalent stress (Von Mises) for different panels given by Nauticus Hull software and the ultimate stress according to DNV classification society. The ship is subjected to various stresses for both sagging and hogging conditions with different signs:

Tension gives positive stress and compression gives negative stress.

Table.3-8 Longitudinal and equivalent (Von Mises) stress distribution for different panels

	Stress magnitude and distribution		
Panels	**Shear stress**	**Total longitudinal stress**	**Equivalent stress (Von Mises)**
Deck (Sagging)	τ = -5.6 N/mm^2	σ_x= -149.8 N/mm^2	σ_e= 150.1 N/mm^2
		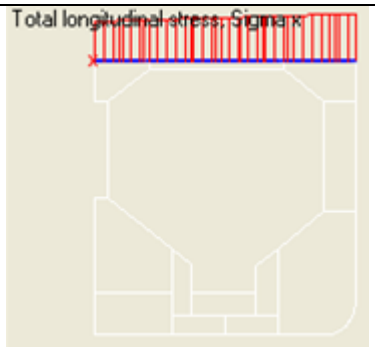	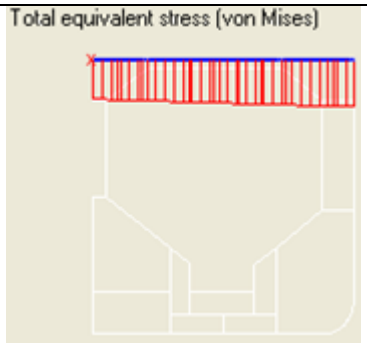
Deck (Hogging)	τ = -5.1 N/mm^2	σ_x= 149.4 N/mm^2	σ_e = 149.7 N/mm^2
		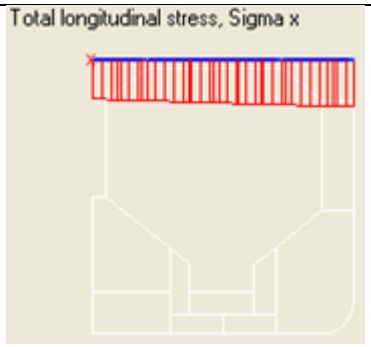	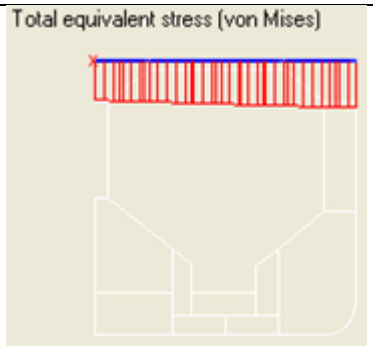
Outer shell Bottom (Sagging)	τ = -1.5 N/mm^2	σ_x= 121.4 N/mm^2	σ_e =121.4 N/mm^2
		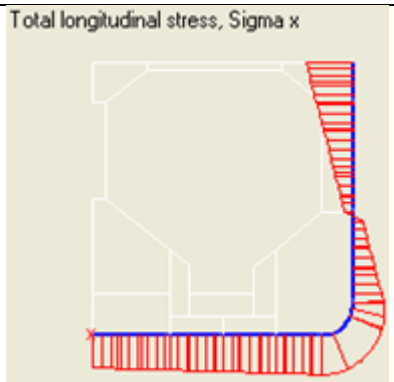	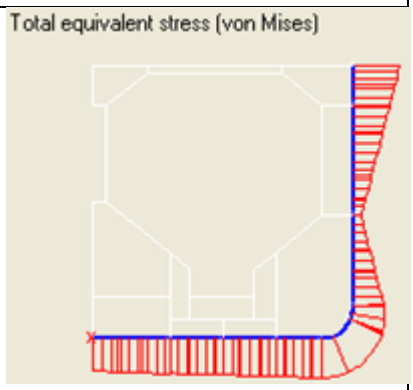
Outer shell Bottom (Hogging)	τ = -1.4 N/mm^2	σ_x = -121.1 N/mm^2	σ_e = 121.1 N/mm^2
		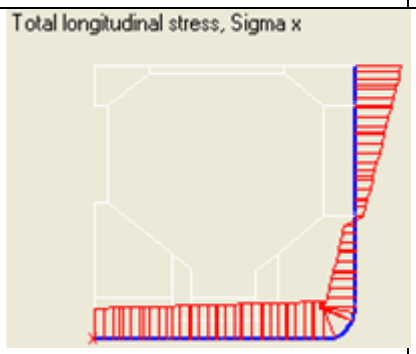	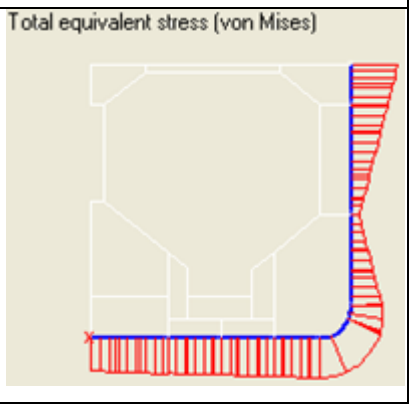

3.5.4. Buckling check

- The phenomenon of buckling is divided into three categories, namely elastic buckling, elastic-plastic buckling and plastic buckling.
- The longitudinal stresses applied in the buckling control are calculated by dividing the still water bending moment and wave bending moment with the section modulus of the hull girder.

The buckling/plastic collapse of the deck and/or bottom structure takes place and a ship's hull may break if the working longitudinal bending moment exceeds the capacity of the cross-section.

- The thicker bottom plating and stocky longitudinal in the bottom cause bottom structure collapse in form of plastic buckling rather than elastic buckling.
- Plate buckling strength is an important aspect in offshore steel construction design. Each plate should be checked as it influences on the strength and stability of the whole construction. Particular attention should be paid to the calculation of the ship's hull, which consists of a large number of longitudinal and transverse panels.
- For stiffened panels, it is supposed that the main support members including longitudinal girders, transverse webs and deep beams are designed with proper proportions and stiffening systems, their instability results the failure of the stiffened panels they support.
- The stress values applied on different elements of the mining ship hull are given as a result by Nauticus Hull software, and because we obey all the DNV rules during the scantling calculation, all stress are less than the ultimate capacity of the buckling strength. See buckling stress values in table.3-9. For more details refer to Naticus Hull report. Appendix.A1.
- For this current bulk carrier with longitudinal stiffening system, particular attention should be given to buckling of the main deck ship where the cross-deck strips are arranged in the longitudinal system.
- The buckling and ultimate strength of the structure depends on a variety of geometric and material properties, loading characteristics, boundary conditions and local damage related to fatigue cracking, corrosion and damaging.
- The self-unloading mining bulk carrier is subjected to various loads which may in different cases leads to critical buckling stresses, for instance the deck panel, which supports the mining lifting system in the amid ship, the crane and the boom in the aft part, in addition to the bottom supporting the riser system. To avoid the failure of the hull structure, the reinforcement should be maximum in those areas.

Table.3-9 Buckling check stresses for different bulk carrier ship members

	Deck		Side		Bottom		bulkhead	
Stress values	Applied stress	Buckling strength	Applied stress	Buckling strength	Applied stress	Buckling strength	Applied stress	Buckling strength
Plates	160	173	134.6	188.5	120	191.4	121.1	173.4
Longitudinal Stiffeners	150	200	70	207	121	211	86	178
Transversal stiffeners	160	235	160	235	160	235	160	235

3.5.5. Global results of scantling

The coefficients used for scantling calculation are shown in table.3-10.

Table.3-10 Summary of data used in the local rule requirements

Coefficients	Values
Material factor, f_1, bottom	1
Material factor, f_1, deck	1
Stress factor f_{2B} (f_2 at bottom) (Rules)	0.710
Stress factor f_{2D} (f_2 at deck) (Rules)	0.875
Speed factor, C_{av}	0.202
Speed/flare factor, C_{af}	0.500
Wave coefficient, C_W	10.037
Wave coefficient, C_{WO}	10.037
Wave coefficient, C_{WU}	10.037

The position of the vertical center of gravity of the mining ship studied is Y_{cg} = 10.2 m after applying the load of 12 t/m^2 which is in the acceptable range. Refer to table.3-11.

It can be noted that increasing the height of double bottom in comparison to other bulk carriers raise the position of the center of gravity of the cargo.

Table.3-11. Global results of the scantling

Data	Values	Unites
Moment of inertia about the horz. neutral axis, Ih	499.45	[m^4]
Moment of inertia about the vert. neutral axis, Iv	1266.91	[m^4]
Section modulus, bottom (z = 0 mm)	48.93	[m^3]
Section modulus, deck line (z = 22800 mm)	39.66	[m^3]
Section modulus, at side (y = 21600 mm)	58.65	[m^3]
Height from base line to the neutral axis	10.21	[m]
Total area (plates)	5.3	[m^2]
Total area (profiles)	1.6	[m^2]
Total Cross sectional area	6.90	[m^2]
First moment of the area above the neutral axis, s	26.36	[m^3]
I/s	18.95	[m]

3.5.6. Hull girder section modulus of ship

Hull girder section modulus of ship is calculated based on the gauging results from all structural components (plates and stiffeners) in a girth belt, or a transverse section.

Hull girder strength is a critical design parameter, it is viewed as the primary measure of the strength of a hull girder. This is true as ships are designed to operate within the material elastic range of its steel structure.

- The section modulus for both deck and bottom is more detailed in tables (3-12, 3-13) for midship section and actual cross section (105 m from AP).
- The general results of section modulus in deck and bottom of the bulk carrier show a good accordance to DNV standards.
- For the moment of inertia, its seen an ecces of the exact value because of the impossible accurate scantling dimensions for ship members, this analysis is more detailed in the report given by Nauticus Hull software. See Annex.A1.see table.3-14.

Table.3-12 Hull girder section modulus at midship section

Midship section	Bottom	Deck	Unites
Minimum section modulus, Z_o	32.48	32.48	[m^3]
Sagging (2262340 knm)	34.8	34.8	[m^3]
Hogging (2474100 knm)	34.8	34.8	[m^3]
Rule section modulus amidships	34.8	34.8	[m^3]
Minimum moment of inertia	214.55		[m^4]
Minimum section modulus at side	20.40		[m^3]

Table.3-13 Hull girder section modulus at actual position (105 m from AP)

Frame 140	Bottom	Deck	Unites
Section modulus (Sagging (2262340 knm))	34.8	34.8	[m^3]
Section modulus (Hogging (2474100 knm))	34.8	34.8	[m^3]
Rule section modulus	34.8	34.8	[m^3]
Minimum moment of inertia	214.55		[m^4]

Table.3-14 Hull girder strength summary

	Actual	Rule	Status (%) (100=rule)	Unites
Cross-sectional area	6.90			[m^2]
Height to the neutral axis	10.21			[m]
Moment of inertia	499.45	214.551	232.8	[m^4]
Section modulus, bottom	48.93	34.805	140.6	[m^3]
Section modulus, deck line (z = 22800 mm)	39.66	34.805	114.0	[m^3]

3.6. Bloc weight estimation

Reduces weight of hull structures designed for a very large carrier plays an important role as the economic efficiency is the most significant aspect . It is known that the traditional allowable working stress approaches with high safety and reliability . It means that the hull structure weight is higher actual requirement of marine structures.

The reference chosen for the scantling is frame 140 (105 m from AP) within frame 120 and 160 . The estimation of the bloc weight has to be done manually , the calculation of the volume of all elements is required to find the weight of this block after multiplying by lenght and the material density (ρ steel NS).

For total the areas of longitudinal members given by Nauticus Hull software includes plates stiffeners, girder and bulkheads and, its required to compute the total area of transvers stiffeners.

A detailed description of the results is presented in table.3-15.

Table.3-15 Computation of the bloc weight (Frame 120 to 160)

Item	Computation	magnitude	Unite
Area of plates	A_{plates}	10.64	[m^2]
Area of longitudinal members	A_{Long}	3.2	[m^2]
Area of transvers stiffeners	$A_T = \Sigma$ (web height . thickness)	0.63	[m^2]
Total area	A_{Total}	14.43	[m^2]
Lenght of bloc	L_{Bloc}= Nr frames . Frame spacing	30	[m]
Volume of the bloc	$V_{total\ block} = L_{Bloc} . A_{Total}$	432.9	[m^3]
Density of steel NS	$\rho_{NS\ steel}$	7.850	[t/m^3]
Total weight of the bloc	$W = \rho_{steel} . V_{total\ block}$	3398.265	[tones]

3.7. Analysis of results

The results from mining ship structural design can be summarized in the following remarks:

- At sea, the self-unloading mining ship is subjected to cyclical shearing and bending actions induced by continuously changing wave pressures acting on the hull.
  The stresses in the hull section caused by shear forces and bending moments are carried by continuous longitudinal structural members. These structural members are the strength deck, side shell and bottom shell plating and longitudinals, inner bottom plating and longitudinals, double bottom girders and topside and hopper tank sloping plating and longitudinals, which are generally defined as the hull girder.

- Comparing to other ship's , the self-discharging mining ship is exposed to significant loads produced by the ship's equipments including the crane, the boom installed in the deck, the lifting mining system of the riser in deck and bottom during operations, fuel tanks pressure and holds loaded by minerals and nodules (sagging bending moment when cargoes weight is incorrectly coocentrated in the middle of the ship and hogging when it is in the extremities) Such as those, which induce stresses in the hull structure, not to mention the dynamic effects resulting from the motions of the ship itself. Heretofore it has been difficult to arrive at the minimum scantlings for a large ship's hull of 227 m length by first principles alone, since the forces that the structure might be required to withstand in service conditions are uncertain. Accordingly, it must be assumed that the allowable stress includes a sufficient factor of safety, or margin, for these uncertain loading factors.

- The still water hull loadings vary quite slowly. For example when the mining ship is in port, there are gradual changes in bending moments, shears, and perhaps the torsional moments as cargo is discharged and loaded, fuel oil and stores taken aboard, etc.

- ✓ Ultimate sagging moments of resistance in intact and damaged hulls are considerably less than ultimate hogging moment. The hull collapse occurs in a mode that combines vertical and horizontal bending moments, which leads to a combined collapse of the ship hull.

- ✓ The length of the current mining ship produces higher longitudinal stresses required additional strengthening and a greater displacement for the same cargo weight, where the breadth related more to statical stability in order to ensure that this is sufficient in all possible conditions for loading.

- ✓ The shape of topside tanks provides sufficient stability to prevent dangerous cargo shift, and bilge hoppers contribute to convenience in collecting the cargoes on discharge.

- ✓ The most important issue arising from the density and storage of heavy cargo in holds is a very low position of the center of mass when a ship is fully loaded. This results in very favorable initial stability (large value of metacentric height), at the same time it causes a very short period of rolling and high accelerations bringing about inertial forces acting on ship structures, outfitting and its cargo. It is then suggested to design an elevated double bottom to keep the center of gravity higher. In addition the stability of self-unloading mining ship must be checked taking into consideration the effects of the heeling moment due to the sliding of the cargos.

- ✓ Ship structural design has very significant influence on the accident resistance; the collision energy absorption capability depends on the ship structure scantling, including the thickness of outer shell, inner shell, side stringers, transverse webs, width of the side ballast tank and width of lower and upper wing tanks.

- ✓ It is very important to take measures to avoid collision of self-discharging mining ship in service; the damage induced by collision reduces the ultimate resistance of the ship hull girder and the degree of reduction, varies with the damage type, position and amounts.

- ✓ The main factors that have contributed for the bulk carrier's hull structure failure are the corrosion and existence of structural cracks in the cargo holds.
  If a foremost hold of self-unloading mining ship is flooded, the bulkhead between the two holds may not be able to resist the pressure forces exerted by the sloshing of cargo and water mixture. If the bulkhead collapses, flooding could rapidly occur throughout the entire cargo length of the ship and the vessel is likely to sink.

4. BASIC CONSIDERATIONS IN SELECTING MINING EQUIPMENT

Seabed mining is a highly technological process due to the types of equipment and technical knowhow which need to be employed to overcome environmental challenges and successfully exploit a resource. This section lists some of the key considerations in developing a system for exploitation of the seabed described by (Bashir, Kim, Kiosidou, Wolgamot, Zhang, 2012).

4.1. Riser deployment system

The issue to be discussed early in the design phase is whether the mining ship needs a tower for deploying the riser by itself. Present technologies for oil and gas extraction and the related development of riser technology (Di Silvestro, Casola, Fatica, Mameli, Prandi, 2006), allow for the installation and deployment of the riser built in a shipyard as a whole, which takes place by means of a towing operation and positioning the riser in deep water with the use of buoyancy elements. Risers are towed to the field and several methods for this type of riser erection have been worked out. The towing operation may take place on sea surface, or the riser may be towed submerged, also in horizontal position.

Such an approach provides even more space on a mining ship, which can be used for additional cargo or other equipment. In case of a design where a mining ship should deploy riser by itself a lot of space is needed for riser sections and an installation tower must be erected on a ship.

4.2. Production Support Vessel

The PSV is similar to many of the vessels involved in oil and gas, dredging, or transportation industries, where its purpose is to supply a large deck space and a stable platform from which the mining operations are controlled and undertaken. The PSV and its supporting vessels support all mining, recovery and offshore loading activities. The PSV maintains its position over the deposit on the sea-floor using either dynamic positioning or anchoring. Dynamic positioning systems consist of several electric or diesel-powered thruster propellers that are controlled by a computer system using Global Positioning System technology as a reference.

It was also noted (Baker, Beaudoin) that the vessel will need to reposition the various sea-floors mining machines and to optimize the motions of barges and/ or bulk carriers moored alongside. Once the ore is pumped from the seafloor to the PSV, it will be transferred to a transportation barge or bulk carrier.

The requisite ocean surface production support system must be available. This could in the form of a production support vessel similar to the types used in oil and gas production.

The choice of this system is governed by many factors, of which the following constitute some of the most critical:

- **Daily production rate**

The volume of the minerals to be produced at any given field dictates whether a storage facility onboard is required, as well the size of the support system;

- **Configuration of the riser system**

This includes the weight and number of risers and depends on the water depth and the production rate;

- **Presence of processing unit onboard**

The decision whether to have a processing unit on- or off-board influences the sizes and the facilities on the support vessel.

4.3. Lifting system

The second report of the ECOR Panel on Marine Mining (September 2008) has mentioned that a number of methods have been investigated for transporting the ore from the sea-floor to the surface. To date, the majority of work has centered on a fully enclosed Riser and Lifting System (RALS), technology from the oil and gas industry. The purpose of the RALS is to:

• receive the mineral ore particles (mined slurry) excavated from sea-floor deposits by the Seafloor Production Tool/Collector;

• lift the mined slurry vertically to the dewatering plant inlet on the deck of the PSV, using a Subsea Lift Pump or an Airlift System and a vertical riser system suspended from the PSV;

• send the return water back to the sea. Much of the RALS and its components will be taken directly from the offshore oil and gas industry where these items are field proven in similar applications.

M Bashir, SH Kim, E Kiosidou, H Wolgamot and W Zhang, have presented some interesting lifting systems:

- Pneumatic lifting by airlift;
- Mechanical lifting by a single bucket lift;
- Hydraulic lifting by multiple centrifugal slurry pumps;
- Hydraulic lifting by a positive displacement pump;

The Fig.4-1 shows a typical deep sea mining system. It consists of a Seafloor Mining Tool (SMT, excavation/cutting), a vertical transport system (VTS) and a mining support vessel (MSV).

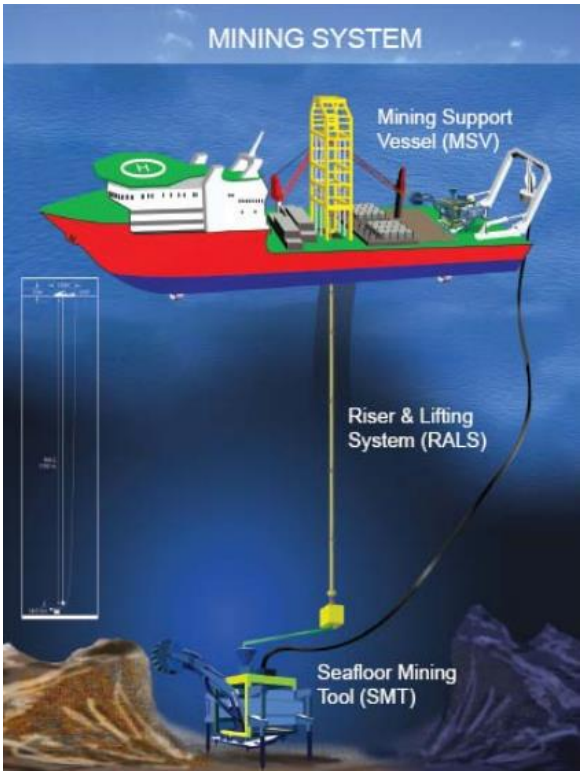

Figure.4-1 Schematic layout of a deep sea mining system consisting of a SMT, VTS and a MSV.

http://shipwreck.net/pdf/Scott+MineralDepositsintheSeaECOR110908.pdf

4.4. Water depth

One of the challenges facing the mining on the sea bed is the water depth of between 4000m–6000m where minerals are found. In order to select the most appropriate systems and equipment for mining, the effect of water depth on the equipment in installation, operation and recovery phases needs to be understood. Some of the most important depth dependent effects are:

- Temperature , hydrostatic pressure increases linearly with depth;
- Physical distance of the seafloor from the production vessel influences how the vessel communicates with the seabed, how material can be transported, etc.

4.5. Powering

Seabed operations are generally regarded as an energy intensive system because of the huge amount of energy required for powering the collective units of the entire system.

The key components of that require powering are:

• REE mud collection equipment;

• Pump stations and leaching tanks;

• Production support vessel (Ocean surface monitoring devices).

There are five forces that affect the seafloor mining tool, they are as following: gravity, buoyancy, hydraulic drag force, tension of the riser and added mass forces.

4.6. Hydrodynamics

The hydrodynamic forces acting on the equipment during installation, and to some extent during operation, could have a significant impact on the success of seabed minerals exploitation.

The loading conditions for the installation and recovery of seabed equipment are derived from the hydrodynamics of the operating environment in addition to the self-weight of the equipment. Another aspect of the mining installations that requires thorough hydrodynamic analysis is the power cable (umbilical). The umbilical will be used to connect a power supply to the REE mud collector, the leaching tank and any other seabed installation that requires power for its operations. In performing the installation analyses of this equipment, considerable attention should be paid to the prediction of hydrodynamic forces due to currents, waves, tidal movement etc.

4.7. The basic categories of deep water risers

The risers are specially made for each purpose, giving different properties which decide the riser's physical behavior, both statically and dynamically. The most important parameters affecting the dynamics of a steel riser are cited by Uwa Eigbe, Colin Mckinnon and Mike Thompson (2001) as follow:

• Riser length and external diameter;
• Cross sectional area and wall thickness;
• Elasticity and top tension;
• Density of the riser contents.

Some of these parameters are closely related. The top tension level is dependent on the weight of the riser, i.e. the cross sectional area, the length of the riser and the density of the internal fluid. The riser elongation is proportional to the modulus of elasticity times the cross sectional area according to (Rustad, 2007). The main types of deep water risers are:

- Top tensioned;
- Spar risers (specific category of top tensioned risers);
- Free standing (uncoupled configuration for Semisubmersibles and FPSO's);
- Highly compliant (coupled compliant and simple catenary designs for the different production units);
- Flexible risers as distinct from rigid (metallic) risers.

All deep water risers are subject to fatigue loading, dynamic bending stresses and vortex induced vibration. A marine riser system is presented in fig.4-2.

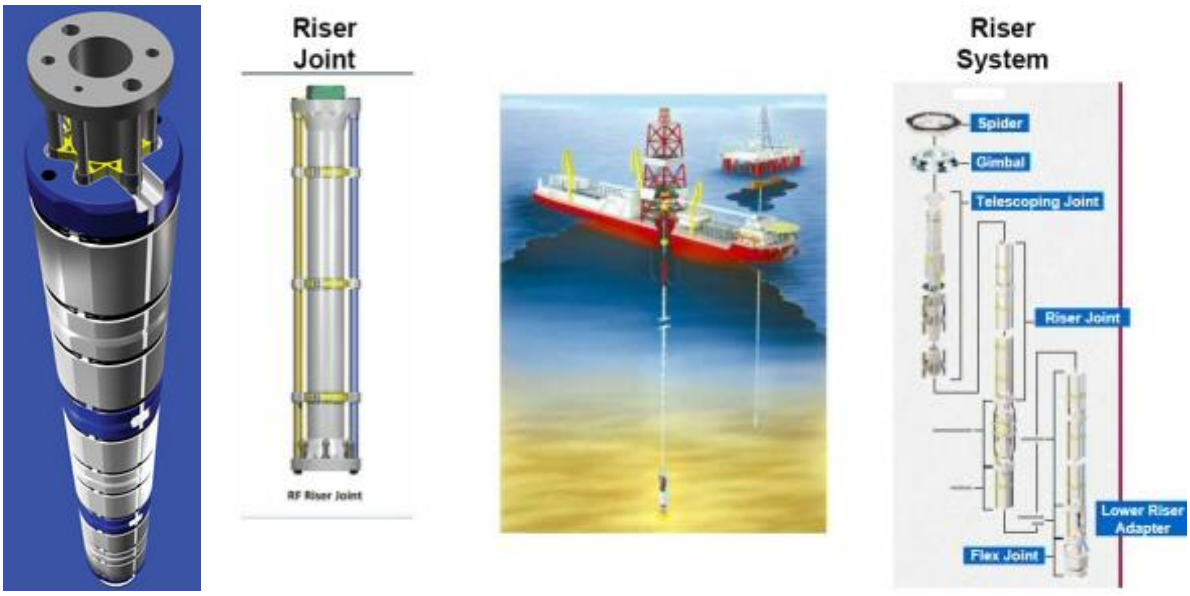

Figure.4-2 Marine riser system
http://www.lonestarbit.com/energy/riser.html
http://www.evergreen-maritime.com/products/detail-en63.html

4.8. A riser subjected to increasing pure bending

A riser must sustain installation loads and operational loads. In addition external loads such as those induced by waves, current, uneven seabed, trawl board impact, pullover, expansion due to temperature changes need to be considered.

Experience has shown that the main load effect on offshore pipes is bending combined with longitudinal force while subjected to external hydrostatic pressure during installation and internal pressure while in operation.

A marine riser subjected to increasing pure bending will fail due to local buckling/collapse or fracture as a result of increased deformation of the cross section and reduced slope in the stress-strain curve. Up to a certain level of deformation, the decrease in moment of inertia will be counterbalanced by increased pipe wall stresses due to strain hardening. When the loss in moment of inertia can no longer be compensated by the strain hardening, the moment capacity has been reached and catastrophic cross sectional collapse will occur if additional bending is applied.

5. RISER DESIGN REQUIREMENTS AND LOADS

5.1. ABS rules

The American Bureau of Shipping (ABS,2006) is a classification society, with a mission to promote the security of life, property and the natural environment, primarily through the development and verification of standards for the design, construction and operational maintenance of marine-related facilities.

The ABS Guide applies to classification of design, construction and installation of risers for offshore and marine applications, as well as the periodic surveys required for maintenance of classification. Serviceability of risers is also addressed, but only to the extent that proper functioning of the pipe and its components affects safety.

ABS will certify or verify design, construction and installation of offshore risers when requested by the owner or mandated by government regulations to verify compliance with this guide, a set of specific requirements, national standards or other applicable industry standards. If ABS verification is in accordance with this guide and covers design, construction and installation, then the riser is also eligible for ABS classification.

The satisfaction of individual requirements may require comprehensive data, analyses and plans to demonstrate adequacy. This especially applies for risers located in frontier areas, such as those characterized by relatively great water depth or areas with little or no previous operating experience.

5.2. Riser Configuration

A top tension riser system essentially consists of pipes connecting a floating installation with well heads at the seabed.

The top tension riser configurations covered by the criteria provided in this chapter are:

• High pressure production risers anchored to a wellhead with one or two concentric pipes acting as outer riser and/or inner riser plus the production tubing.

• High pressure drilling risers anchored to a wellhead with one or two concentric pipes acting as outer riser and/or inner riser plus drilling strings, using a surface Blow Out Preventer (BOP)

• Single pipe low pressure drilling risers anchored to a subsea BOP

• Single pipe export risers anchored to a subsea riser base.

5.3. Load combinations and design load cases

The risers are to be designed to satisfy the functional requirements under loading conditions corresponding to the internal environment, external environment, system requirements and service life defined by the project.

The risers are to be designed for the load combination that yields the most unfavorable conditions in terms of overall stress utilization. All potential external and internal loads are to be identified and load combinations developed to represent superposition that may occur within defined degrees of probability. In preparing load cases, the probable duration of an event (e.g., installation) is to be taken into account in the selection of concurrent environmental conditions. Extreme environmental events are unlikely to coincide, and therefore, the design process is to take caution to exclude unrealistic load combinations.

Load cases for the riser systems are to be defined to reflect manufacturing, storage, transportation, testing, installation, operation, retrieval and accidental events. Imposed loads are to be classified as either functional, environmental or construction and may be continuous or incidental, unidirectional or cyclic in nature. Accidental loads are to be considered separately, following review of risk factors for the particular development, and are to be applied under agreed combinations with functional and environmental loads. The design of the risers is to be based on design load cases, which are to be defined in the project-specific design basis documentation.

5.4. Design criteria

It is to be verified that the each riser is capable of withstanding all loads that are reasonably anticipated over its specified design life. The risers are to be designed to meet all applicable design criteria with the following failure modes considered:

- Burst;
- Leakage;
- Yielding;
- Local buckling;
- Global buckling;
- Fatigue;
- Wear and tear;
- Cross sectional out of roundness;

5.5. Wall thickness sizing

The wall thickness of risers is to be checked against all applicable design criteria for all load cases based on the following conditions:

• Transportation;

• Collapse during installation;

• In-service collapse during normal operation;

• Burst at maximum internal pressure during wellhead shut-in;

• Burst under hydro test;

The reduced wall thickness due to manufacturing tolerances, wear and tear and seabed abrasion needs to be accounted for in the design.

5.6. Global analysis

5.6.1. Static analysis

Nonlinear static strength analysis is to be conducted to define the risers' global configuration and to check the adequacy of initial wall thickness selection. The most reasonable configuration from all potential solutions is to be determined through consideration of design water depth, the maximum static offset, top tension requirement, articulation angle at riser top connection, floating installation motions and the most onerous current direction and profile.

Sufficient margins need to be added to account for the amplifications due to the most severe dynamic responses of risers.

5.6.2. Dynamic analysis

Dynamic analysis is to be conducted for the risers subjected to each design load case defined in the project-specific Design Basis documentation. The extreme responses of risers are to be determined and checked against the relevant design criteria.

The risers can be analyzed using a regular wave, a frequency domain random wave approach, or a time domain random wave approach.

Based on the regular wave analysis, load cases critical to the design of risers are to be identified and further analyzed using the random wave approach to validate the regular wave analysis results and to determine if any undue conservatism is made.

For the random wave approach, the time domain analysis is recommended so that more accurate evaluations of the extreme response of risers can be obtained. Frequency domain analysis may be used for preliminary purposes, but the results need to be verified by the time domain analyses.

5.6.3. Fatigue analysis

- **General**

The fatigue damage in the risers is induced by three main sources:

• First order (wave frequency) wave loading and associated motions of floating installation

• Second order (low frequency) drift motions of floating installation

• Vortex-Induced Vibration (VIV) of risers due to current and heave motion of floating installation **,** riser installation, vibrations of hull structure, riser internal fluid slugging and pressure pulses, and cyclic riser-soil interactions may also add fatigue damage to the risers. The overall fatigue life is to be determined by combining the fatigue damage from each contributing source. An appropriate weighting factor needs to be applied to individual fatigue damage prior to the combination.

- **First and second order motion-induced fatigue analysis.**

Depending on the required level of detail and accuracy, the motion-induced fatigue analyses are to be carried out for a set of sea state windows selected from the sea state scatter diagram. For each sea state window, a representative sea state is to be selected and applied to the floating installation and risers. The random sea analysis in the time domain is to be conducted for a sufficiently long duration so that the statistical features of riser responses can be accurately captured.

The fatigue damage at a specific point of riser pipe body or riser end connection is to be obtained by counting the stress cycles and using the appropriate Stress Concentration Factors (SCFs) and S-N curve defined in the design basis documentation. The maximum damage accumulation around the circumference of the riser body is to be considered as the fatigue damage at a specific location along the riser length. The resultant fatigue damage from each sea-state is to be factored by the associated probability of occurrence and then summed according to the Palmgren-Miner's rule to determine the annual fatigue damage.

Validation study needs to be conducted to verify the adequacy of finite element meshing, the convergence of statistics and the sufficiency of the number of selected critical sea state windows, loading directions and stress bins so as to produce a reliable calculation of fatigue damage.

- **VIV fatigue analysis**

The VIV fatigue analysis is to be conducted to assess the magnitude of VIV-induced fatigue damage on risers, and to determine whether VIV suppression devices are required to mitigate the vibration. Dedicated analysis software is to be used to perform the analysis.

Each of the anticipated directional current profiles with one-year return period is to be used in the long term (during the service life of the risers) VIV fatigue analysis. Responses to both uniform and sheared current profiles need to be accounted for. The VIV fatigue damage due to each current profile is to be factored by the associated occurrence probability and then summed up according to Palmgren-Miner's rule to determine the annual VIV fatigue damage.

The short term VIV fatigue analysis associated with the duration of 100-year return period current during the service life of the risers is to be considered with 100-year return period current profiles coming from different directions. The damage from the most critical current profile is to be factored by the associated occurrence probability and then added to the total VIV fatigue damage.

Whenever VIV suppressors are determined to be necessary, the VIV fatigue analysis is to be reevaluated to determine the lengths and locations of VIV suppressors and the improvement on fatigue behavior obtained.

5.6.4. Design sensitivity analysis

Parametric studies are to be carried out to assess the effects of variations in riser responses accounting for variables such as:

- Riser length and weight;
- Drag coefficients;
- Floating installation offsets and motions;
- External environmental loads;
- Internal fluid densities;
- Riser-soil interactions.

5.7. Definitions of design loads

Loads acting on risers can be divided into environmental, functional and accidental loads. Typical design loads may be categorized in the table.5-1

Table.5-1 Categorization of design loads for risers

Environmental Loads	Functional Loads	Accidental Loads
Wind	Weight in air of:	Impacts from dropped
Waves	- Pipe	objects
Current	- Coating	Impacts from collision
Tides	- Anodes	between risers
Surge	- Attachments	Mooring or tendon failure
Marine growth	Buoyancy	Loss of floating installation
Sea ice	Towing	station
Seabed subsidence	External hydrostatic pressure	keeping capability
Hydrothermal aging	Internal pressures:	Tensioner failure
	- Mill pressure test	
	- Installation	
	- Storage, empty/water filled	
	- In place pressure test	
	- Operation	
	Installation tension (pipes)	
	Installation bending	
	Top tension (risers)	
	Makeup (connectors)	
	Boundary conditions:	
	- Reel	
	- Stinger	
	- Rock berms	
	- Seabed contours	
	- Top constraints (risers)	
	Soil interaction	
	Loads due to containment:	
	- Weight	
	- Pressure	
	- Temperature	
	- Fluid flow, surge and slug	
	- Fluid absorption	
	Inertia ,Pigging and run tools	

5.8. Combinations of wind, current and waves

The worst combinations of wind, current and waves are to be addressed in the design. When current and waves are superimposed, the current velocity and direction are to be added as vectors to the wave induced particle velocity and direction prior to computation of the total force, and where appropriate, flutter and dynamic amplification due to vortex shedding are to be taken into account.

Because risers have small diameters compared to the wavelengths being considered, semi-empirical formulations such as Morison's equation are considered to be an acceptable basis for determining the hydrodynamic force acting on a riser:

$$F = F_D + F_i \tag{34}$$

Where:

The drag force for a stationary pipe is given by :

$$F_D = ½\, \rho\, D\, C_D\, U_n^2 \tag{35}$$

The inertia force for a stationary pipe is given by :

$$F_1 = \rho\, (\frac{\pi\, D^2}{4})\, C_M\, a_n \tag{36}$$

Where :

C_M : Inertia coefficient based on the displaced mass of fluid per unit length

a_n :Component of the total fluid acceleration vector normal to the axis of pipes

The lift force for a stationary pipe located on or close to the seabed is given by:

$$F_L = \frac{1}{2}\, C_L\, \rho\, U_n^2\, A_t \tag{37}$$

Where :

F_L : Lift force per unit length

C_L : List coefficient (dimensionless)

A_t : Projected area per unit length in a plan normal to the direction of force

For risers that exhibit substantial rigid body oscillations due to the wave action, the modified form of Morison's equation , given below may be used to determine the hydrodynamic force :

$$F= F_D + F_t = \frac{1}{2}\, \rho\, D\, C_D\, (U_n - Ú_n)|\, U_n - Ú_n\, | + \rho\, (\frac{\pi\, D^2}{4})\, a_n + (\frac{c}{g})\, (\frac{\pi\, D^2}{4})\, C_m\, (a_n - á) \tag{38}$$

$Ú_n$: component of the velocity vector of riser normal to its axis

C_m : added mass coefficient , $C_m = C_M - 1$

á : component of the acceleration vector of the riser normal to its axis

The values of u_n and a_n are to be determined using recognized wave theory appropriate to the wave heights, wave periods and water depth at the installation location, as well as the elevation at which the load is calculated.

6. VIBRATION OF STRUCTURES INDUCED BY FLUID FLOW

6.1. General

Fluid around a structure can significantly alter the structure's vibrational characteristics.

The presence of a quiescent fluid decreases the natural frequencies and increases the damping of the structure. A dense fluid couples the vibration of elastic structures which are adjacent to each other. Fluid flow can induce vibration. A turbulent fluid flow exerts random pressures on a structure, and these random pressures induce a random response. The structure can resonate with periodic components of the wake.

If a structure is sufficiently flexible, the structural deformation under the fluid loading will in turn change the fluid force. The response can be unstable with very large structural vibration once the fluid velocity exceeds a critical threshold value.

Vibration induced by fluid flow can be classified by the nature of the fluid structure interaction. Effects which are largely independent of viscosity include added mass and inertial coupling. Unsteady pressure on the surface of a structure, due to either variations in the free stream flow or turbulent fluctuations, induces a forced vibration response. Strong fluid-structure interaction phenomena result when the fluid force on a structure induces a significant response which in turn alters the fluid force as mentioned by (Blevins, 1990).

6.2. Riser vibration

6.2.1. Added mass and inertial coupling

If a body accelerates, decelerates, or vibrates in a fluid, then fluid is entrained by the body. This entrainment of fluid, called the added mass or virtual mass effect, occurs both in viscous and in inviscid, i.e., ideal, fluids. It is of practical importance when the fluid density is comparable to the density of the structure because then the added mass becomes a significant fraction of the total mass in dynamic motion.

Velocity potential $\Phi(x, y, z, t)$ which is a function of the special coordinates and time, such that the velocity vector is the gradient of a potential function:

$$V = \nabla\Phi \tag{39}$$

V(x, y, z, t) is the fluid velocity vector. The potential function Φ satisfies Laplace's equation:

$$\nabla^2\Phi = 0 \tag{40}$$

The boundary condition is that on the surface of the body; the normal component of velocity must equal the velocity of the body:

$$\frac{\partial\Phi}{\partial n} = \mathrm{V}\cdot \mathrm{n} \tag{41}$$

On the surface S ,where n is the unit outward normal vector. The pressure in the fluid is given by the Bernoulli equation :

$$p = -\rho\frac{\partial\Phi}{\partial t} - \frac{1}{2}\rho V^2 \quad (42)$$

Where ρ is the fluid density and V is the magnitude of velocity. The force exerted by the fluid on the body is the integral of the fluid pressure over the surface.

$$\overrightarrow{F} = \int_S pn\, dS \quad (43)$$

The added mass per unit length is found and the result is:

$$m = \rho\pi a^2 \quad (44)$$

Where a is the cylinder radius. This added fluid mass is equal to the mass of fluid displaced by the cylinder.

Added mass and inertial coupling occur in elastic and rigid bodies, but the added complexity of elasticity and the three-dimensional motions make a closed-form solution impossible for most elastic bodies.

In the case of quasi-two-dimensional structures (such as long span tubes or rods), the axial variation in the motion occurs relatively slowly over the span, and two-dimensional results for sections are applicable.

Concentric cylindrical shells coupled by a fluid annulus are important in the design of nuclear reactor containment vessels. Approximate solutions are required for both the vessels and the fluid. A classification of flow-induced vibration is presented in table.6-1.

Table.6-1 A classification of flow-induced vibration.

Inertial coupling effect	Unsteady flow induced vibration	Flow-structure coupled vibration
Added mass	Turbulence induced vibration	Vortex induced vibration
Inertial coupling	Ocean wave induced vibration	Galloping on a flutter
Instability due to parallel flow	Sonic fatigue	Fluid elastic instability

6.2.2. Wave induced vibration of structures

Waves induce vibration of structures, such as marine pipelines, oil terminals, tanks, and ships, by placing oscillatory pressure on the surface of the structure. These forces are often well-represented by the inviscid flow solution for many large structures such as ships and oil storage tanks. For most smaller structures, viscous effects influence the fluid force and the fluid forces are determined experimentally.

Consider an ocean wave approaching the vertical cylindrical structure as shown in figure.6-1.

The wave is propagating in the X direction. Using small-amplitude (linear) inviscid wave theory, the wave is characterized by the wave height (h) (vertical distance between trough and crest), its angular frequency ω, and the associated wavelength (λ) (horizontal distance between crests), and d is the depth of the water.

The wave potential Φ satisfies Laplace's equation and a free-surface boundary condition.

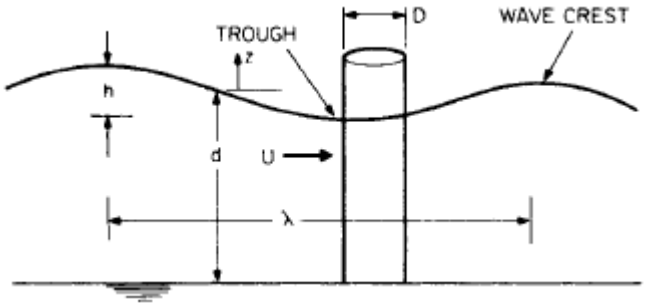

Figure.6-1 A circular cylindrical structure exposed to ocean waves. (Blevins. 1990)

This component of wave velocity induces substantial fluid forces on structures, such as pilings and pipelines, which are oriented perpendicular to the direction of wave propagation.

The forces which the wave exerts on the cylinder in the direction of wave propagation can be considered the sum of three components:

(1) Buoyancy force associated with the pressure gradient in the laterally accelerating fluid;

(2) Added mass force associated with fluid entrained during relative acceleration between the fluid and the cylinder;

(3) Force due to fluid dynamic drag associated with the relative velocity between the wave and the cylinder.

The first two force components can be determined from inviscid fluid analysis as discussed previously. The drag component of force, however, is associated with fluid viscosity.

Thus, the inline fluid force per unit length of cylinder due to an unsteady flow is expressed as the sum of the three fluid force components:

$$F = \rho A \acute{U} + C1\rho A\left(\acute{U} - x\right) + \frac{1}{2}\,\rho\,\left|\acute{U} - x\,\right|(\,U - x)DCD \tag{45}$$

Flexible structures will resonate with the wave if the structural natural period equals the wave period or a harmonic of the wave period. Since the wave frequencies of importance are ordinarily less than 0.2 Hz (wave period generally greater than one cycle per 5 sec), such a resonance occurs only for exceptionally flexible structures such as deep-water oil production risers and offshore terminals.

The above discussion considers only fluid forces which act in line with the direction of wave propagation. These in-line forces produce an in-line response. However, substantial transverse vibrations also occur for ocean flows around circular cylinders.

These vibrations are associated with periodic vortex shedding, which is discussed below.

6.2.3. Vortex-induced vibration

Many structures of practical importance such as buildings, pipelines, and cables are not streamlined but rather have abrupt contours that can cause a fluid flow over the structure to separate from the aft contours of the structure. Such structures are called bluff bodies. For a bluff body in uniform cross flow, the wake behind the body is not regular but contains distinct vortices of the pattern shown in figure.6-2 at a Reynolds number R_d = UD/v greater than about 50, where D is the width perpendicular to the flow and v is the kinematic viscosity. The vortices are shed alternately from each side of the body in a regular manner and give rise to an alternating force on the body.

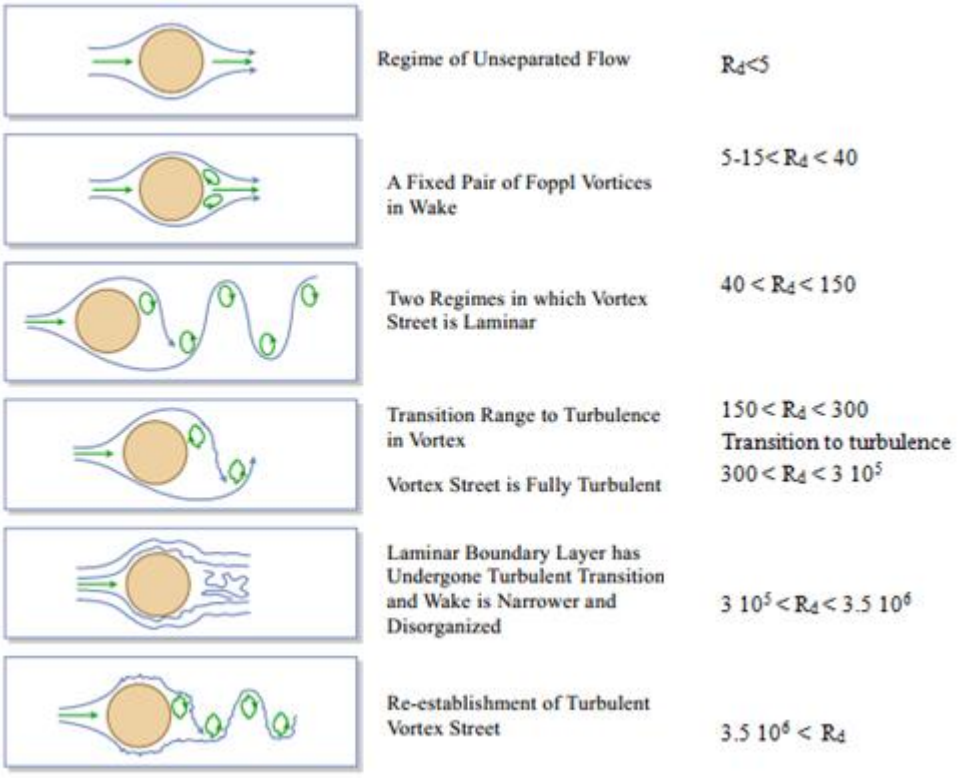

Figure.6-2 Regimes of fluid flow across smooth circular cylinders (Lienard, 1966).

As the flow velocity is increased or decreased so that the shedding frequency f_s approach the natural frequency f_n of an elastically mounted cylinder so that:

$$fn = fs = \frac{SU}{D} \qquad so \qquad \frac{U}{fn\,D} = \frac{U}{fsD} = \frac{1}{S} = 5 \tag{46}$$

The vortex shedding frequency suddenly locks on to the structure natural frequency.

The resultant vibrations occur at or nearly at the natural frequency of the structure and vortices in the near wake input energy to the cylinder. Large amplitude vortex induced structural vibration can result.

The shedding frequency is entrained by the cylinder natural frequency. Entrainment persists until velocity is increased at which point lock-in is broken and the shedding frequency abruptly returns to its natural value.

6.3. Suppression of vortex-induced vibrations

A number of fairings, strakes, and ribbons have been attached to the exterior of circular cylindrical structures to reduce vortex-induced vibrations as shown in fig.6-3, These devices act by disrupting the near wake and disturbing the correlation between the vortex shedding and vibration. They do, however, increase the steady drag from that which is measured on a stationary structure.

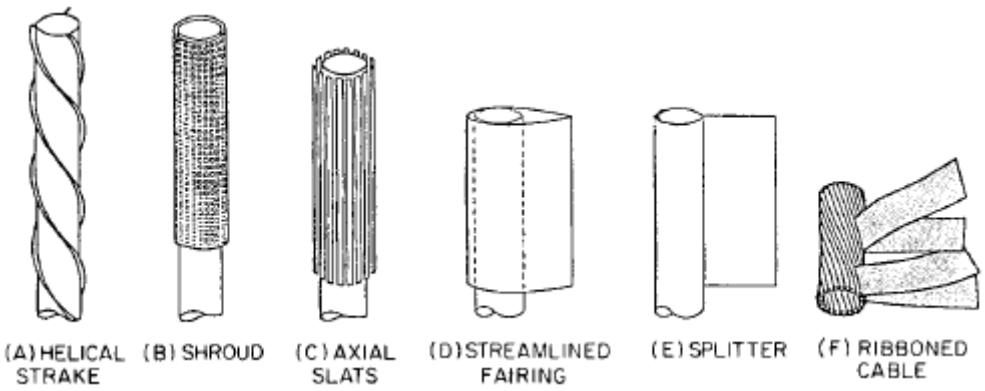

Figure.6-3 Riser configurations for reducing vortex-induced vibration from (Blevins, 1990)

Vortex shedding may induce severe vibration of a cylindrical structure such as a chimney, free-standing tower, guyed mast, bridge columns, etc. Very strong oscillations have been observed in all-welded structures where the damping ratio is extremely low, sometimes they are particularly prone to fatigue failure, as the endurance limit may be only a fraction of the strength if heavy notches, flaws, attachments, or other adverse details are present. In other cases, the motion is intolerable because of its physiological effects or swaying of antennas. For these reasons, suppression of vibration is often desirable.

Blevins noted that in some cases, vibration can be reduced by increasing the structural damping. This can be accomplished by additional dampers attached to an independent support or to a special mass suspended from the structure and suitably tuned or by hanging chains.

Reynolds number is the governing parameter for the flow around a stationary circular cylinder but other influencing parameters can become governing over a certain value. Those parameters were described by (Huera Huarte, 2006) as fellow:

6.4. Important parameters for the analysis of vortex shedding

• Reynolds number (Re) important parameter to characterize the flow regime.

• Aspect ratio L/D relation between the length and the diameter of the cylinder.

Roughness ratio calculated as k/D where k is the equivalent sand roughness parameter. It measures the importance of the surface roughness to the diameter of the structure.

• Turbulence intensity measures relative to the free stream flow velocity that indicates the amount of disorder of the flow. Usually it is expressed as the ratio between the RMS value of the velocity and the free stream velocity.

6.5. Important parameters for the analysis of VIV

• ***Damping ratio (ζ)***

It is an expression for the ability of the structure to dissipate energy during a cycle of vibration.

• ***Reduced velocity (Vr)***

$$Vr = \frac{VT}{d} = \frac{V}{fD} \tag{47}$$

• ***Mass ratio (m^*)***

Ratio between the mass per unit length (m) of the structure and the displaced mass of fluid when oscillating.

$$m^* = \frac{m}{\rho \frac{\pi}{4} D^2} \tag{48}$$

• ***Lock-in***

A cylinder is said to be “locked in” when the frequency of oscillation is equal to the frequency of vortex shedding. In this region the largest amplitude oscillations occur.

Shedding frequency: $\omega_v = 2\pi f_v = 2\pi S_t (U/d)$

Natural frequency of oscillation: $wn = \sqrt{\frac{k}{m+ma}}$

6.6. Strouhal number

According to Fedele and Stoesser (2013), vortex shedding is a phenomenon that occurs when the current flow of a body of water is disrupted by an obstruction, in this case a bluff body. When placed in a fluid flow most bodies create a separated flow across a substantial proportion of their surface. An unsteady flow is created due to the detachment of the stream of water that collides with the device. The turbulence these vortices create are pockets of energy that are usually viewed by the engineering world as problems occurring naturally in air and water which can cause fatigue and failure to its man-made structures. Therefore, the behavior of vortices caused by the external flow of air or water past upright edifices has conventionally been studied by engineers and scientist defensively to find ways to eliminate or guard against the affects of vortex shedding in their designs. In air, vortices create lift-induced drag on an aircraft and also cause vibrations against skyscrapers that can possibly cause the failure of the structure in both instances.

The frequency of vortex shedding, can be expressed non-dimensionally as the Strouhal number which is derived from the average frequency (f) of the lift coefficient, non-dimensional free stream velocity (U) and cylinder diameter(D). Relationship between Strouhal number and Reynolds number for circular cylinders is shown in fig.6-4. Strouhal number is practically constant in the subcritical regime, with a value of approximately 0.2. S_t is defined by:

$$S_t = \frac{f\,D}{U} \tag{49}$$

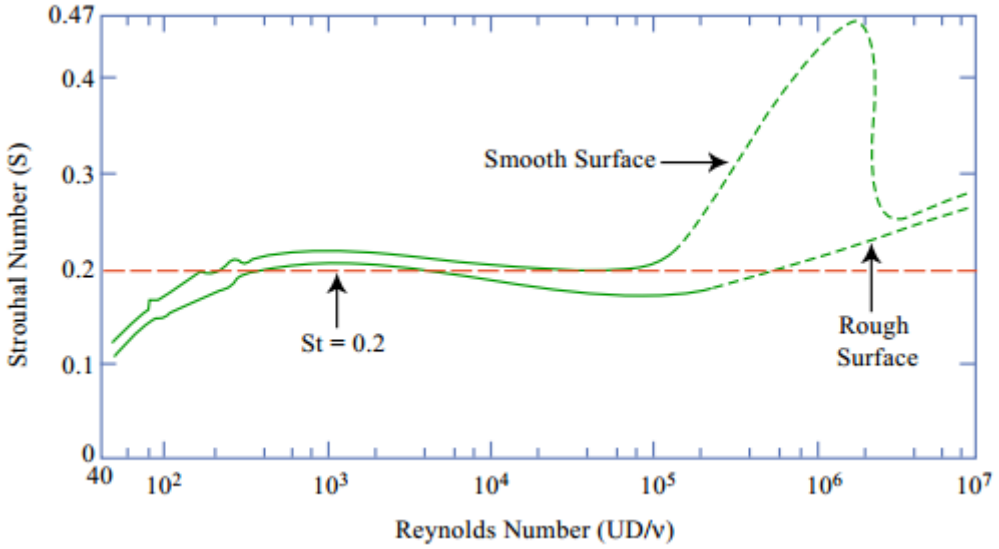

Figure.6-4 Relationship between Strouhal number and Reynolds number for circular cylinders. Data from Lienhard (1966) and Achenbach and Heinecke (1981). S~0.21 (1-21/Re) for 40<Re<200, Roshko (1955).

7. NUMERICAL MODELLING

7.1. Calculation tool

Computational Fluid Dynamics tools are becoming standard in many fields of engineering involving flow of gases and liquids; numerical simulations are used both in the design phase to select between different concepts and in the production phase to analyze performance. Industrial CFD applications require high flexibility in the grid–generation procedure for complex configurations, short turnaround time, and easy to use environments. At present, several commercial packages are available for the CFD industrial community; these packages are usually integrated systems which include a mesh generator, a flow solver, and a visualization tool. Often the numerical techniques adopted in these CFD codes are well accepted algorithms published in the open literature; the selection of one technique with respect to others is usually based on robustness and reliability.

7.2. Overview of physical models in Fluent Ansys

Ansys Fluent provides comprehensive modeling capabilities for a wide range of incompressible and compressible, laminar and turbulent fluid flow problems. Steady-state or transient analyses can be performed. To permit modeling of fluid flow and related transport phenomena in industrial equipment and processes, various useful features are provided. These include porous media, lumped parameter (fan and heat exchanger), stream wise-periodic flow and heat transfer, swirl, and moving reference frame models. The moving reference frame family of models includes the ability to model single or multiple reference frames. A time-accurate sliding mesh method, useful for modeling multiple stages in turbo machinery applications, for example, is also provided, along with the mixing plane model for computing time-averaged flow fields. (FLUENT 12.0 .Theory Guide, 2009).

7.3. CFD and fluid model

The complexity of the hydrodynamic equations makes obtaining an analytical solution very unlikely. Therefore, numerical solutions should be considered. In the Fluent computer program that will be used in this study, the governing equations will be discretized using the finite volume technique. The discretized equations, along with the initial and boundary conditions, will be solved to obtain a numerical solution.

All kinds of fluid flow and transport phenomena are governed by basic conservation principles such as conservation of mass, momentum and energy. All these conservation principles are solved according to the fluid model which gives set of partial differential equations, called the governing equations of the fluid. The following part elaborates on the theoretical background of CFD and the way it is employed for this particular case.

7.4. Methodology

Numerical investigation was performed using commercial software Gambit and Fluent. Ggambit package was used to generate mesh of the flow domain around several riser geometries; these mesh files were then exported to Fluent to solve the integral aerodynamic parameters. This section describes in detail the numerical technique to solve fluid flow:

7.4.1. Newton's second law and momentum equation

Newton's second law states that the rate of change of momentum of a fluid particle equals to the sum of the forces acting on a particle. The forces acting on a body are a combination of both surface and body forces. When this law is applied for Newtonian fluid (viscous stress is proportional to the rates of deformation) resulting equations are called as Navier Stokes equations.

The conservation of mass and momentum can be written as;

$$\frac{\partial \rho}{\partial t} + \rho \frac{\partial Ui}{\partial xj} = 0 \tag{50}$$

$$\rho \frac{\partial Ui}{\partial t} = -\frac{\partial p}{\partial xi}\frac{\partial \tau ij}{\partial xj} + \rho Fi \tag{51}$$

$$\tau ij = \mu(\frac{\partial Ui}{\partial xj} + \frac{\partial Uj}{\partial xi} - \frac{2}{3}\frac{\partial Uk}{\partial xk}\delta ij) \tag{52}$$

For incompressible flow ρ= constant, which from the conservation of mass equation implies

$$\frac{\partial Ui}{\partial xi} = 0 \tag{53}$$

Implying that a fluid particle experiences no change in volume. Thus the conservation of mass and momentum reduce to:

$$\frac{\partial Ui}{\partial t} + Uj\frac{\partial Ui}{\partial xj} = -\frac{1}{\rho}\frac{\partial Ui}{\partial xi} + v\nabla^2 Ui + Fi \tag{54}$$

$$\frac{\partial Ui}{\partial xi} = 0 \tag{55}$$

Where the viscous stress tensor can now be written as :

$$\frac{\partial}{\partial xj}\left(\frac{\partial Ui}{\partial xj} + \frac{\partial Uj}{\partial xi} - \frac{2}{3}\frac{\partial Uk}{\partial xk}\delta ij\right) = \frac{\partial^2 Ui}{\partial xj \partial xj} = \nabla^2 Ui \tag{56}$$

The kinematic viscosity is :

$$v = \frac{\mu}{\rho} \tag{57}$$

The non-dimensional incompressible Navier-Stokes equation is given as;

$$\frac{\partial Ui}{\partial t} + Uj\frac{\partial Ui}{\partial xj} = -\frac{\partial p}{\partial xi} + \frac{1}{Re}\nabla^2 Ui \tag{58}$$

$$\frac{\partial Ui}{\partial xi} = 0 \tag{59}$$

7.4.2. Mass conservation principle and continuity equation

The mass conservation principle states that the rate of increase of mass in a fluid element is equal to the net rate of flow of mass into a fluid element. Applying this physical principle to a fluid model results in a differential equation called continuity equation.

The equations for continuity and momentum may be expressed in the dimensionless form as follows:

Continuity :

$$\frac{\partial u}{\partial x} + \frac{\partial v}{\partial y} = 0 \tag{60}$$

X-momentum :

$$\frac{\partial u}{\partial t} + \frac{\partial}{\partial x}(uu) + \frac{\partial}{\partial y}(vu) = -\frac{\partial p}{\partial x} + \frac{1}{\mathrm{Re}}\left(\frac{\partial^2 \mathrm{u}}{\partial x^2} + \frac{\partial^2 u}{\partial y^2}\right) \tag{61}$$

Y-momentum:

$$\frac{\partial v}{\partial t} + \frac{\partial}{\partial x}(uv) + \frac{\partial}{\partial y}(vv) = -\frac{\partial p}{\partial y} + \frac{1}{\mathrm{Re}}\left(\frac{\partial^2 \mathrm{v}}{\partial x^2} + \frac{\partial^2 v}{\partial y^2}\right) \tag{62}$$

7.4.3. Finite volume method

The finite volume method is one of the numerical techniques applied in well-established commercial CFD codes to solve the governing equations of the fluid. The basic and foremost step of CFD is dividing the computational domain (geometry of the region of interest) in to number of smaller regions called control volumes or cells and the collection of these cells is called a grid or a mesh, also, the calculated scalar values are stored at the center of the control volumes.

Fluent uses the finite volume technique to convert the general transport equation in to a system of algebraic equations and it uses different iterative methods to solve the algebraic equations. The following are the key steps in order to find the solution for the transport equation of a physical quantity, the steps are as follows:

- Division of geometry in to smaller regions (control volumes) using a computational mesh.
- Integration of the governing equations of fluid over all the control volumes of the domain.
- Discretization-conversion of the resulting integral equations into algebraic equations.
- Finding a solution to the system of algebraic equations by an iterative method. (Versteeg and Malalasekra, 2007).

7.4.4. Choosing a turbulence model

According to the theory guide (2009), it is an unfortunate fact that no single turbulence model is universally accepted as being superior for all classes of problems. The choice of turbulence model will depend on considerations such as the physics encompassed in the flow, the established practice for a specific class of problem, the level of accuracy required, the available computational resources, and the amount of time available for the simulation. To make the most appropriate choice of model for our application, we need to understand the capabilities and limitations of the various options.

7.4.5. Fluent Ansys meshing

Mesh generation is one of the most critical aspects of engineering simulation. It was mentioned in the Ansys website that too many cells may result in long solver runs, and too few may lead to inaccurate results. Fluent Meshing technology provides a means to balance these requirements and obtain the right mesh for each simulation in the most automated way possible.

The Meshing technology has been built on the strengths of stand-alone, class-leading meshing tools. The strongest aspects of these separate tools have been brought together in a single environment to produce some of the most powerful meshing available.

The highly automated meshing environment makes it simple to generate the following mesh types:

- Tetrahedral
- Hexahedral
- Prismatic inflation layer
- Hexahedral inflation layer
- Hexahedral core
- Body fitted Cartesian

Cut cell Cartesian Consistent user controls make switching methods very straight forward and multiple methods can be used within the same model. Mesh connectivity is maintained automatically.

Different physics requires different meshing approaches. Fluid dynamics simulations require very high-quality meshes in both element shape and smoothness of sizes changes. Structural mechanics simulations need to use the mesh efficiently as run times can be impaired with high element counts. Fluent Ansys meshing has a physics preference setting ensuring the right mesh for each simulation.

7.5. Computational models

7.5.1. Description of the problem

The purpose the simulation is to illustrate the solution of an unsteady 2D and 3D flow past a circular cylinder, streamlined fairing and straight cables geometry of mining riser and to study the vortex shedding process.

In this section different geometries of risers are designed in Gambit package to perform a numerical simulation around them using Fluent software in an unsteady regime by studying forces, moments, pressures velocities and vorticities distribution.

The studied models are similar to the real object, but to save the computations time (CPU), the simulation is done for only some risers sections because of its large length (5000 m).

The riser section is 2m length inclined by 70° to model a real mining operation (Inclined pipe).

Two examples of forces acting upon marine risers are the external forces caused by wave motion and sea currents and the inner forces due mainly to a unique multiphase flow known as the slug flow regime. The inner flow into the riser consists of a liquid phase (crude oil, minerals) and of a gaseous phase (used to increase the rising flow velocity in the pipe). However, other fundamental boundary forces must be taken into account to analyze riser behavior in the environment in which it works and to deduce on the torsional moments and power requirement of the towing system of the vertical riser used for mining operations.

The most important dimensions of the studied marine steel riser are presented in table.7-1.

Table.7-1 Characteristics of the studied cylindrical mining riser

Item	Magnitude	Units
External diameter (D_0)	0.7	[m]
Inner diameter(D_i)	0.4	[m]
Wall thickness (t)	0.15	[m]
Riser length (L)	5000	[m]
Elasticity (E)	206.82×10^9	[N/m^2]

For the control parameters refer to table.7-2.The results of Reynolds and Strouhal number for different velocity are in table.7-3.

Table.7-2 control parameters of the simulation

Input data	Magnitude	Units
Temperature (T)	288	[K]
Sar water density(ρ)	1025	[kg/m^3]
Dynamic vescosity (μ)	0.001003	[kg/s m]
Riser diameter (D)	0.7	[m]
Lenght of riser section (L)	2	[m]
Strouhal number (St =f D/U)	0.2	-
Riser inclination	70	degree
Weted Area for cylindrical riser	4.396	[m^2]
Weted Area for streamlined fairing riser	5.652	[m^2]
Weted Area for straight cables model riser	6.908	[m^2]

Table.7-3 Reynolds and Strouhal number associated to each velocity.

U(m/s)	Reynolds Nr	f(Hz)	Strouhal Nr
0.2	1.4 10^5	0.05	0.175
0.4	2.8$10^5$	0.11	0.192
0.6	4.2$10^5$	0.17	0.198
0.8	5.7$10^5$	0.22	0.192
1.0	7.1$10^5$	0.28	0.196

7.5.2. Computational domain

Unsteady 2D turbulent flow over a cylinder

The geometry is placed at 10 cm from the upstream and 20cm from the downstream. The velocity of fluid at the inlet is various from 0.2 to 1 m/s. The Reynolds numbers are based on flow velocity U_x and riser diameter D.the computaional domaine is presented in Fig.7-1.

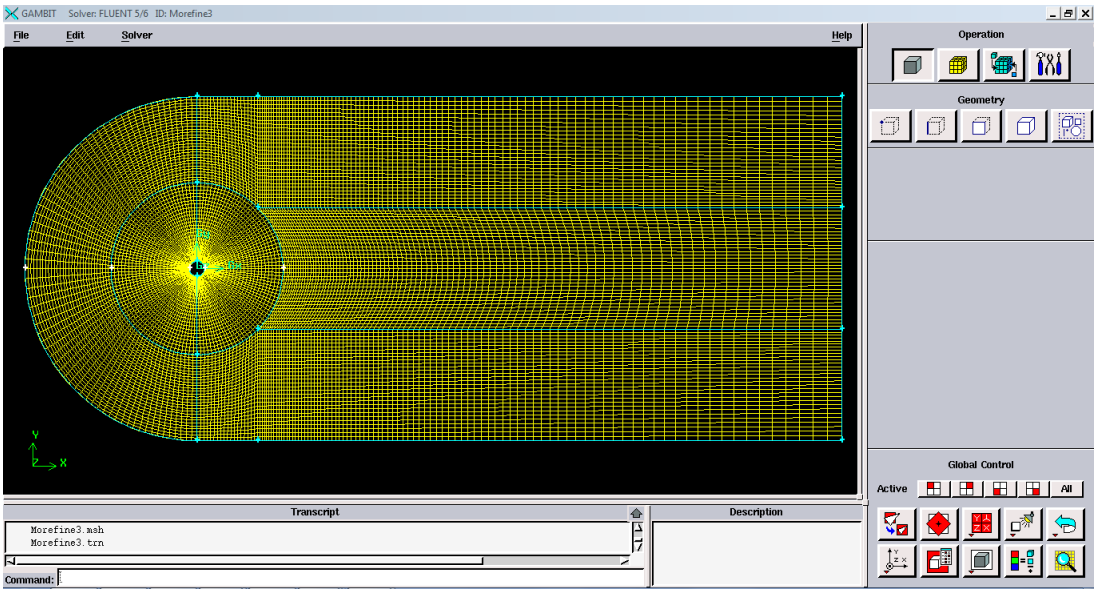

Figure.7-1 Computational 2D domain for a cylinder using Gambit package

Unsteady 3D turbulent flow

Consider a cylinder of 0.7 m diameter and 2m length, inclined with 70° presenting the real physical problem in mining application, the computational 3D domain consists of an upstream of 10m to downstream of 10m and 5m on each cross-stream direction.

The computational domain for cylindrical, streamlined fairing and straight cables model are shown is figures (fig.7-2, fig.7-3, and fig.7-4).

The grid size is represented in table.7-4.

Table.7-4 Grid Size for the three configurations

	Cells	Faces	Nodes
Cylinrical model	177180	545533	191487
Streamlined fairing model	543083	1131294	118064
Straight cables model	513965	1078175	111621

The mesh generation software, Gambit has been used throughout this work to generate the geometry and meshes. we have created the computational domain using Top-down approach. The node distributions in all the edges were specified in order to give a better control on the grid distribution.

This would be important in order to obtain finer meshes around the obstacles in the domain and coarse meshes in other regions where there is not much ‘action’ taking place.

In gambit, the velocity inlet conditions on the velocity field are imposed at the inlet boundaries the outflow conditions on are imposed at the outlet boundaries. Wall conditions (no-slip conditions) are imposed on both the side surfaces and on the upper-lower surfaces.

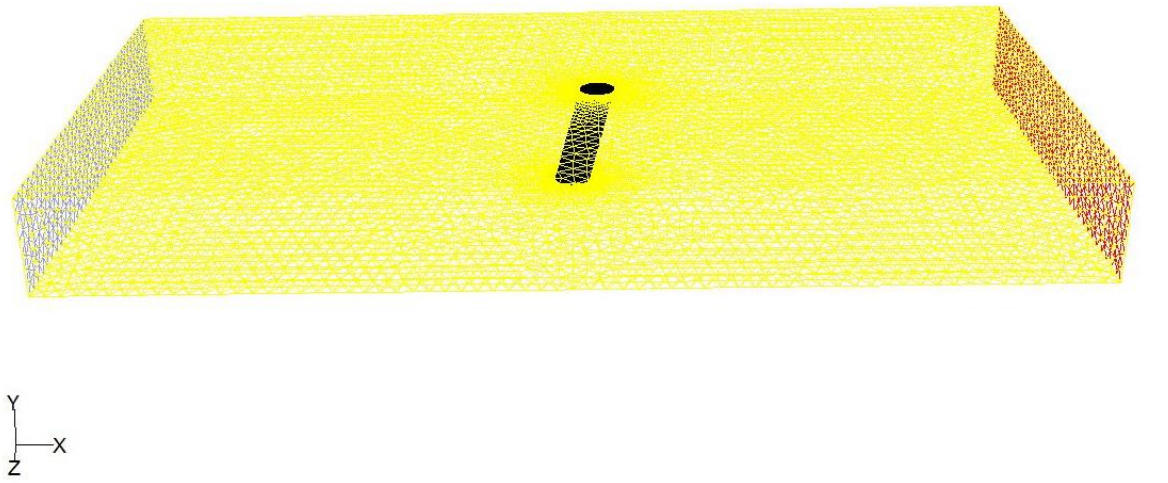

Figure.7-2 Computational domain for cylindrical model

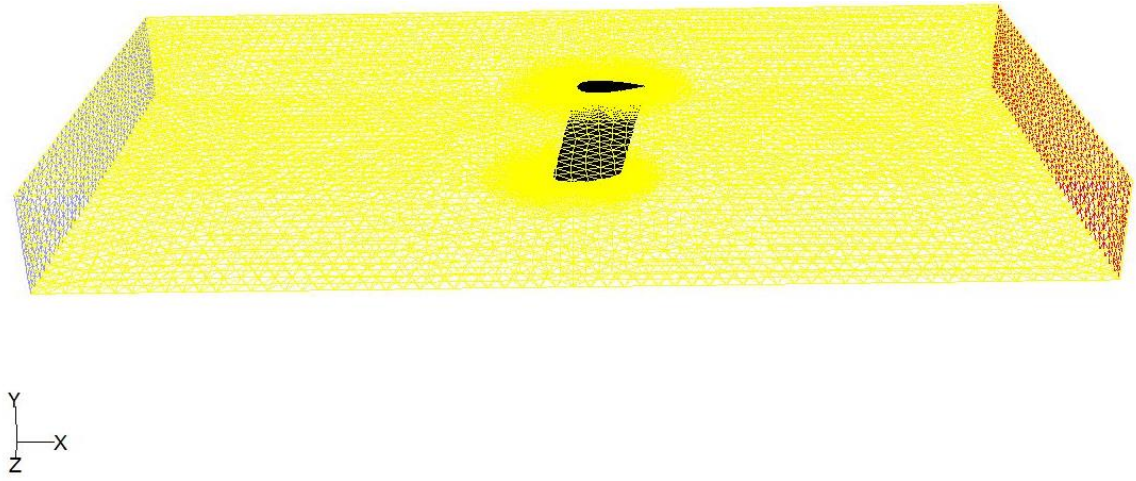

Figure7-3 Computational domain for streamlined fairing model

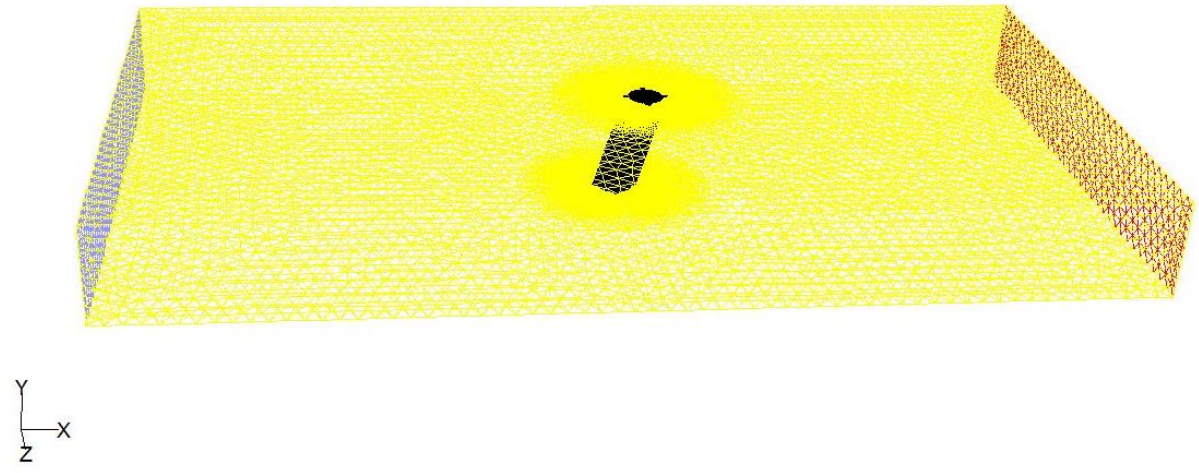

Figure.7-4 Computational doain for Straight cables model

8. RESULTS AND ANALYSIS

8.1. Simulation of a 2D flow over a cylinder

The flow past a two-dimensional cylinder is one of the most studied of aerodynamics. It is relevant to many engineering applications. The flow pattern and the drag on a cylinder are functions of the Reynolds number $Re_D = UD/\mu$, based on the cylinder diameter D and the undisturbed free-stream velocity U. Recall that the Reynolds number represents the ratio of inertial to viscous forces in the flow. The drag is usually expressed as a coefficient

$$C_d = d / (\tfrac{1}{2}\rho U^2 D) \tag{58}$$

8.1.1. Laminar case

The flow decelerates and stagnates upstream of the cylinder (high pressure zone).

• It then accelerates to the top of the cylinder (lowest pressure).

• The origins of the flow separation from a surface are associated with the pressure gradients impressed on the boundary layer by the external flow.

Next it must decelerate against a high pressure at the near stagnation point.

• At higher Reynolds numbers ($10^3 < Re < 10^5$), the flow becomes fully separated. An adverse pressure gradient exists over the near portion of the cylinder resulting in a rapid growth of the laminar boundary layer and separation.

➢ **Vorticity contours**

The Figure.8-1**,** indicating physical phenomenon around the circular cylinder such as the generating process of the vortex shedding and the downstream movement.

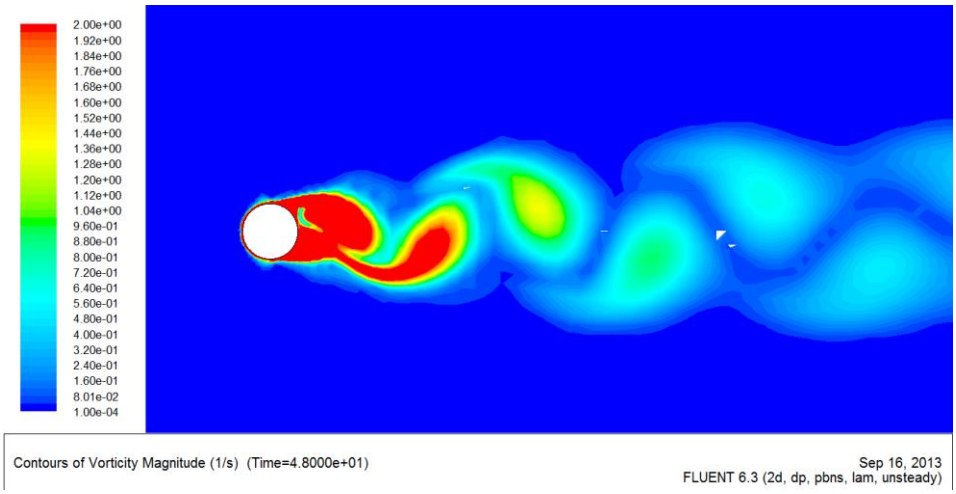

Figure.8-1 Vorticity contours for laminar 2D flow past a cylinder

- **Pathlines vorticity**

The figure.8-2 shows the shed vortex generated in the wake region of the cylinder.

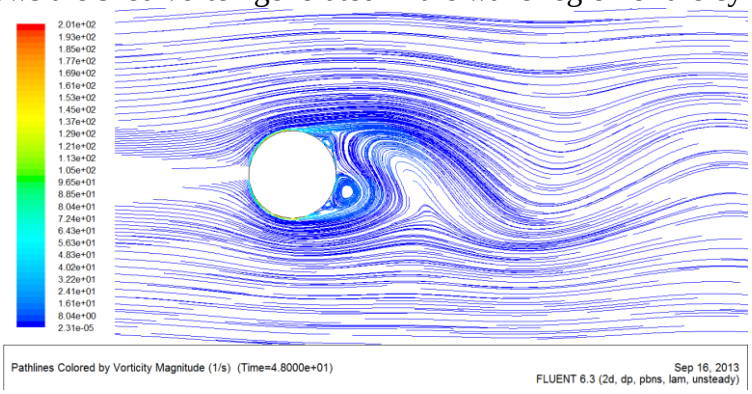

Figure.8-2 Pathlines vorticity for laminar 2D flow past a cylinder

- **Drag coefficient**

As the Reynolds number increases, the boundary layer transitions to turbulent, delaying separation and resulting in a sudden decrease in the drag coefficient. See fig.8-3.

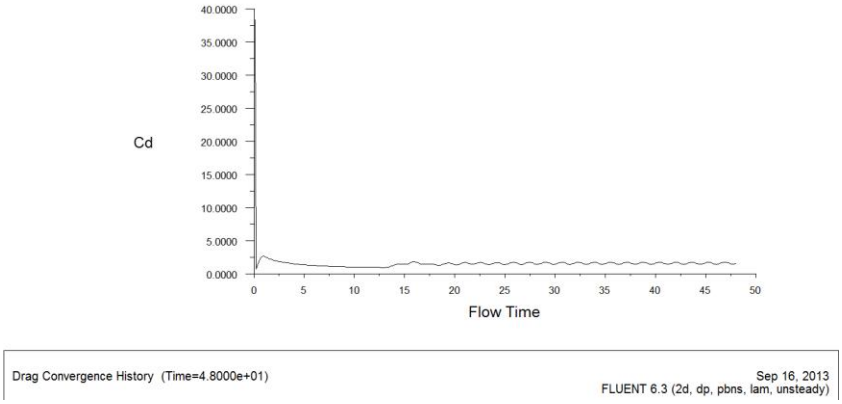

Figure.8-3 Drag coefficient for laminar 2D flow past a cylinder

- **Lift coefficient**

From Cl graph, it can be seen clear sinusoidal pattern which is a sign of a sustained vortex shedding process, the lift coefficient maintained constant amplitude over time. See figure8.4.

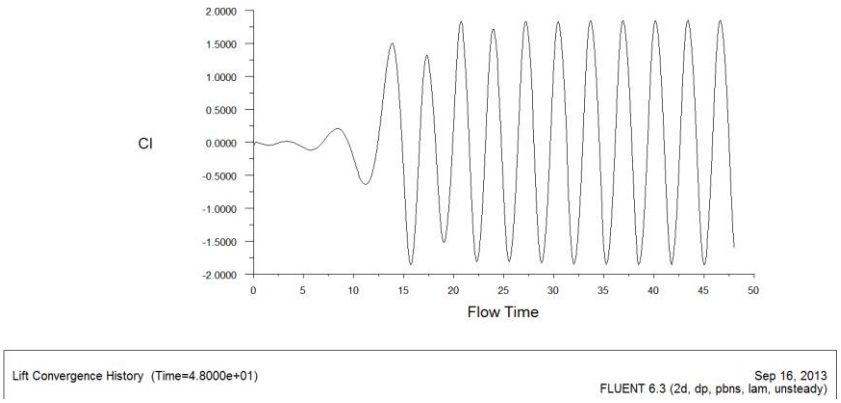

Figure.8.4 Lift coefficient for laminar 2D flow past a cylinder

8.1.2. Turbulent case

From the results, As the Reynolds number increases, flow begins to separate behind the cylinder causing vortex shedding which is an unsteady phenomenon. we can apply either a steady state or an unsteady (time dependent) solver to capture these effects, as appropriate.

The resultants Reynolds number are presented in table.8-1.

Table.8-1 Reynolds number associated to various velocities

U(m/s)	Reynolds Nr
0.2	$1.4\ 10^5$
0.4	$2.8\ 10^5$
0.6	$4.2\ 10^5$
0.8	$5.7\ 10^5$
1.0	$7.1\ 10^5$

- **Vorticity contours**

• In turbulent flow, the boundary layer is defined as the thin region on the surface of a body in which viscous effects are important.

• The boundary layer allows the fluid to transition from the free stream velocity to a velocity of zero at the wall.

• The contour shows the incipient vortex at the top end and shed vortex at the bottom end in the wake of the cylinder.

• The vorticity magnitude increases with increase of the flow velocity.

• The vorticity structure of the flow showed that the wake was much narrower at the higher Reynolds number. See fig.8-5.

V=0.2 m/s

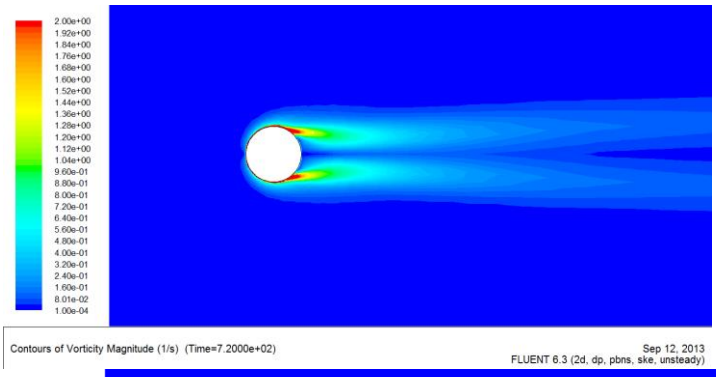

V=0.4 m/s

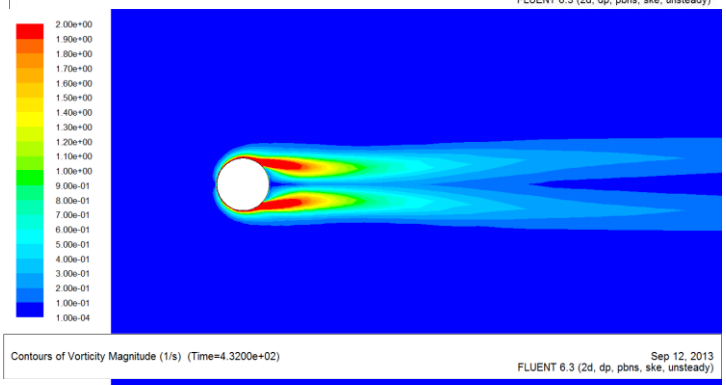

V=0.6 m/s

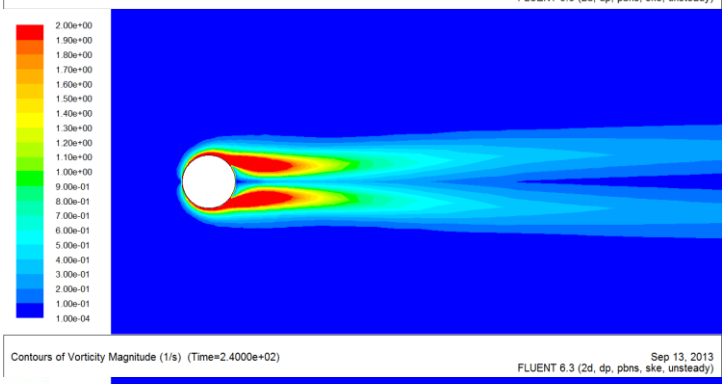

V=0.8 m/s

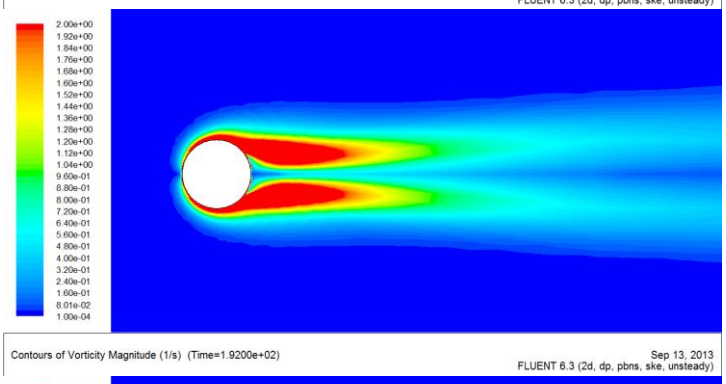

V=1 m/s

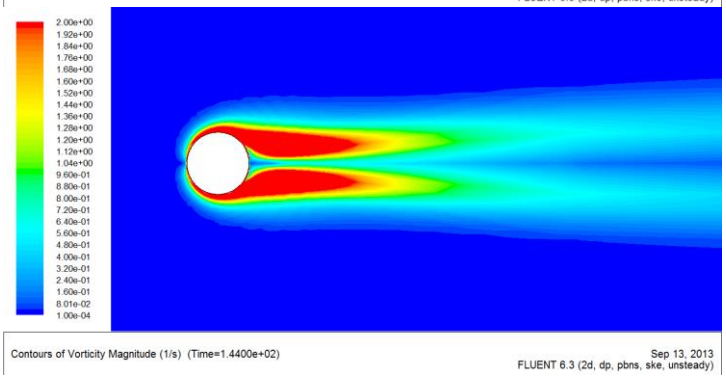

Figure.8-5 Vorticity contours for turbulent 2D flow over a cylinder for variable speed

- **Pathlines vorticity**

The vortexes are more clear in pathlines in the wake region of the cylinder, the relative relation between the flow velocity and the vorticity for V=1 m/s is shown in fig.8-6.

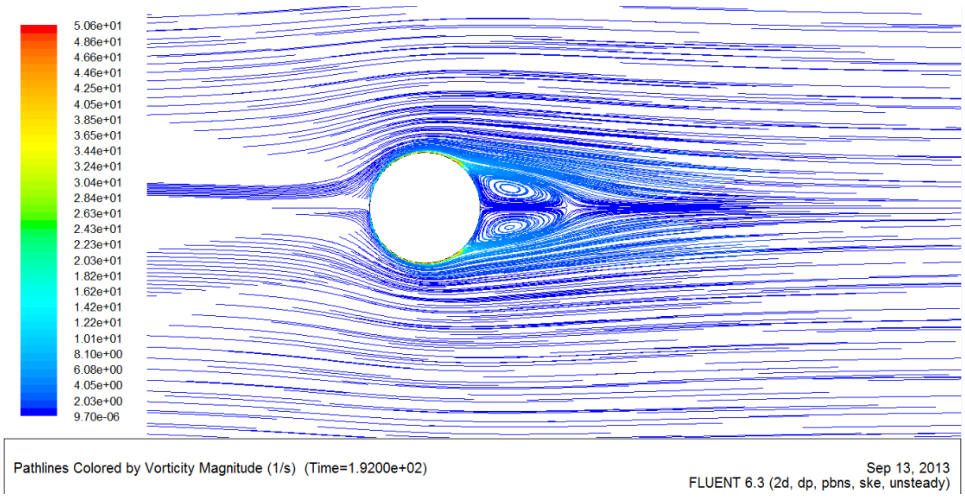

Figure.8-6 Pathlines vorticity for turbulent 2D flow over a cylinder

- **Wall function Y Plus**

The values of Y^+ are dependent on the grid and the Reynolds number of the flow, and are meaningful only in boundary layers. The value of Y^+ in the wall-adjacent cells dictates how wall shear stress is calculated.

In the studied case which is fully turbulent model, the Y+ values are slightly high and maximum is about 250. The lift coefficient can be better predicted if the Y+ value is kept in the range of 30-150. In order to meet this condition, the cells adjacent were refined to wall using Adapt option.

Fluent breaks each cell into four parts such that the first cell is at half the distance as compared to the original mesh, as shown in fig.8-7 .It can be seen that non-conformity exists in the mesh after adaption.

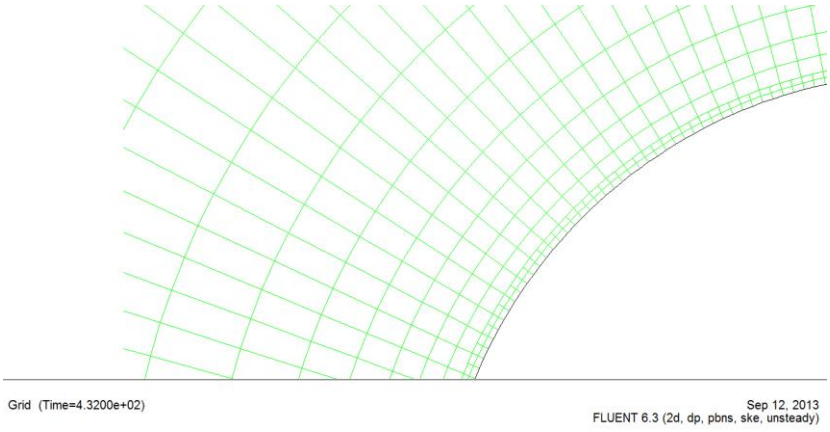

Figure8.7. Grid resolution for turbulent flow after adaption

After adaption, the Y+ values have reduced and most of the cells are below 150.

This shows that the grid resolution is well within the recommended range. See to fig.8-8.

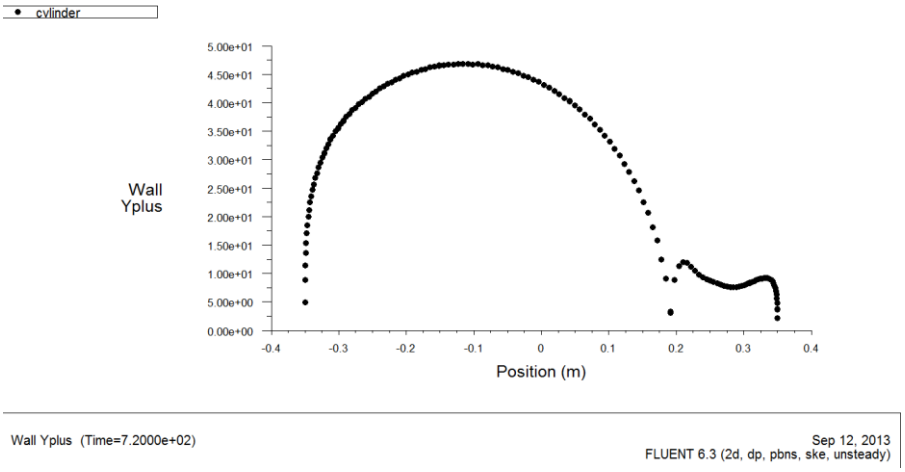

Figure.8-8 Wall Y^+ value for turbulent flow after adaptation

- **Drag and Lift coefficient**

The components of the resultant force acting on the riser immersed in the fluid are the drag force and the lift force.

- The drag force acts in the direction of the motion of the fluid relative to the cylinder.
- The lift force acts normal to the flow direction.
- Both are influenced by the size and shape of the cylinder and the Reynolds number.
- In order to predict the drag on an object correctly, it's needed to correctly predict the pressure field and the surface shear stress. This, in turn, requires correct treatment and prediction of boundary layers and flow separation, it is also important to solve with higher order schemes for key parameters of interest.

For accurate drag, lift predictions, the boundary layer and flow separation need to be modeled accurately. This requires the use of:

- A suitable grid.
- A suitable turbulence model.
- Higher order discretization.
- Deep convergence using the force to be predicted as a convergence monitor.

- **Drag coefficient**

The results indicate that the drag coefficient is gradually reduced as the Reynolds number increases in function of time. Then C_D reaches its lowest value, it looks stable but there are some small oscillations which are not clear, may be due to the turbulence model used which is K-Epsilon. See Fig.8-9 showing Drag coefficient for flow speed V=1 m/s.

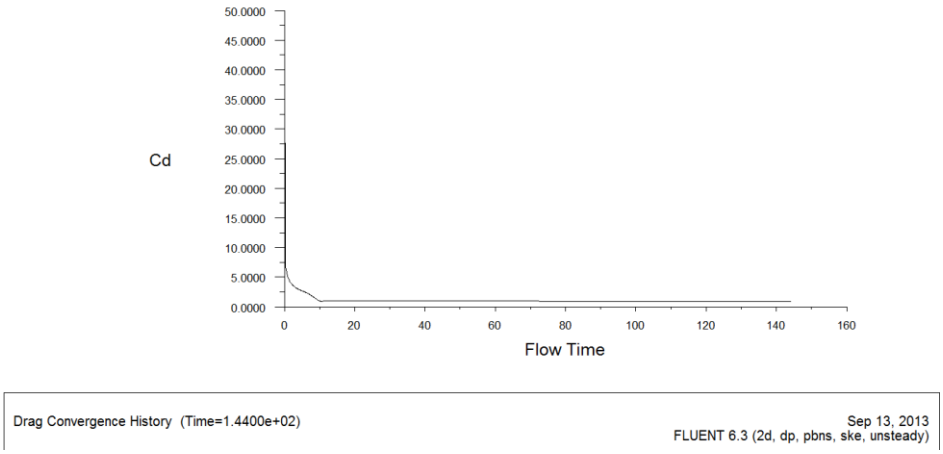

Figure.8-9 Drag coefficient for 2D turbulent flow

Lift coefficient

The graph shows small oscillation at the beginning when the flow heats the cylinder then the lift coefficient goes to zero when Reynolds number increases, this justifies the fully turbulent model, it can be better predicted in laminar turbulence model, refer to fig.8-10. For V=1 m/s.

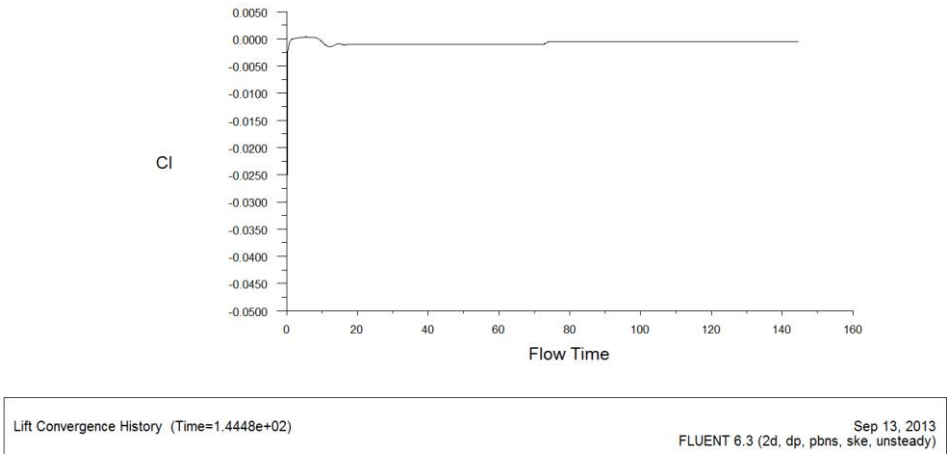

Figure.8-10 Lift coefficient for 2D turbulent flow

8.1.3. Comparison of Strouhal number with experiments

The Strouhal number which indicates vortex shedding characteristics obtained during this study were compared to that of previous experimental studies (Norberg, 2003). See table.8-2. Comparison with reference data shows good correspondence. See figures (Fig.8-11, Fig.8-12).

Table.8-2 Strouhal number performed for various Reynolds number

U m/s)	Reynolds Nr	f(Hz)	Strouhal Nr
0.2	$1.4\ 10^5$	0.05	0.175
0.4	$2.8\ 10^5$	0.11	0.192
0.6	$4.2\ 10^5$	0.17	0.198
0.8	$5.7\ 10^5$	0.22	0.192
1.0	$7.1\ 10^5$	0.28	0.196

The results matches fairly good with the value (0.183) as reported in the literature by (Williamson and G.L. Brown, 1998) [23]

Numerical result of the Strouhal number is represented in the fig.8-11.

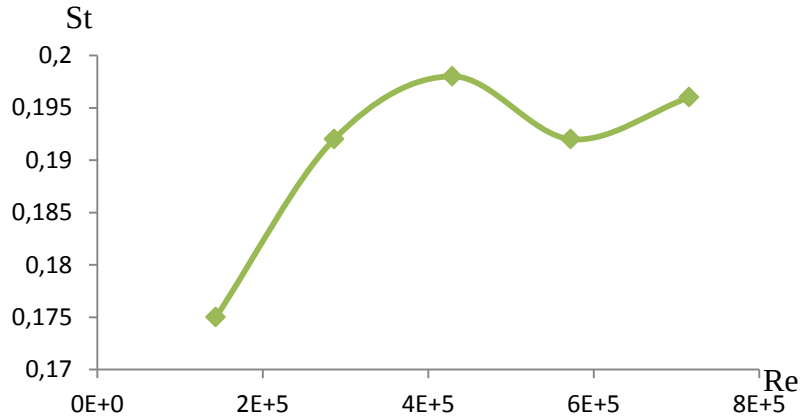

Figure.8-11 Strouhal number as a function of Re

Experimental results shown in fig.8-12 indicate that the Strouhal number increases continuously. The found results were 96% consistent with Norberg's results over an entire range.

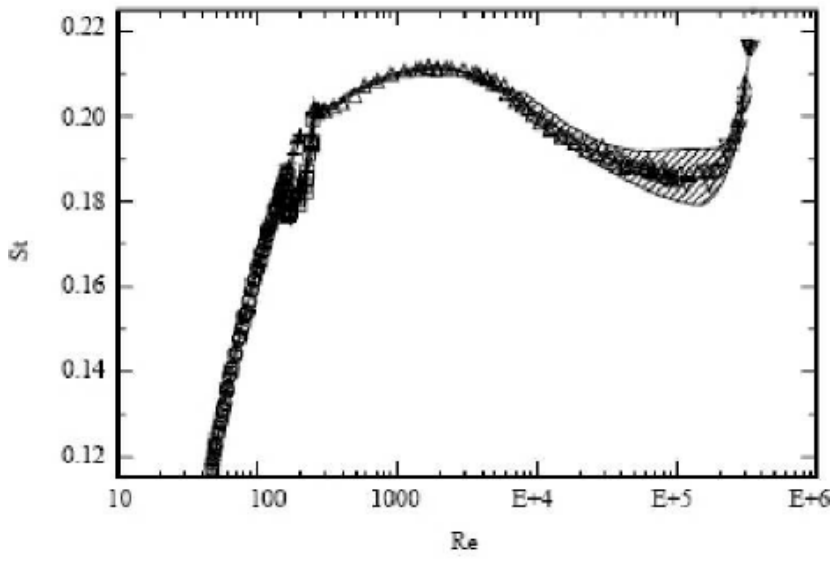

Figure.8-12 Experimental result of Strouhal number as a function of Re, from (Norberg, 2003)

8.2. Simulation of 3D flow past cylindrical, streamlined & straight cable riser

The flow pattern including pressure, velocity, vorticity is presented for flow speed V=1 m/s for different riser configurations.

The total results for flow speed from 0.2 to 1 m/s are detailed in annex.A3.

8.2.1. Comparison of drag coefficient for cylindrical riser with experiments

Incompressible high-Reynolds-number flows around a circular cylinder are analyzed by direct integration of the Navier-Stokes equations using finite-difference method.

The cylinder drag coefficient is presented in function of Reynolds number, (C_D decreases when Re increases). A comparison of numerical result (Fig.8-13) found using Fluent Ansys package with the previous experiments (Fig.8-14) shows a good coincidence.

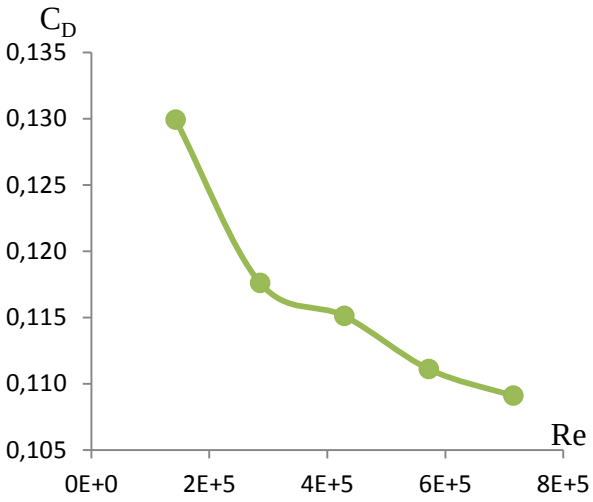

Figure.8-13 Numerical result of cylinder drag coefficient as a function of Re

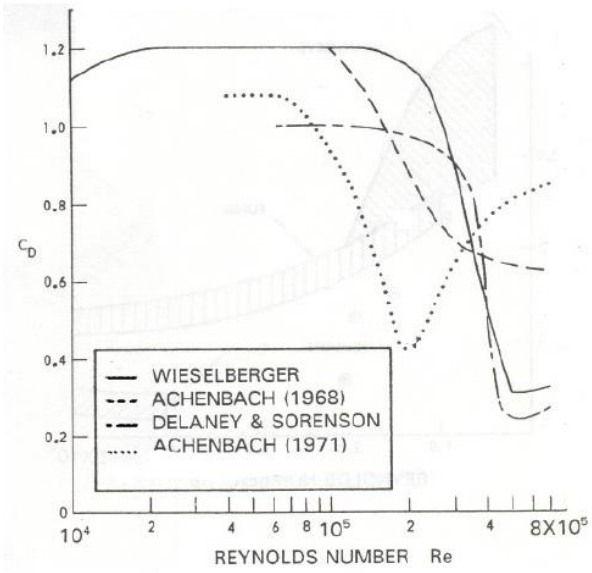

Figure.8-14 Cylinder drag coefficient as a function of Re, from ((Wieselberger (1921), Achenbach (1968), Delaney & Sorenson (1953), Achenbach (1971))

8.2.2. Pressure contours

A turbulent fluid flow exerts pressures on a structure which induce a random response.

The pressure acting on the riser geometries increases with increase of flow speed.

The maximum pressure (576 Pa) is given for the straight cables riser geometry resulting from the cables while the minimum pressure (519 Pa) is applied on the streamlined riser similar to NACA profile. For cylindrical riser configuration P=527 Pa. See Figures (Fig.8-15, Fig.8-16, Fig.8-17).

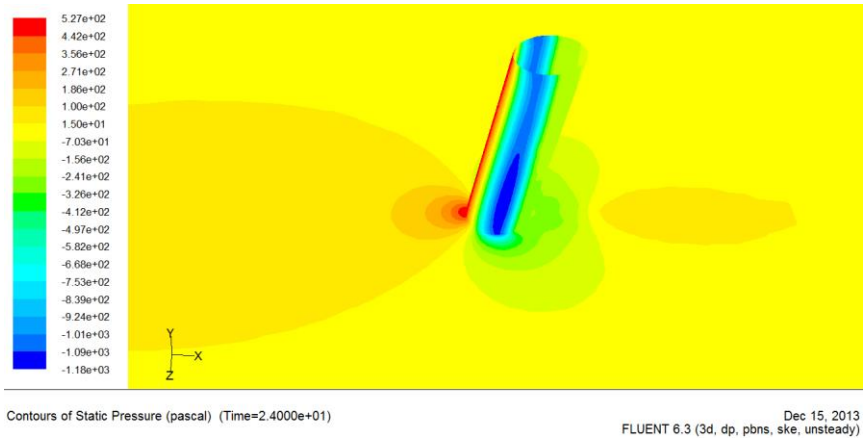

Figure.8-15 Pressure contours of 3D turbulent flow past cylindrical riser

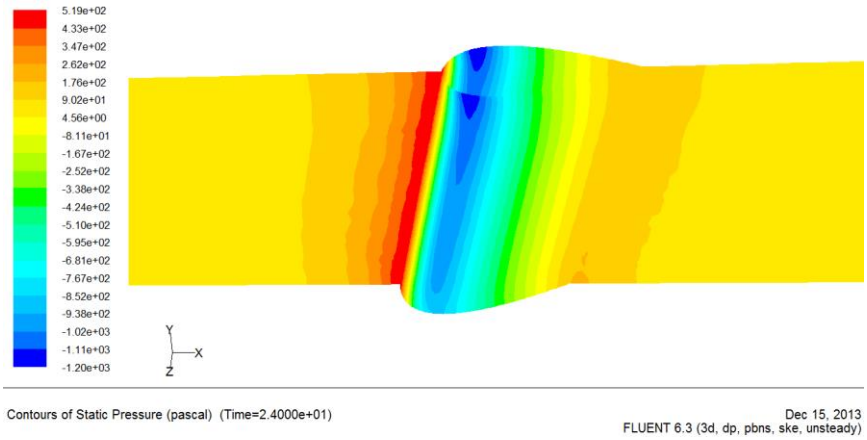

Figure.8-16 Pressure magnitude of 3D turbulent flow past streamlined fairing riser

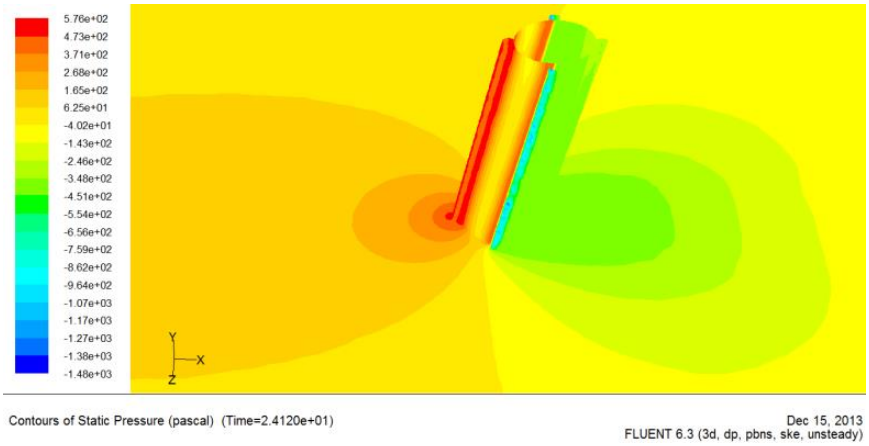

Figure.8-17 Pressure contours of 3D turbulent flow past straight cables riser

8.2.3. Velocity magnitude contours

Figures (Fig.8-18, Fig.8-19, Fig.8-20) show clearly that the flow speed outside wake is much higher than inside while it reaches the maximum upstream. (Separation of boundary layer).

straight cables riser the maximum flow speed is 1.68 m/s which is minimum comparing to other models(1.76 m/s for cylindrical and 1.73 m/s for streamlined model) , because the fixed cables make an obstacle which decrease the velocity of turbulent flow.

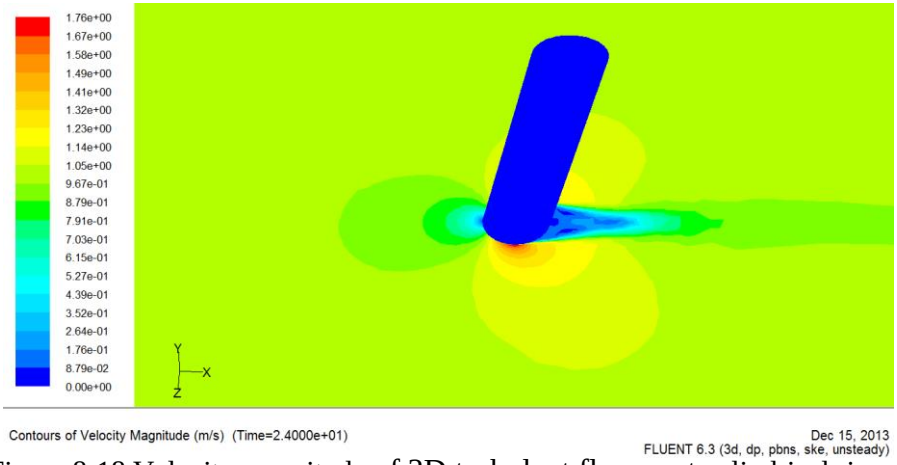

Figure.8-18 Velocity magnitude of 3D turbulent flow past cylindrical riser

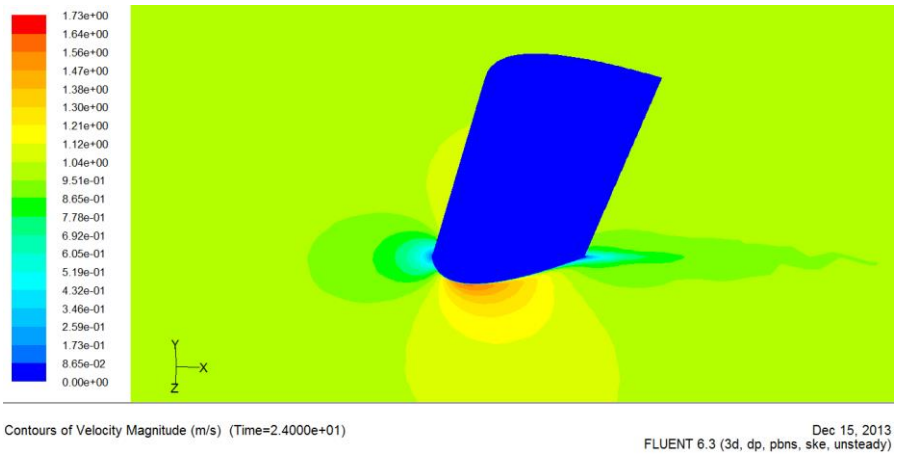

Figure.8-19 Velocity magnitude of 3D turbulent flow past streamlined fairing riser

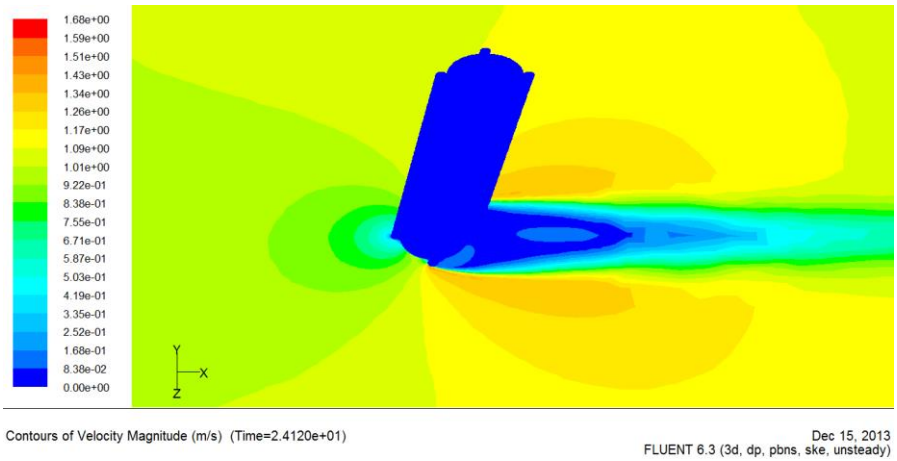

Figure.8-20 Velocity magnitude of 3D turbulent flow past straight cables riser

8.2.4. Velocity vectors

The velocity distribution is well presented with vectors showing the difference between the three riser geometries. See Figures (Fig.8-21, Fig.8-22, and Fig.8-23)

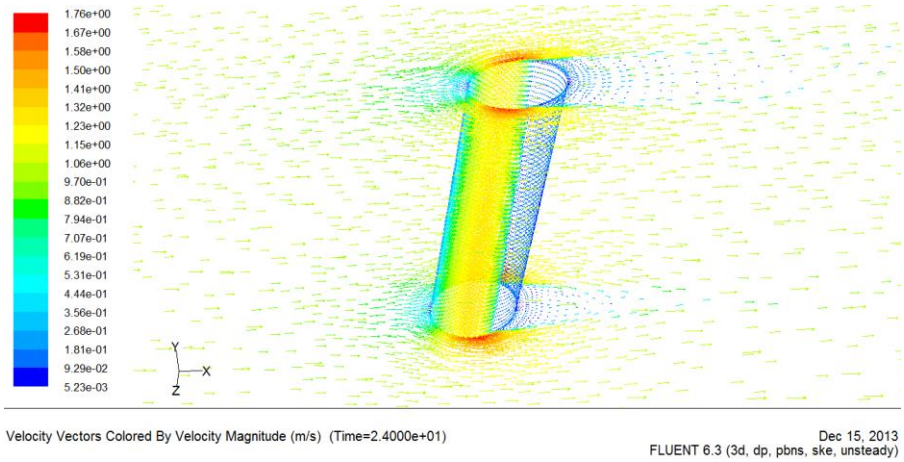

Figure.8-21 Velocity vectors of 3D turbulent flow past cylindrical riser

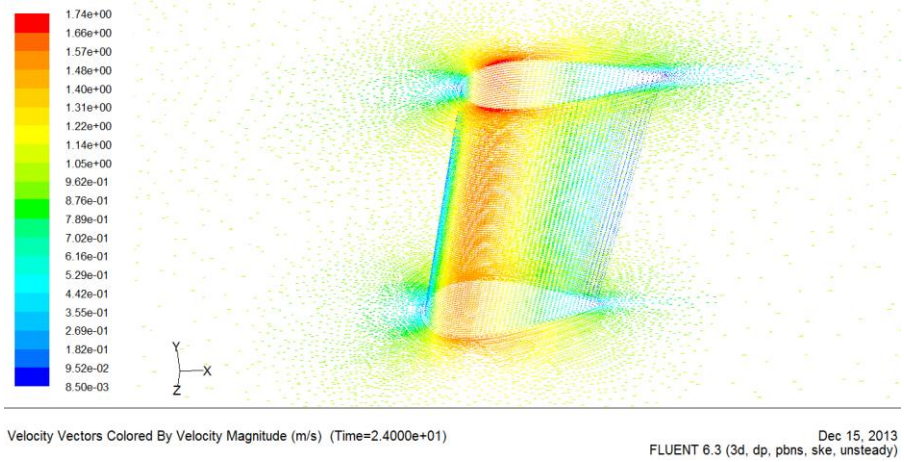

Figure.8-22 Velocity vectors of 3D turbulent flow past streamlined fairing riser

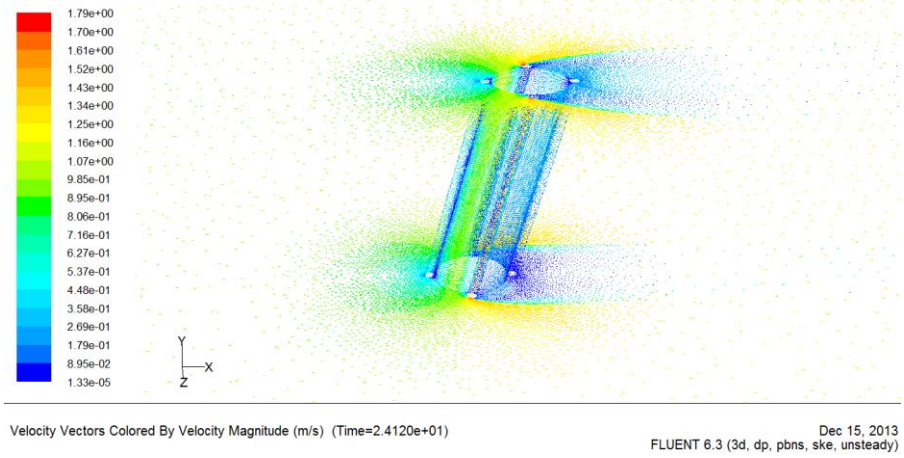

Figure.8-23 Velocity vectors of 3D turbulent flow past straight cables riser

8.2.5. Vorticity magnitude contours

Vorticity gathers at down crossing points in upper layer and gathers at up crossings in lower layer, See figures (Fig.8-24,Fig.8-25,Fig.8-26)

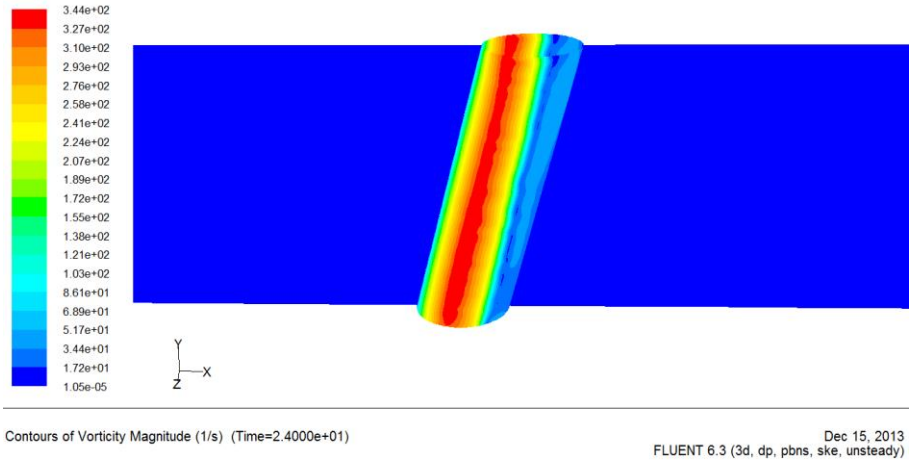

Figure.8-24 Vorticity magnitude of 3D turbulent flow past cylindrical riser

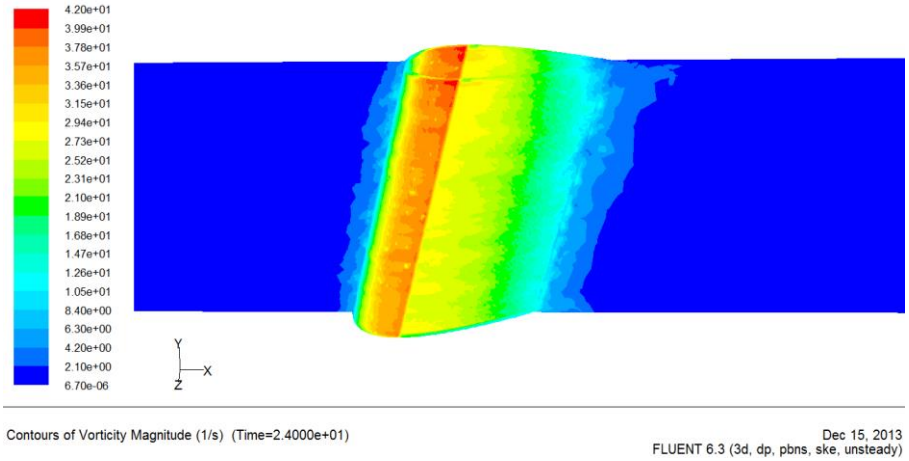

Figure.8-25 Vorticity magnitude of 3D turbulent flow past streamlined fairing riser

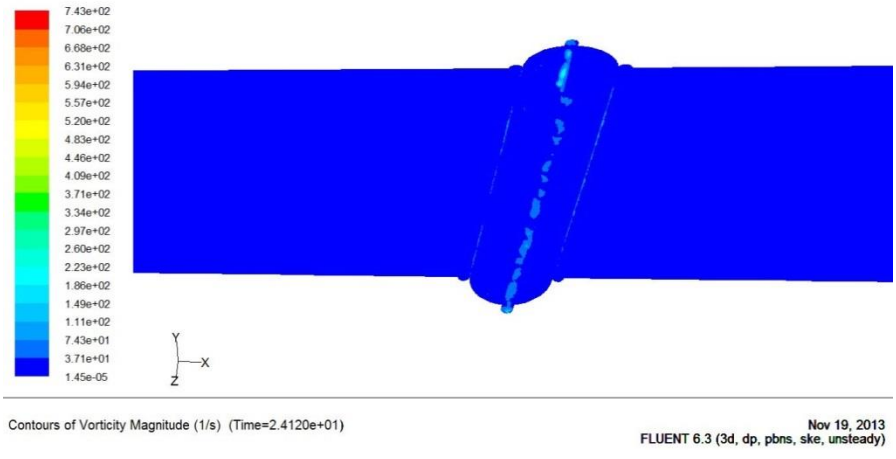

Figure.8-26 Vorticity magnitude of 3D turbulent flow past straight cables riser

8.2.6. Pathlines vorticity

The vortex shedding phenomena is presented in figures (Fig.8-27, Fig.8-28, and Fig.8-29) for three riser configurations; it's generated in the wake region of each model.

The vortex intensity is low for streamlined fairing riser, medium for the cylindrical riser and maximum for straight cables riser geometry (Cables generate significant vortex shedding)

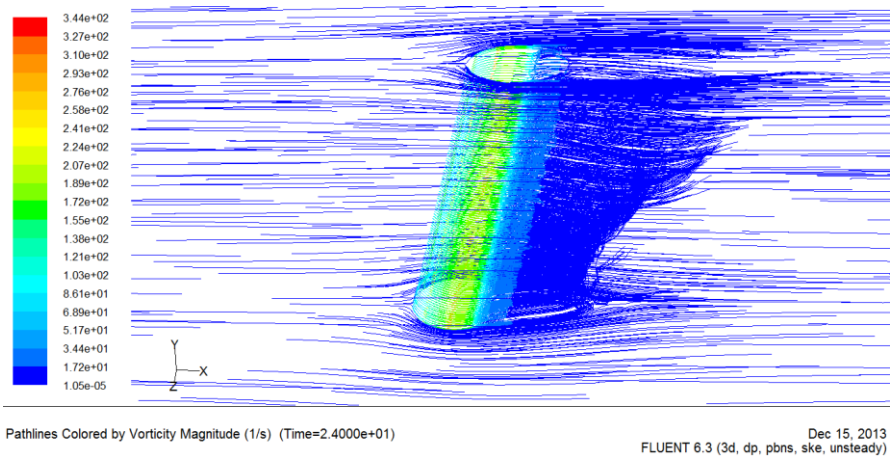

Figure.8-27 Pathlines vorticity of 3D turbulent flow past cylindrical riser

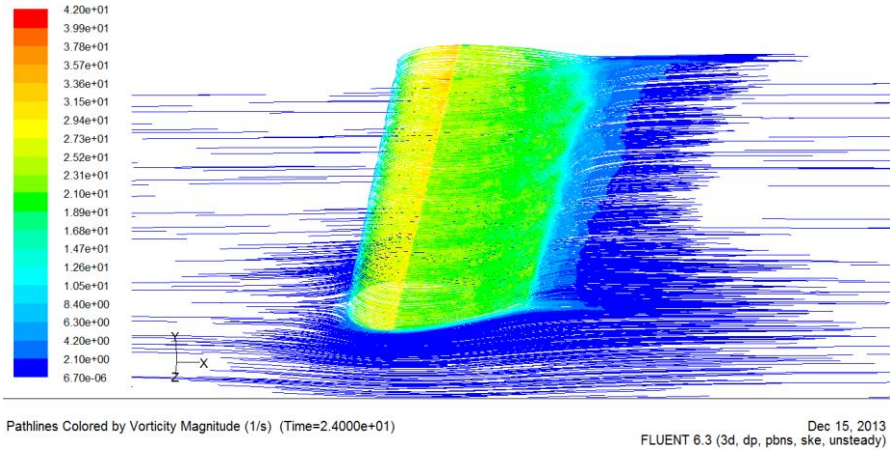

Figure.8-28 Pathlines vorticity of 3D turbulent flow past streamlined fairing riser

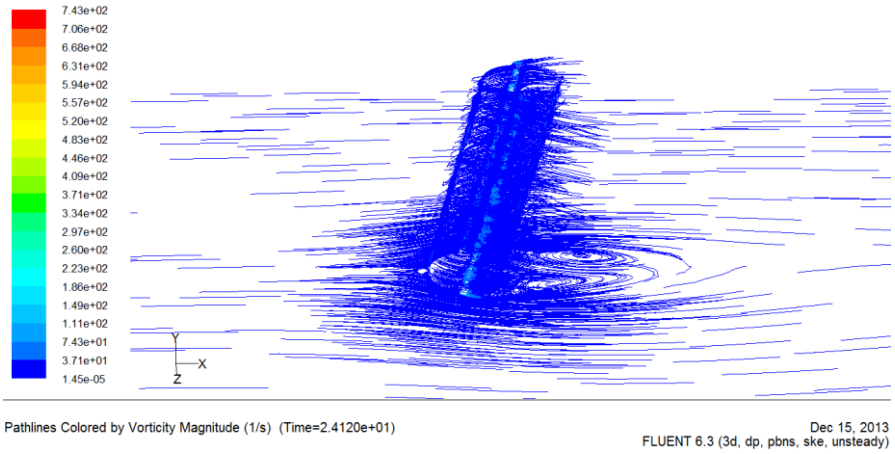

Figure.8-29 Pathlines vorticity of 3D turbulent flow past straight cables riser

8.3. Drag and lift force for the three riser models

The results of the drag and lift coefficients and forces are presented in table.8-4 for the three riser models.

For C_D and C_L graphs resulting from the simulation according to the time flow for V=1 m/s, refer to the appendixes.A2, and it is more detailed in Annex.A2.

Table.8-4 C_D and C_F for three riser configurations

U (m/s)	Drag coefficient	Drag	Lift coefficient	Lift
Cylindrical configuration				
0.2	0.129	11.707	-0.033	-3.032
0.4	0.117	42.396	-0.030	-11.012
0.6	0.115	93.390	-0.029	-24.274
0.8	0.111	160.272	-0.028	-41.687
1.0	0.109	245.758	-0.028	-63.934
Streamlined fairing configuration				
0.2	0.035	4.406	-0.0075	-0.928
0.4	0.031	15.710	-0.0067	-3.343
0.6	0.030	33.494	-0.0064	-7.184
0.8	0.029	57.593	-0.0063	-12.430
1.0	0.028	87.861	-0.0061	-19.056
Straight cables configuration				
0.2	0.371	42.988	-0.0989	-11.467
0.4	0.370	171.845	-0.0989	-45.877
0.6	0.374	390.938	-0.1001	-104.410
0.8	0.371	688.900	-0.0992	-184.003
1.0	0.372	1079.487	-0.0995	-288.361

- Overall pipe drag penalty caused by the effective vortex suppression is within the range acceptable from the ship thrust requirement point of view.
- Figures (Fig.8-30, Fig.8-31, and Fig.8-32) show little dependence of the drag and lift coefficient on the flow velocity.
- The negative values of C_L mean that there is a minimum lift force acting on the riser.
- The streamlined fairing model generates the minimum drag and lift force because of its shape similar to NACA profile, comparing to the straight cables riser configuration which induces the maximum C_D and C_L caused by the cylindrical cables.

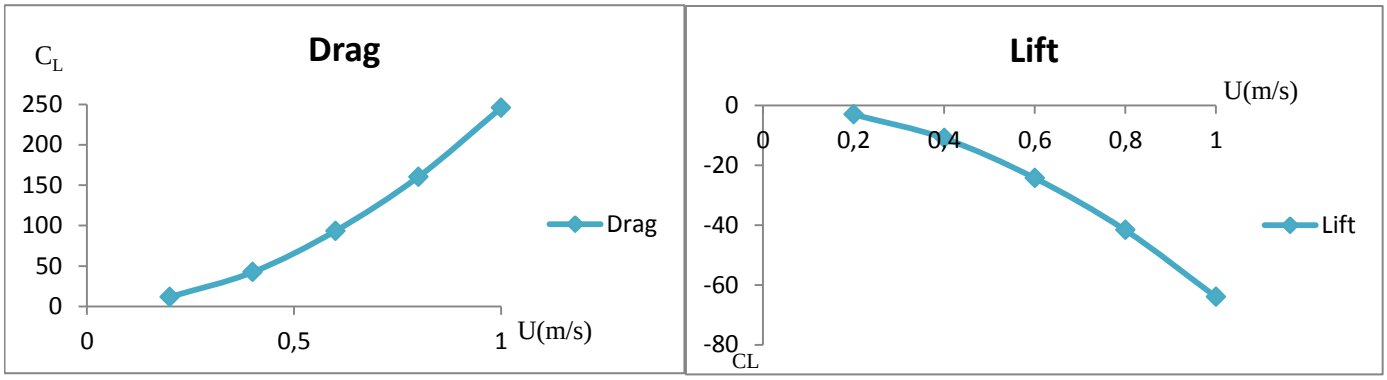

Figure.8-30 Drag and lift force according to the flow velocity for cylindrical riser model

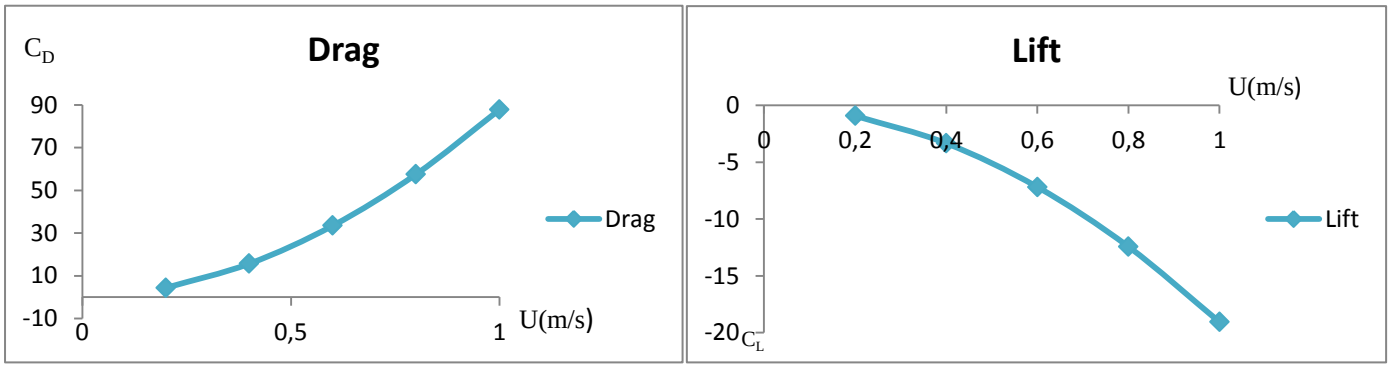

Figure.8-31 Drag and lift force according to the flow velocity for streamlined fairing riser model

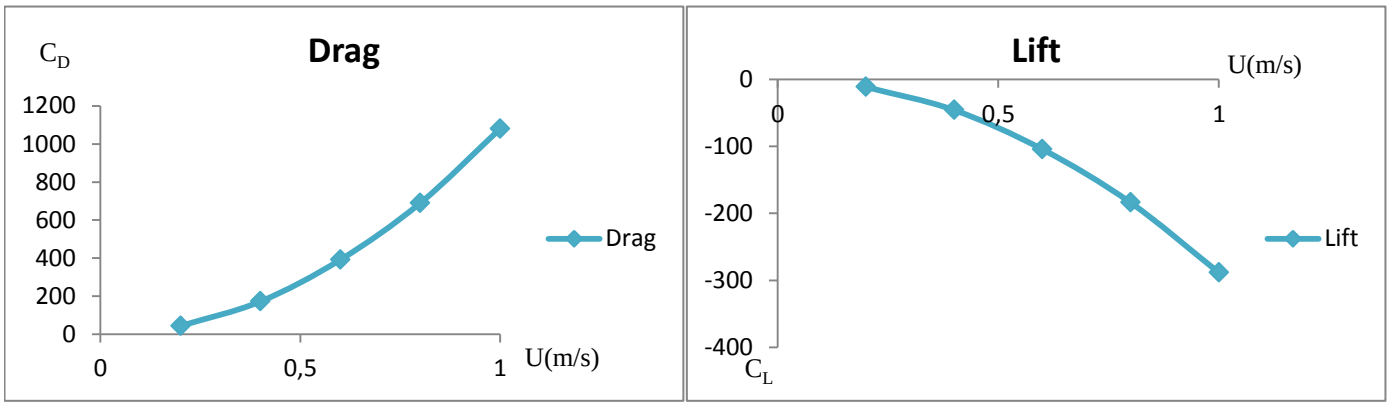

Figure.8-32 Drag and lift force according to the flow velocity for straight cables riser model

8.4. Torsional moments for three riser models

Hydrodynamic torsional moment was one of the postulated causes for potential detorquing for the heavy riser in the deep-ocean mining operations.

The resultant torsional moments associate to the studied riser configurations for different flow velocities is presented in table.8-4.

Table.8-4 Torsional moments associated to each riser configuration for various velocities

	Torsional moments M_x (Nm)		
U (m/s)	Cylindrical model	Streamlined fairing model	Straight cables model
0.2	7.93	1.60	33.22
0.4	27.63	4.64	132.82
0.6	58.47	8.58	302.28
0.8	90.45	13.52	532.59
1.0	150.81	18.95	834.56

- Probable riser twist at the level of the pipe length can be caused by flow-induced torsional moment on the straight-down cable configuration.
- Figures (Fig.8-33, Fig.8-34, and Fig.8-35) show a significant torsional moment for straight cable riser model induced by the flow, this comparing to the streamlined fairing configuration which gives the minimum torsional moment among the three studied riser models.

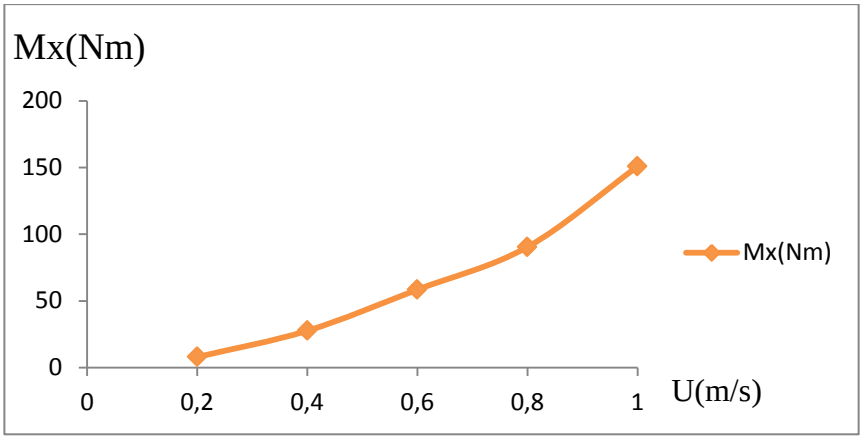

Figure.8-33 Torsional moment according to the flow velocity for Cylindrical riser model

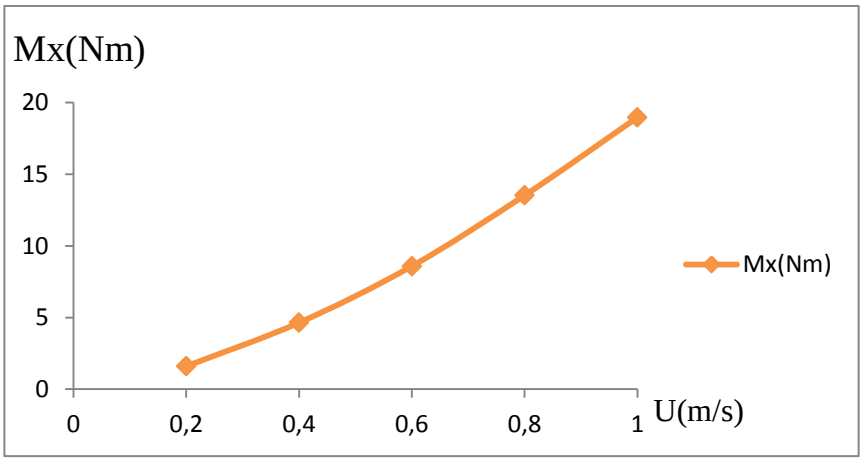

Figure.8-34 Torsional moment according to the flow velocity for Streamlined fairing riser model

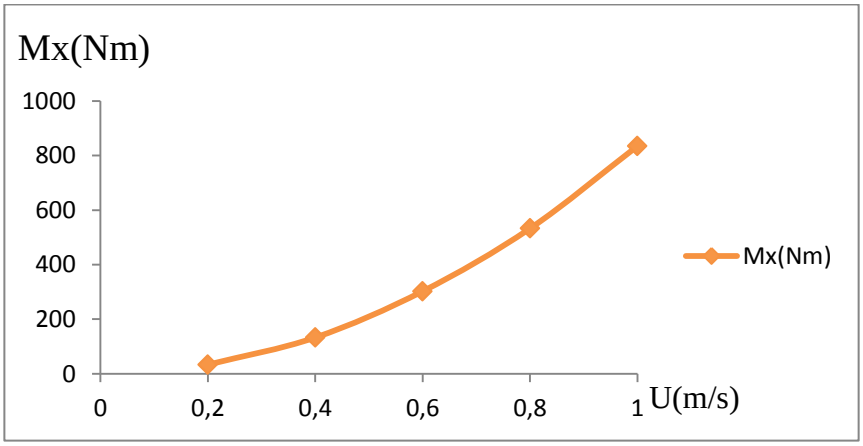

Figure.8-35 Torsional moment according to the flow velocity for Straight cables riser model

8.5. Power requirements for towing the risers from deep seafloor

The cylinder motion through the ambient fluid generates a drag force, F_D, and corresponding 'towing' power, (F_D.U).

For different flow velocities the drag force is calculated then the power needed for towing the riser from the seabed is deduced on. The powers magnitudes is presented in table.8-5.

the resultants powers are presented in the fig.8-31,the power is computed according to drag force neglecting the lift force for the total length of the riser (L=5000m) as shown in figures(Fig.8-36, Fig.8-37, Fig.8-38)

$$F_D = 1/2\ C_D\ \rho\ (2\ \pi\ r\ L)\ U^2$$

$$P=U.\ F_D$$

Table.8-5 Power requirements for different riser configurations

	Power (kw)		
U (m/s)	Cylindrical model	Streamlined fairing model	Straight cables model
0.2	5.85	1.61	26.26
0.4	42.39	11.49	210.15
0.6	140.02	36.74	716.53
0.8	320.38	84.21	1683.96
1.0	614.37	160.52	3297.83

- The power requirement for towing the whole riser from deep seafloor of 5000m varies according to the vortex suppression configuration.
- Comparing the power requirements for the three riser configurations, it's clear that the power is higher for the straight cables model, those cables generate significant drag which leads to maximum power.
- The streamlined model generates a small power because of the small drag force, comparing to the cylindrical riser configuration.

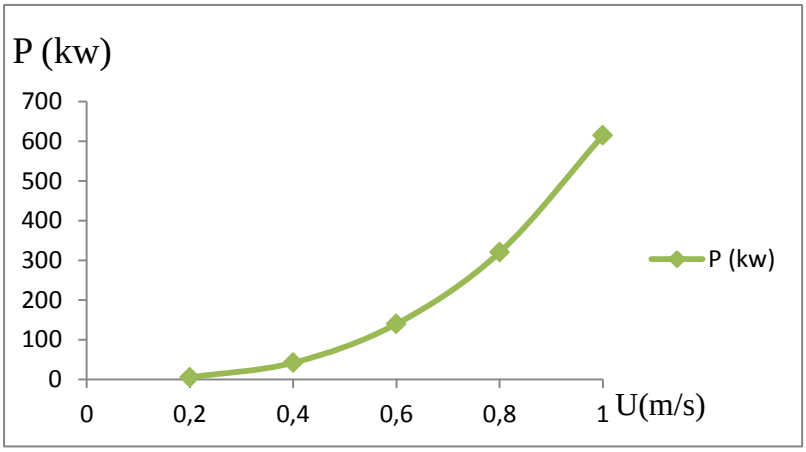

Figure.8-36 Power requirement according to the flow velocity for cylindrical riser model

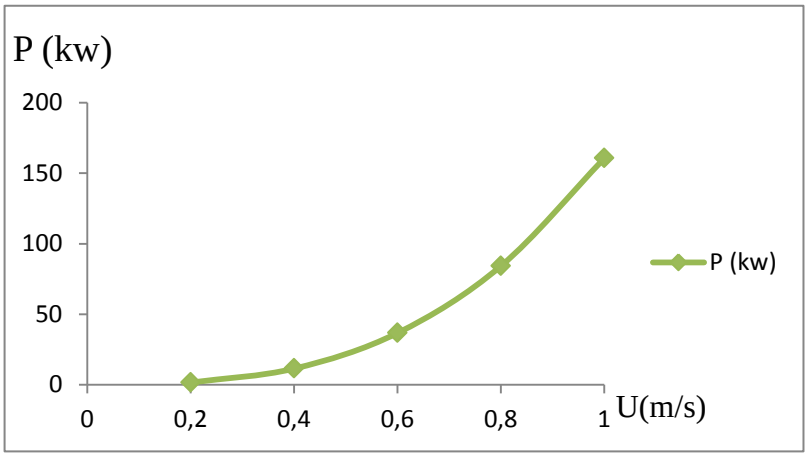

Figure.8-37 Power requirement according to the flow velocity for streamlined fairing riser model

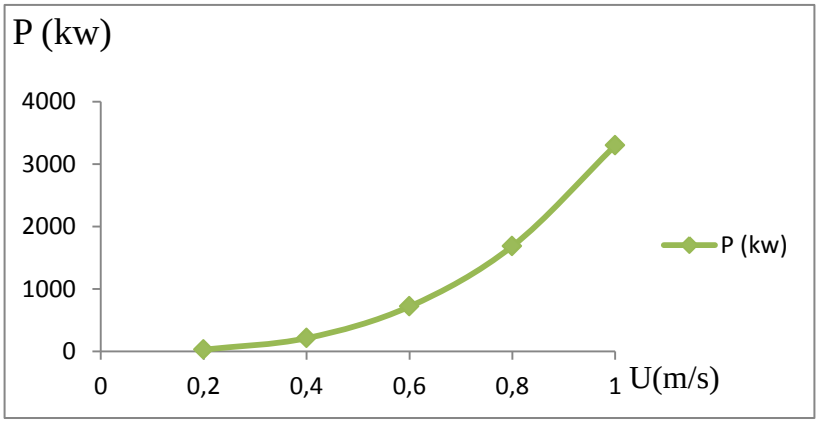

Figure.8-38 Power requirement according to the flow velocity for straight cables riser model

8.6. Analysis of results and recommendations

When a long structure is placed perpendicular to the oncoming flow, higher vibration modes can be excited as the flow velocity is increased, through the successive synchronizations of its structural modes with the local shedding frequency.

The case of vertical long riser, most relevant to mining and offshore applications, has been extensively studied using numerical computations. the following key points can be concluded:

8.6.1. Flow visualization

- The studied riser geometries show a strong dependence of pressure, vorticity on relative flow velocity. Refer to figures (Fig.8-15 to Fig.8-29).

  Flow past a circular cylinder is one of the classical problems of fluid mechanics; the geometry of mining riser suggests a steady and symmetric flow pattern.
- For lower value of Reynolds number, the flow is steady and symmetric; any disturbance introduced at the inlet gets damped by the viscous forces.

  As the Reynolds number is increased, the disturbance at the upstream flow cannot be damped. This leads to the important periodic phenomenon downstream of the cylinder, known as `vortex shedding'.
- Flow instability produces vortices that grow alternately on each side of the riser. The shedding of a vortex is produced when the shear layer of the next upcoming vortex interacts with the opposite side shear layer, cancelling its vorticity because of its different sign. This process is repeated at each side of the riser, generating the vortex street in the wake region.
- Unsteady pressure on the surface of a structure, due to either variations in the free stream flow or turbulent fluctuations, induces a forced vibration response. Strong fluid-structure interaction phenomena result when the fluid force on a structure induces a significant response which in turn alters the fluid force.
- The shedding frequency increases with the flow velocity until it equals the cylinder natural frequency and large amplitude riser vibrations begin.

  The vibrations result from this strong coupling between the string’s dynamics and its induced wake. The structure can resonate with periodic components of the wake.
- Vibration of a riser in a fluid flow can increase of the mean drag on the riser and cause the vortex shedding frequency shift from the natural shedding frequency to the frequency of riser oscillation. This is called synchronization or lock-in.

8.6.2. Vortex suppression configurations

The Numerical result of cylinder drag coefficient as a function of Re of the bare cylinder agree well with the previous experiments. This implies that the simulations data for the rest of the configurations are reliable.

The cylindrical model, the streamlined fairing, and straight cables models have been shown to be effective in destroying regular vortex-shedding patterns and reducing vortex-induced oscillatory forces on the riser models. For these models, vortex-shedding intensity is at low level, vortex frequency is irregular, and the unsteady lift is minimum.

The results were presented on a comparative basis with comprehensive parametric analyses:

- **Cylindrical riser model**

A wealth of experimental data exists for the circular cylinder because it is one of the most widely studied bodies in the field of fluid mechanics.

The flow pattern is presented in figures (Fig.8-15, Fig.8-18, Fig.8-21, Fig.8-24, and Fig.8-27) and drag force on the cylinder are functions of the Reynolds number based on the riser diameter (*D)* and the undisturbed free-stream velocity (*U)* , cylindrical riser is subjected to torsional moment and bending stress resulted from waves and currents loads.

- **Streamlined riser model**

For this model, the flow pattern is shown in figures (Fig.8-16, Fig.8-19, Fig.8-22, Fig.8-25, and Fig.8-28).

The streamlined riser configuration is similar to NACA profile, it generates a minimum drag force, significant lift and small torsional moment, it also requires a least towing power from the seafloor. The streamlined geometry shows a good effectiveness in reducing the vortex shedding intensity (vortexes damping) comparing to other riser geometries .

The big contact area of the streamlined riser model generates big axial forces and bending moments which makes it not useful in the industry.

- **Straight cables riser model**

The flow pattern is presented in figures (Fig.8-17, Fig.8-20, Fig.8-23, Fig.8-26, and Fig.8-29)

- A significant drawback of the cables is that they considerably increase the riser drag more than twice, and by consequence, it generates big power for towing the whole riser from the seabed. Significantly increase the unsteady lift, and intensify the vortex-shedding effect, as compared to the bare cylinder. None of which is desirable for the riser during the mining operations.

- Straight-cables around the riser encounter flow-induced torsional moment; this may create unfavorable restrictions on the riser heading control, and potential detorquing.

- A proposed method for producing straked configurations in ocean mining applications is to wrap the cables around the pipe rather than to run the cables straight down the riser.

- Among the three riser geometries studied, the straight cables model could be the most effective in reducing the vortex shedding intensity if a particular number of cables are installed along it with a specific pitch angle, but at the same time this configuration can provide a set of flow-induced torsional moment from which potential pipe torsional deformations can be estimated.

- Furthermore, proper arrangements of multiple elastic joints and axial dampers installed along a marine riser can reduce the static bending deflection and the axial stress and bending moments. These asymmetric arrangements induce external flow-induced torsional moment, substantially twisting the riser, and moreover induce lateral force, pushing the riser in the lateral direction and leads to problems such as fatigue damage, pipe girth weld failure which can affects also the mining ship hull.

- Mining ships are subjected to vertical movement (heave) causes vertical force acting on the riser, which can be transferred down and results in unwanted stresses in the structure.
  Heave compensators are used to reduce the effect of ship heave on the vertical transport system. Otherwise, the mining operations would require calm seas, with large amounts of time spent waiting for good weather.

CONCLUSIONS

On designing a self-unloading mining ship, loading patterns and sequences reflecting the specific gravities of intended cargoes and ballasting patterns in various operation modes strength features and limitations of the ship should be taken into consideration.

Structural design of self-unloading mining ship shows that accidental stress or severe structural damage caused during charging or discharging of self-unloading mining ship due to shear forces, vertical or horizontal bending moments could ultimately lead to catastrophic structural failure either alongside or at ocean.

In view of this, it is recommended that terminal operators and members of the ship regularly inspect the ship hull structure including the cargo holds before all loading and after all discharging operations, hatch covers and ballast tanks with a view to detecting damage and defects.

The evaluation of the ultimate strength of mining ship hull using NAUTICUS Hull software is believed to be an adequate estimation of the ultimate load capacity of the ship.

Determining the load effects is one of the major objectives in the reliability assessment of the hull structure strength.

The weakest areas in the self-unloading mining ship are the cargo holds frames, the bulkhead between two holds, hatch covers, amid ship of double bottom and deck panels subjected to stress applied by the mining lifting system when towing and launching the riser, especially when the riser is subjected to bending or torsional moment induced by the waves and currents In addition to the crane area and boom system in the aft part of ship.

Particular attention should be paid to these areas of such ships and where necessary, additional support and reinforcements should be provided. This includes improved hull girder longitudinal strenght and double bottom strength , greater strength of transverse watertight bulkheads and also cover the robustness of side shell.

The design and operation of marine risers are complex processes based on a limit state design approach, and requirements for safety and reliability mean that an extensive amount of engineering analysis is required. Production in deep sea fields gives rise to even higher loads and stresses, all foreseeable failure scenarios are considered and the system is designed against the failure mode that is most critical to structural safety.

Unsteady conditions that occur in the ocean make it impossible to get totally correct predictions of the riser motion which strongly affect the flow field, and therefore need to be fully coupled

with the fluid motion; fluid structure interaction (FSI) which is a crucial consideration in the design of many systems must be implemented.

Marine risers are long structures and the critical ratio L/D tends to be very large which makes it difficult to perform CFD simulations since the required number of elements in the mesh tends to be enormous. Moreover the flow around the riser is characterized by vortex patterns that are naturally fully three dimensional and complex to predict.

Flow-induced vortex shedding for riser are of major importance in many engineering fields because of potential riser stresses, bending and torsional deformation during deep sea mining operations.

As an outcome of the simulation of 3D turbulent flow over a mining riser, the streamlined fairing (NACA profile) could be an optimum riser model in alleviating the vortex shedding , but its complex geometry causes significant stresses and creates more problems in use.

The straight cables configuration can generate the least vortex-shedding intensity, minimum lift and minimum increase in drag, and little torsional moments. If the geometry is arranged in helical form with a specific pitch angle.

In order to hit the target of developing a commercial deep ocean mining technology and to develop new configurations for riser systems which are robust to the loads imposed by the design extreme conditions, it is required to analyze the structural integrity of deep sea pipes following extreme events, and to perform a flow computation over diverse riser models to ensure the safety of the riser and the mining ship.

The self-unloading mining ship is a new project in mining applications ,and because of its suspected structural failure, the classification societies has to set new or revised unified requirements to give higher safety and survival margins.

The analysis of problems involved in the design of a self-unloading mining ship reveals several issues which should be carefully studied during more detailed design phases. One of the most important systems of such a ship, strongly affecting the adopted design solutions, is the unloading system. Much additional weight is required for mining equipment and self-unloading machinery; also the hull structure will need to be additionally strengthened due to the nature of cargo and the planned location of ship operations, remote from ship repair services.

The achieved results regarding the structural design can be used as a starting point for the design iterations to follow. Further research and development works will be devoted to detailed structural design and analysis of the self–discharging mining ship, seakeeping calculations, stability analysis, as well as capital and operation costs.

REFERENCES

Journal article	A. Pollio and M. Mossa, 2006.”A comparison between two simple models of a slug flow in a long flexible marine riser” .Technical University of Bari, Department of Water Engineering and Chemistry, Bari Italy
	Tomasz Abramowski and Tomasz Cepowski , 2013.”Preliminary Design Considerations for a Ship to Mine Polymetallic Nodules in the Clarion-Clipperton” , Proceedings of the Tenth ISOPE Ocean Mining and Gas Hydrates Symposium Szczecin, Poland, September 22-26, 2013
	M Bashir, SH Kim, E Kiosidou, H Wolgamot, W Zhang, 2012. ”A Concept for Seabed Rare Earth Mining in the Eastern South Pacific” University of Southampton Research Repository Prints Soton.
	Di Silvestro, R, Casola, F, Fatica, G, Mameli, A, Prandi, A, 2006. ”Novel Tow Methods for Deepwater Riser Towers Transportation in West-of-Africa Environment” Offshore Technology Conference, Paper 17892.
	Uwa Eigbe, Colin Mckinnon Mike Thompson. JP Kenny Ltd, Staines, Middlesex. England Christopher J. Wajnikonis, JP Kenny Inc, Houston, Texas. USA, 2001. ”An interactive approach to deep water riser systems analysis and design”
	Lienard, J. H.: 1966. ”Synopsis of Lift, Drag and Vortex Frequency Data for Rigid Circular Cylinder” Washington State University, College of Engineering, Research Division Bulletin 300.
	Achenbach, E. and Heinecke, E., 1981. ”On Vortex Shedding From Smooth and Rough Cylinders in the Reynolds Numbers From 6 10^3 to 5 10^6 ” J. Fluid Mech. 109, 239-251.
	Roshko, A, 1953. ”On the Development of Turbulent Wakes from Vortex Streets”.National Advisory Committee for Aeronautics Report NACA TN-2913.
	H.Versteeg, W.Malalasekra, 2007. “An introduction to computational fluid dynamics” .Pearson Prentice Hall, 2nd Ed.
	C.H.K. Williamson and G.L. Brown, 1998. ”A Series in to represent the Strouhal- Reynolds number relationship of the cylinder wake” J. Fluids Struct.12, 1073.
	Norberg, C, 2003. ”Fluctuating lift on a circular cylinder: review and new experiments” .Journal of Fluids and Structures 17, 57–96.
	Delaney, NK, and Sorenson, NE, 1953. "Low-speed drag of cylinders of various shapes" NACA TN 3038.
Book	Elaine Baker and Yannick Beaudoin. ”Deep Sea Minerals - Vol 3 - Cobalt-rich Ferromanganese Crusts - page 46”.
	ANSYS FLUENT 12.0 .Theory Guide. April 2009
	Achenbach, E (1968). "Distribution of local pressure and skin friction around a circular cylinder in cross-flow up to Re = 5 x 10^6 " J Fluid Mech, Vol 34, p 625.
	Achenbach, E (1971). "Influence of Surface Roughness on the Cross- Flow around a circular cylinder" J Fluid Mech, Vol 46, p 321.

Chapter	IACS, 2001, International Association of Classification Societies
	Det Norske Veritas (DNV) , January 2012 . ”Rules for classification of ships PART 3 CHAPTER, New buildings hull and equipment – main class Hull structural design, ships with length 100 meters and above.
	Second Report of the ECOR Panel on Marine Mining, September 2008 ”Mineral Deposits in the Sea”.
	American Bureau of Shipping, 2006. ”ABS guide for building and classing subsea riser systems” .Incorporated by Act of Legislature of the State of New York 1862.
	R. D. Blevins. 1990.”Vibration of structures induced by fluid flow”, chapter 29, part i.
	Wiesenberger, C, 1921. “Neuere feststellunger uber die gesteze des flussigkeits and luftwiderstands” Phys Z, Vol 22, p 321.
Internet document	International Maritime Solid Bulk Cargoes Code (IMSBC), issued by IMO. Source. Available from: http://www.bulkcarrierguide.com [05 January 2014].
	Nauticus Hull package. Source. Available from: http://www.dnv.com [20 December 2013].
	Francesco Fedele , Thorsten Stoesser. "HYVOS Hybrid Vortex Oscillating System”Source. Available from:http://savannah.gatech.edu/people/ffedele/Research/researchsite/OMHtmlExport/Vortex_Shedding.htm [23 December 2013].
	Ansys meshing. Source. Available from: http://www.ansys.com/Products/Workflow+Technology/ANSYS+Workbench+Platform/ANSYS+Meshing [30 November 2013]
	Riser system. Source. Available from: http://www.lonestarbit.com/energy/riser.html http://www.evergreen-maritime.com/products/detail-en63.html [29 december 2013]
Thesis	Anne Marthine Rustad, 2007. ”Modeling and Control of Top Tensioned Risers”. Department of Marine Technology, Norwegian University of Science and Technology
	Francisco J. Huera Huarte, April 2006. ”Multi-mode Vortex-Induced Vibrations of a Flexible Circular Cylinder”. Department of Aeronautics, University of London, England.

ACKNOWLEDGEMENTS

First of all, I am so grateful to my sponsor, Erasmus Mundus EMSHIP program, for providing me the opportunity to upgrade my knowledge in Ship Design field. I would like to express my sincere appreciation to all my professors in the University de Liège, Ecole Centrale de Nantes and West Pomeranian University of Technology, Szczecin.

A special gratitude I give to my university project manager, Prof. Zbigniew Sekulski, whose contribution in stimulating suggestions and encouragement, useful to coordinate my project especially in writing this report.

I greatly appreciate the supports from my company supervisor Prof. Tomasz Abramovski director of Interoceanmetal organization (IOM), who gave the permission to use all required materials to complete my tasks during the internship.
Furthermore, I would also like to acknowledge with much appreciation the crucial role of the staff of West Pomeranian University of Technology, Szczecin.

I take this opportunity to record our sincere thanks to the coordinator of the EMSHIP project Prof. Philippe Rigo whose has invested his full effort in guiding all cohorts to achieving the goal. It is my great honor to be his student and under his instruction.

This thesis was developed in the frame of the European Master Course in “Integrated Advanced Ship Design” named “EMSHIP” for “European Education in Advanced Ship Design”, Ref.: 159652-1-2009-1-BE-ERA MUNDUS-EMMC.

APPENDIXES

A1. Self-unloading mining ship structural design

- **Designed hull shape of self-unloading mining ship**

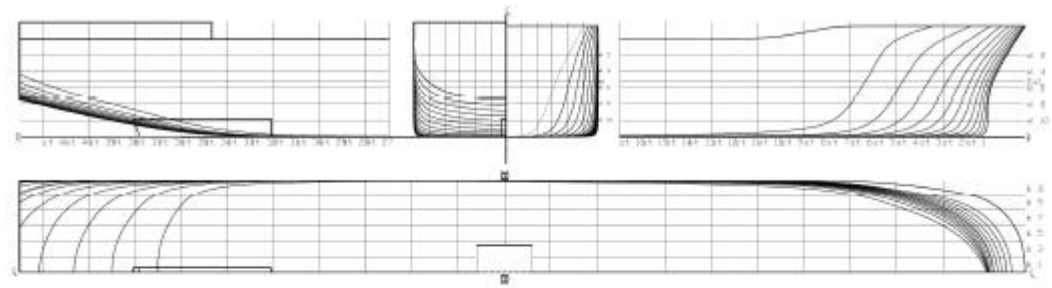

The designed hull shape of the mining ship

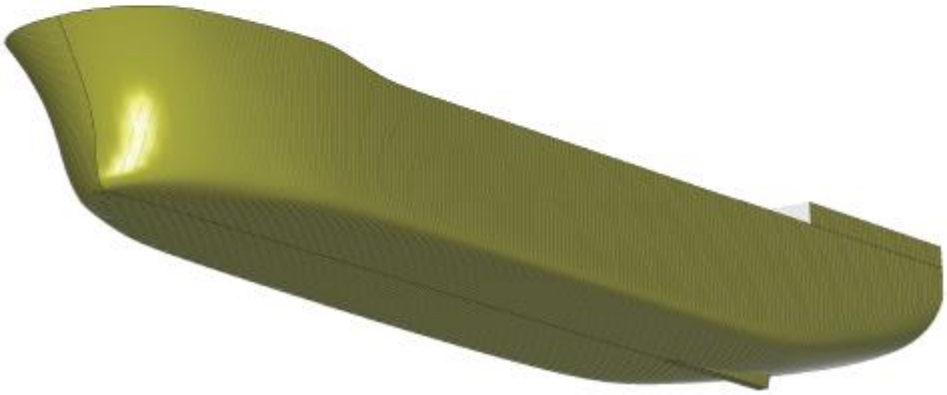

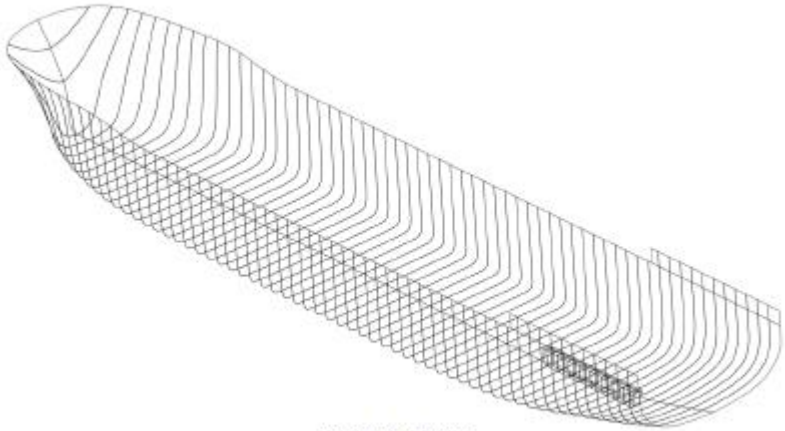

3D view of hull shape

Figure.1 Shape of the proposed self-unloading mining ship hull

- **Summary of input and output data of the scantling using Nauticus Hull according to DNV rule requirements**

For further details, refer to Nauticus Hull report Annex. A1.

➢ ***Main data of the designed ship***

SECTION SCANTLINGS

Hull Section Scantlings according to DNV Rules for ships with L > 100 m

Rule edition ..... : Jan. 2009
Program version ..... : 11.50.5860

Ship Identification
Vessel ID: mining ship

ID No ..... : mining ship
Date/Sign ..... : 2013-11-23 Student

Cross Section Identification
Frame 140

Midship section? ..... : No
Distance from AP ..... (m) : 105.000
Date/Sign ..... :

Database: C:\Documents\DNV\Nauticus\Vessels\mining ship\CrossSections\LABAS.PW

Main Dimensions

Length betw. perpendiculars, Lbp	(m) :	227.000
Rule length, L	(m) :	220.190
Breadth moulded, B	(m) :	43.200
Depth moulded, D	(m) :	22.600
Draught moulded, T	(m) :	12.900
Block coefficient, Cb	:	0.845
Min. design draught at AP	(m) :	8.000
Min. design draught at FP	(m) :	8.000
Waterplane area coefficient, Cwp		0.950

➢ ***Data used in DNV rules requirements***

Summary of data used in the Local Rule Requirements

Distance from AP to considered section	(m) :	105.000	
Moment of inertia about the horz. neutral axis, Ih	(m4) :	499.449	
Moment of inertia about the vert. neutral axis, Iv	(m4) :	1266.915	
Section modulus, bottom	(m3) :	48.930	
Section modulus, deck line (z = 22800 mm)	(m3) :	39.662	
Height from base line to the neutral axis	(mm) :	10207	
STRESS FACTOR, f2:			
f2B (f2 at bottom)	:	0.710	(Rules)
f2D (f2 at deck)	:	0.875	(Rules)
DESIGN BENDING MOMENTS:			
Still water bending moment, sagging	(kNm) :	2262340	(Input)
Still water bending moment, hogging	(kNm) :	2474100	(Input)
Wave bending moment, sagging	(kNm) :	3983033	(Input)
Wave bending moment, hogging	(kNm) :	3616815	(Input)
MOTION PARAMETERS:			
Acceleration parameter, ao	:	0.339	(Rules)
Period of roll, Tr	(s) :	19.377	
Pitch angle, theta	(rad/deg) :	0.100 / 6	(Rules)
Roll angle, Fi	(rad/deg) :	0.324 / 19	(Rules)
Vertical acceleration, av	(m/s2) :	2.754	(Rules)
Ballast draught, Tb	(m) :	8.000	(Input)

NOTE: The wave bending moments are given as input.

NOTE - Sloshing pressure

The sloshing pressure (ref. DNV Rules Pt.3 Ch.1 Sec.4 C305) is applicable within Ls/4 from the tank ends, but is used in this cross-section also.

NOTE - Impact pressure

The impact pressure is not included in the calculations (ref. DNV Rules Pt.3 Ch.1 Sec.4 C305).
Here the sloshing length Ls > 0.13L and/or the sloshing breadth Bs > 0.56B.
The impact pressure should therefore be considered by the user.

A2. Drag and lift coefficient obtained from the simulation of 3D flow around mining riser using Fluent Ansys software.

For flow velocity V=1 m/s, C_D and C_L are presented in function of flow time for 3 riser models.

- *Drag coefficient*

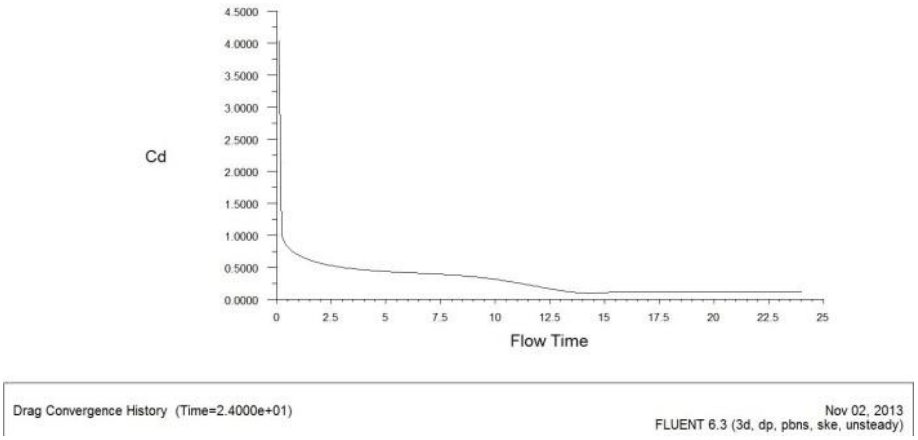

Figure.2 C_D for cylindrical riser configuration

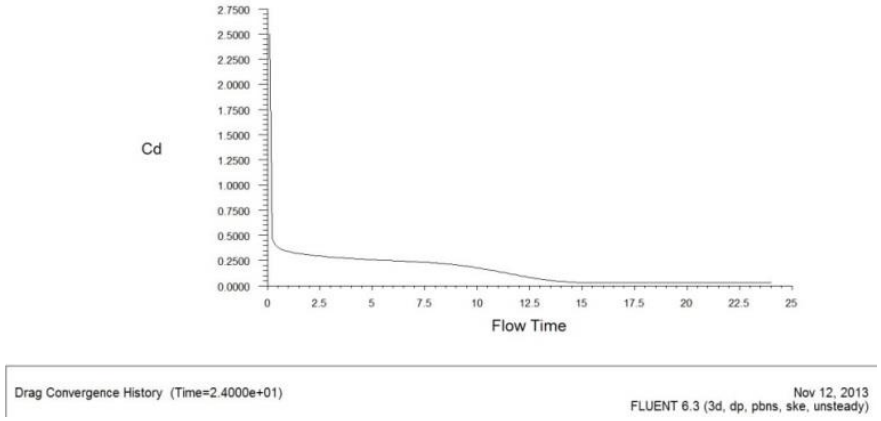

Figure.3 C_D for streamlined fairing riser configuration

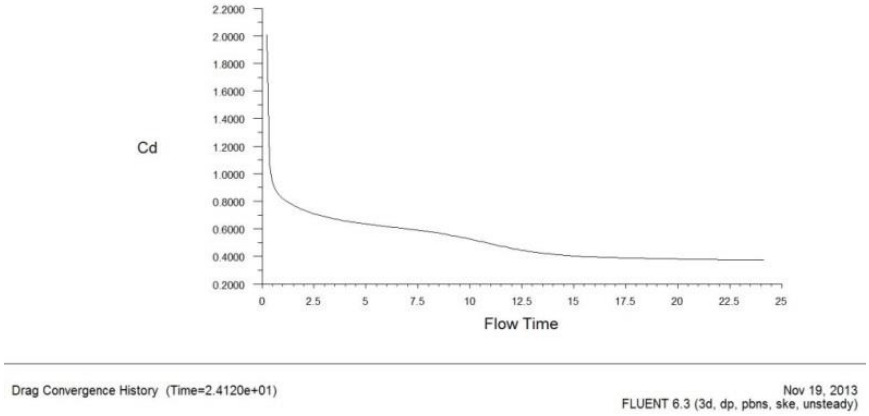

Figure.4 C_D for straight cables riser configuration

- *Lift coefficient*

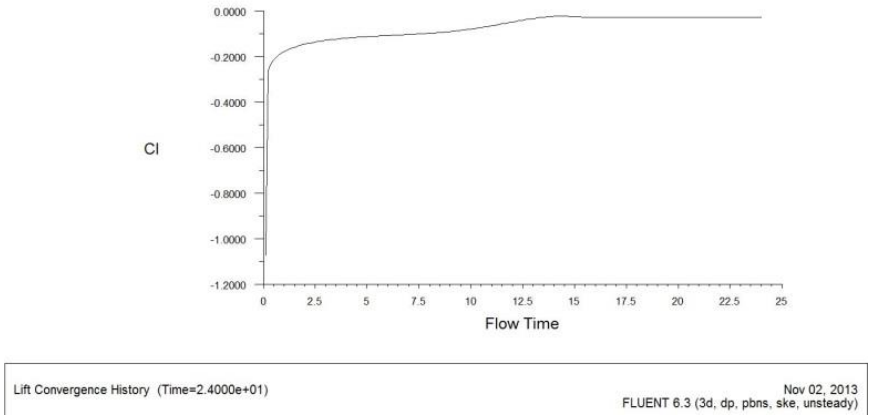

Figure.5 C_L for cylindrical riser configuration

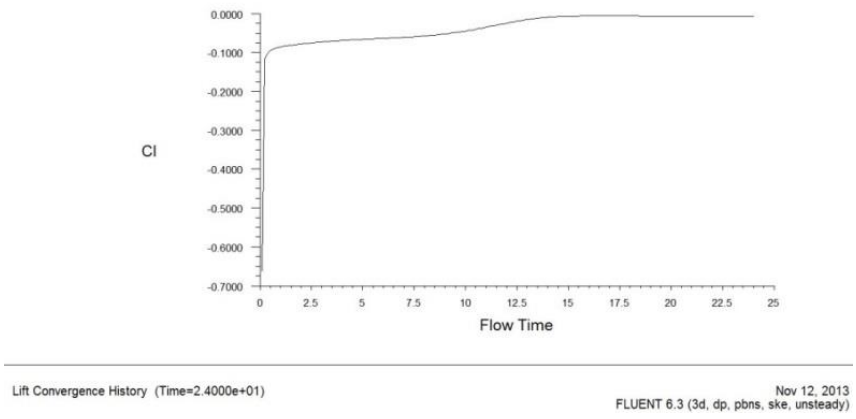

Figure.6 C_L for streamlined fairing riser configuration

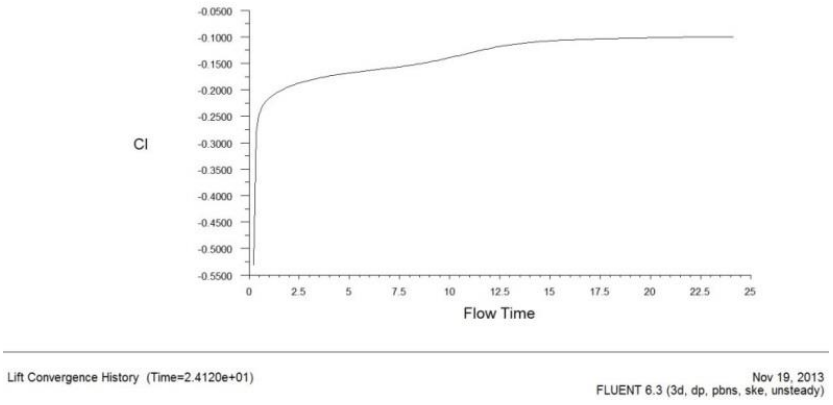

Figure.7 C_L for straight cables riser configuration